

**DESIGN, SYNTHESIS, AND BIOLOGICAL EVALUATION OF
BETULINIC ACID DERIVATIVES AS POTENT ANTI-HIV-1 AGENTS**

Keduo Qian

A dissertation submitted to the faculty of the University of North Carolina at Chapel Hill in partial fulfillment of the requirements for the degree of Doctor of Philosophy in the School of Pharmacy.

Chapel Hill
2008

Dr. Kuo-Hsiung Lee

Dr. Kenneth F. Bastow

Dr. Arnold Brossi

Dr. Alexander Tropsha

Dr. Susan L. Morris-Natschke

Dr. Qian Shi

ABSTRACT

KEDUO QIAN: Design, Synthesis, and Biological Evaluation of Betulinic Acid Derivatives as Potent Anti-HIV-1 Agents (Under the Direction of Kenan Professor Kuo-Hsiung Lee)

The overall goals of this research were to design and synthesize novel betulinic acid (BA) derivatives and to evaluate their biological activities, establish structure-activity relationships (SAR), and investigate mechanism(s) of action. Three specific goals were identified in this study: 1) establish the detailed SAR of C-3 modified BA analogs for HIV-1 maturation inhibitors and further improve antiviral activity profiles; 2) investigate the impacts of C-19 isopropenyl moiety to the antiviral activity and develop 28,30-disubstituted BA analogs as novel HIV-1 entry inhibitors; 3) develop 3,28-disubstituted BA analogs as bifunctional HIV-1 inhibitors.

More than 50 BA derivatives were synthesized and evaluated in HIV-1 replication inhibition assay in this research. Compound **82** with enlarged C-3' substitution of C-3 side chain showed an extremely potent anti-HIV-1 activity with an EC₅₀ value of 0.0006 μ M, which was better than the current clinical trial candidates bevirimat (DSB) in HIV-1_{IIIB} infected MT-2 cell line. In contrast, C-30 substitutions through ether bond do not influence the antiviral potency of the derivatives significantly. Incorporation of water-solubilizing moieties into C-30 position can

improve the hydrophobicity and solubility of the C-28 modified BA derived HIV-1 entry inhibitors significantly, which led to the discovery of **112** with a significant anti-HIV-1 activity (EC_{50} : 0.09 μ M) similar to the previous best hints. The C-28 side chain was further modified to increase the metabolic stability, resulting in the identification of novel 3,28-disubstituted BA analogs **131** and **132**, with better stability and extremely potent antiviral activities (EC_{50} ~0.006 μ M) which are slightly better than that of bevirimat.

In a different project, we discovered that C-3 modification and C-30 modification can increase the anti-proteasome activity of BA dramatically. 3,30-disubstituted BA analogs may be developed into potent proteasome inhibitors and potential anti-cancer agents, which represents another promising direction for the development of BA derivatives.

ACKNOWLEDGEMENTS

First, my sincere gratitude and respect are extended to my advisor, Dr. Kuo-Hsiung Lee for his support, advice, criticism, and encouragement during my graduate studies and research.

I am very grateful to the members of my doctoral committee: Dr. Kenneth F. Bastow, Dr. Arnold Brossi, Dr. Alexandra Tropsha, Dr. Susan Morris-Natschke, and Dr. Qian Shi. They have generously offered their expertise. I have benefited greatly from their advice, criticism, and encouragement.

I am especially thankful to Dr. Donglei Yu and Dr. Kyoko Nakagawa-Goto for their generous sharing of their experience and help with my research.

I am very grateful to Dr. Chin-Ho Chen (Duke University Medical School) for his screening for anti-HIV and anti-proteasome activity, and to Panacos Inc. (Gaithersburg, MD) for their contributions to this research program.

I am especially grateful to Dr. Xiang Wang for his kind help on molecular modeling, and to Dr. Zhiming Wen for his help on metabolic stability assessment.

My thanks are also extended to all the faculties, staffs, students, and especially colleagues of Dr. Lee's laboratory for their support and help.

Finally, I extend my gratitude to my parents, Guibao Qian and Yanmin Wu, for their love and emotional support over these years.

TABLE OF CONTENTS

ABSTRACT	ii
ACKNOWLEDGEMENTS	iv
TABLE OF CONTENTS	v
LIST OF TABLES	x
LIST OF FIGURES	xi
LIST OF SCHEMES	xiii
LIST OF SYMBOLS AND ABBREVIATIONS	xiv

Chapter 1.	Human Immunodeficiency Virus (HIV), Acquired Immunodeficiency Syndrome (AIDS) and Current Anti-HIV Drugs in Clinical Use.....	1
1	Introduction.....	1
2	HIV Classification	2
3	Structure of HIV-1 Virion.....	3
4	Life Cycle of HIV and Possible Anti-HIV Drug Targets	7
5	Approved Antiretroviral Therapy (ART).....	10
5-1	NRTIs	12
5-2	NNRTIs	13
5-3	PIs	13
5-4	Entry Inhibitors.....	14
5-5	Integrase Inhibitors	15
6	HAART and Associated Problems	15

Chapter 2.	HIV Entry Inhibitors and Triterpene Derivatives as Anti-HIV Agents – A Review	17
1	Introduction.....	17
2	Attachment Inhibitors	18
2-1	Nonspecific Attachment Inhibitors.....	18
2-2	CD4-gp120 Binding Inhibitors.....	19
3	Co-receptor Binding Inhibitors	21
3-1	CCR5 Inhibitors.....	22
3-2	CXCR4 Inhibitors.....	29
4	Fusion Inhibitors	31
4-1	Large Molecule Fusion Inhibitors	32
4-2	Small Molecule Fusion Inhibitors – Recent Progress with Triterpene Derivatives as HIV Inhibitors	33
4-2-1	<i>Discovery of RPR103611 and IC9564</i>	<i>34</i>
4-2-2	<i>Mechanism of Action Study of RPR103611 and IC9564.....</i>	<i>37</i>
4-2-3	<i>Current Status of Triterpene Derivatives as Potent HIV-1 Inhibitors</i>	<i>39</i>
5	Conclusion	41
Chapter 3.	Design, Synthesis and Anti-HIV-1 Activity of 3-O-Acyl-Betulinic Acid Derivatives as Maturation Inhibitors.....	43
1	Introduction.....	43
2	Design	44
3	Chemistry.....	45

4	Results and Discussion	51
5	Experimental Section	57
5-1	Chemistry	57
5-2	HIV-1 Replication Inhibition Assay in MT-2 Cell Lines.....	67
5-3	HIV-1 Maturation Inhibition Assay	68
Chapter 4.	Synthesis of 28,30-Disubstituted Betulinic Acid Derivatives as Novel HIV-1 Entry Inhibitors.....	69
1	Introduction.....	69
2	Design	70
3	Chemistry.....	73
4	Results and Discussion	77
5	Experimental Section	82
5-1	Chemistry	82
5-2	HIV-1 _{IIIB} Replication Inhibition Assay in MT-2 Cell Lines	94
5-3	HIV-1 _{NL4-3} Replication Inhibition Assay in MT-4 Cell Lines.....	94
5-4	Cell Fusion Assay.....	94
Chapter 5.	Novel Designed 3,28-Disubstituted BA Analogs with Improved Metabolic Stability as Potent Anti-HIV-1 Inhibitors	96
1	Introduction.....	96
2	Design	97
3	Chemistry.....	99
4	Results and Discussion	103
5	Experimental Section	108

5-1	Chemistry	108
5-2	<i>In Vitro</i> Metabolic Stability Assessment in Human Liver Microsomes	117
5-2-1	<i>Materials</i>	117
5-2-2	<i>Sample Preparation</i>	117
5-2-3	<i>HPLC-MS Conditions</i>	118
5-3	HIV-1 _{IIB} Replication Inhibition Assay in MT-2 Cell Lines ..	119
5-4	HIV-1 _{NL4-3} Replication Inhibition Assay in MT-4 Cell Lines	119
Chapter 6.	Concluding Remarks and Perspectives for Future Directions of Research on BA Derivatives	120
1	BA Derivatives as Potent HIV-1 Inhibitors	120
1-1	SAR Conclusions of BA Derivatives as Potent HIV-1 Inhibitors Targeting Maturation and Entry Processes	120
1-2	Future Research Directions	121
2	Modeling of BA Analogs.....	123
2-1	PASS Prediction of BA and DSB Biological Activities	123
2-2	Pharmacophore Elucidation Using MOE 2007.09	125
2-3	Future Studies on Modeling of BA Analogs Using Variable Selection <i>k</i> NN QSAR Method	129
2-3-1	<i>Introduction</i>	129
2-3-2	<i>Model Validation: Training and Test Set Compound Selection</i>	130
2-3-3	<i>Robustness of QSAR Models</i>	131
2-3-4	<i>Database Mining</i>	132
3	BA Derivatives as Potent Proteasome Inhibitors.....	133
3-1	Introduction	133

3-2	Proteasome Inhibition Activities of DSB and C-30 Modified BA Analogs.....	135
3-3	Future Planned Studies on Novel BA Analogs as Potent Anti-proteasome Agents	139
REFERENCES.....		141

LIST OF TABLES

Table 1-1	HIV genes and gene products.....	5
Table 1-2	Antiretroviral drugs approved by FDA for HIV.....	11
Table 2-1	Structures of 3- <i>O</i> -acyl-BA and dihydro-3- <i>O</i> -acyl-BA derivatives and their anti-HIV-1 activities in acutely infected H9 lymphocytes	40
Table 3-1	Anti-HIV-1 activities for compounds 72-82 , 90 and 93 in acutely infected MT-2 cell lines	52
Table 4-1	Anti-HIV-1 replication activities of 96-113 , 115-120 in HIV-1 _{IIIB} infected MT-2 cell lines	81
Table 4-2	Anti-HIV-1 replication activities of 95-107 and 112 in HIV-1 _{NL4-3} infected MT-4 cell lines	82
Table 5-1	Anti-HIV-1 replication activities of 121-132	107
Table 6-1	Some of the PASS predicted biological activities of BA (44)	124
Table 6-2	Some of the PASS predicted biological activities of DSB (58)	125
Table 6-3	Proteasome inhibition activities of 3-substituted BA analogs.....	136
Table 6-4	Proteasome inhibition activities of 28,30-disubstituted BA analogs.....	138

LIST OF FIGURES

Figure 1-1	Global summary of the HIV/AIDS epidemic, December 2007	2
Figure 1-2	Schematic diagram of HIV virion structure	4
Figure 1-3	Genome of HIV-1	7
Figure 1-4	US-FDA approved NRTIs (date of approval).....	12
Figure 1-5	US-FDA approved NNRTIs (date of approval)	13
Figure 1-6	US-FDA approved PIs (date of approval).....	14
Figure 2-1	Structures of some selected sulfated compounds as HIV nonspecific attachment inhibitors	19
Figure 2-2	Selected structures of CD4-gp120 binding inhibitors.....	21
Figure 2-3	Structures of modified chemokine derivatives as HIV inhibitors.....	23
Figure 2-4	Structures of TAK analogs.....	24
Figure 2-5	Lead optimization and identification of Maraviroc	26
Figure 2-6	Structures of Vicriviroc and Ancriviroc analogs	27
Figure 2-7	Structures of INCB9471 and Aplaviroc.....	28
Figure 2-8	Selected promising CCR5 antagonists as anti-HIV agents.....	29
Figure 2-9	Merck analogs showing potent CCR5 binding affinity.....	29
Figure 2-10	Structures of AMD analogs.....	31
Figure 2-11	C-28 Modified BA as HIV Entry Inhibitors	36
Figure 3-1	Structures of four MSB analogs and other 3- <i>O</i> -acyl BA analogs.....	44
Figure 3-2	Isolation of the four MSB (77-80) isomers by JAI LC-918 recycling preparative HPLC	50
Figure 3-3	Purity confirmation of the four MSB (77-80) isomers by Shimadzu LC-20AT	51
Figure 3-4	Effect of 3'- <i>S</i> -MSB (78) on virus particle production and Gag processing	55

Figure 4-1	Structures of BA and selected C-28 modified BA derivatives	70
Figure 4-2	Structures of Series I (96-107), Series II (108-112) and 113	73
Figure 5-1	Structure of 71	97
Figure 5-2	Structures of 108 , 121-132	99
Figure 5-3	Metabolic stability of 108 and 121	104
Figure 6-1	Design for future BA derived HIV-1 inhibitors.....	123
Figure 6-2	Structures of selected active compounds for pharmacophore model.....	127
Figure 6-3	MOE predicted pharmacophore model for compound 122 , 129-132	128
Figure 6-4	Flowchart of <i>k</i> NN Method	130
Figure 6-5	The workflow of <i>k</i> NN QSAR modeling	131
Figure 6-6	Workflow of the data mining procedures.....	133
Figure 6-7	3,30-disubstituted BA analogs to increase anti-proteasome activity.....	140

LIST OF SCHEMES

Scheme 3-1	Synthesis of compounds 72 and 73	47
Scheme 3-2	Syntheses of compounds 74-81	48
Scheme 3-3	Total syntheses of compounds 77 and 78	49
Scheme 3-4	Synthesis of compound 82	50
Scheme 4-1	General synthetic route for 97-106, 111-112	75
Scheme 4-2	Syntheses of 96, 107-110	76
Scheme 4-3	Synthesis of 113	76
Scheme 5-1	Synthesis of 124	101
Scheme 5-2	Syntheses of 121-123, 125-132	102
Scheme 6-1	General synthetic route for 3, 30-disubstituted BA analogs	140

LIST OF SYMBOLS AND ABBREVIATIONS

AIDS	acquired immune deficiency syndrome
AZT	zidovudine
BA	Betulinic Acid
CDCl ₃	deuterated chloroform
DMAP	4-dimethylaminopyridine
DMF	N,N-dimethylformamide
DMSO	dimethyl sulfoxide
DSB	3 β -O-(3', 3'-Dimethylsuccinyl) betulinic acid
EC ₅₀	effective concentration that is able to suppress HIV replication by 50%
EDCI	N-(3-Dimethylaminopropyl)-N'-ethylcarbodiimide hydrochloride
ELISA	enzyme linked immunosorbent assay
FDA	Food and Drug Administration
HIV	human immunodeficiency virus
¹ H NMR	proton nuclear magnetic resonance
HOBt	N-hydroxybenzotriazole
IC ₅₀	inhibitory concentration which is toxic to 50% of cells
kNN-QSAR	k nearest neighbor quantitative structure-activity relationship
MeOH	methanol
mp	melting point (°C)
mRNA	messenger ribonucleic acid
MS	mass spectrum
MSB	monomethylsuccinyl betulinic acid

NBS	N-bromosuccinimide
NNRTIs	non-nucleoside reverse transcriptase inhibitors
NRTIs	nucleoside reverse transcriptase inhibitors
PIs	protease inhibitors
RT	reverse transcriptase
SAR	structure-activity relationship
THF	tetrahydrofuran
TI	therapeutic index (the ratio of IC_{50} to EC_{50})
TLC	thin-layer chromatography
μ M	micromolar concentration
UNAIDS	the joint United Nations program on HIV/AIDS
WHO	World Health Organization

Chapter 1. Human Immunodeficiency Virus (HIV), Acquired Immunodeficiency Syndrome (AIDS) and Current Anti-HIV Drugs in Clinical Use

1. Introduction

Since the first person was recognized with acquired immunodeficiency syndrome (AIDS) in 1981, this pandemic has rapidly grown into the fourth leading cause of mortality globally. As the world enters the third decade of the AIDS epidemic, AIDS remains an exceptional crisis due to both its emergent and long-term development. It is estimated that human immunodeficiency virus (HIV), the etiologic cause of AIDS, has infected over 60 million people worldwide. Currently, there are approximately 33.2 million people living with HIV (Figure 1-1). In 2007, 2.5 million people were newly infected and 2.1 million people died of AIDS-related illnesses.¹

The four major routes of HIV transmission are unprotected sexual intercourse², contaminated needles³, breast milk, and transmission from an infected mother to her baby at birth⁴. HIV primarily infects vital cells in the human immune system, such as helper T cells (specifically CD4⁺ T cells), macrophages and dendritic cells, resulting in the destruction and functional impairment of the immune system. HIV infection leads to low levels of CD4⁺ T cells through three main mechanisms: firstly, direct viral killing of infected cells; secondly, increased rates of apoptosis in infected cells;

and thirdly, killing of infected CD4⁺ T cells by CD8 cytotoxic lymphocytes that recognize infected cells. A healthy, uninfected person usually has 800 to 1,200 CD4⁺ T cells/mm³ blood. During HIV infection, the number of CD4⁺ T-helper cells progressively declines. When it falls below 200/mm³, the patients become particularly susceptible to many life-threatening opportunistic infections caused by microbes that usually do not infect healthy people, as well as suffer diarrhea, debilitating weight loss, neurologic conditions, and cancers, such as Kaposi's sarcoma and certain types of lymphomas.⁵

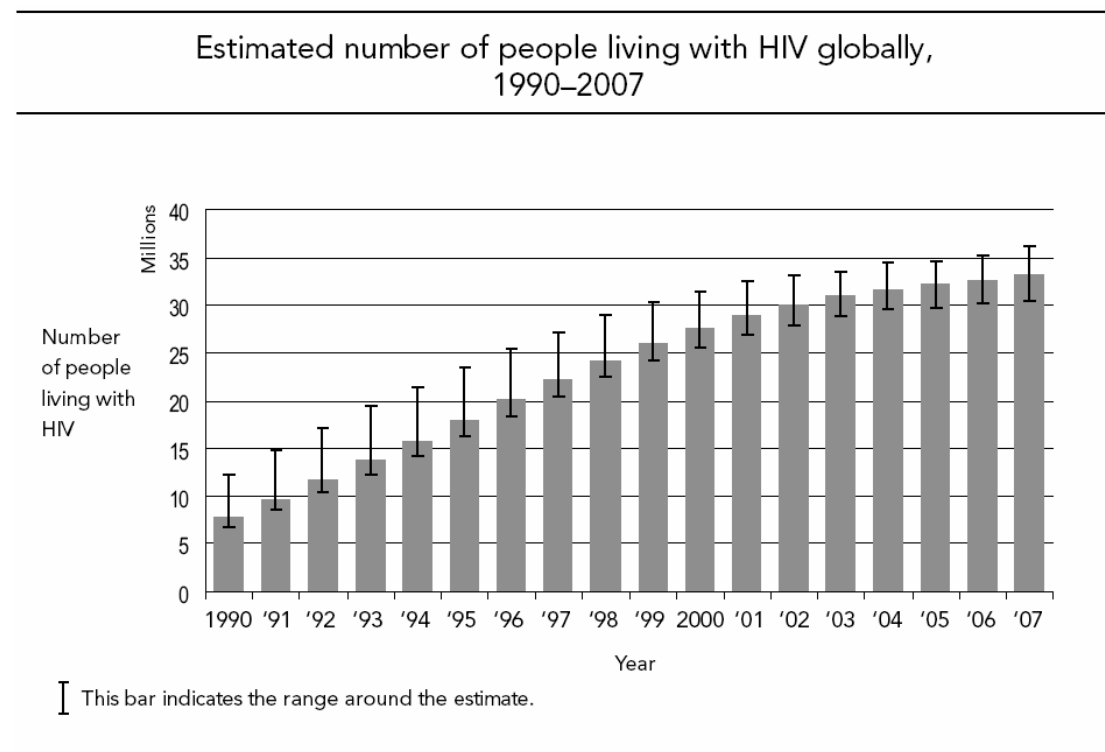


Figure 1-1. Global summary of the HIV/AIDS epidemic, December 2007

2. HIV Classification

HIV is a member of the genus *Lentivirus*, part of the family of *Retroviridae*. *Lentiviruses* have many common morphologies and biological properties. Many

species are infected by lentiviruses, which are characteristically responsible for long-duration illnesses with a long incubation period.⁶ Humans can be infected by two species of HIV: HIV-1 and HIV-2. Together with the related non-human virus, simian immunodeficiency virus (SIV), HIV-1 and HIV-2 comprise the subgenus “primate lentiviruses”. The genomic organization of these viruses is similar, but a high degree of genetic diversity exists.⁷ HIV-1 is thought to have originated in southern Cameroon after jumping from wild chimpanzees (*Pan troglodytes troglodytes*) to humans during the twentieth century.⁸ It is highly virulent and relatively easily transmitted, and is the cause of the vast majority of HIV infections globally. HIV-2 may have originated from the sooty mangabey (*Cercocebus atys*), and is largely confined to West Africa.⁸ Compared to HIV-1, HIV-2 is less transmittable, less pathogenic, shows lower virus loads in the asymptomatic stage, and results in slower disease progression.⁹

3. Structure of HIV-1 Virion

The mature HIV-1 virion is about 120 nm in diameter and roughly spherical.¹⁰ The viral genome contains two copies of single-stranded RNA, which code for the virus's nine genes, enclosed by a conical capsid (CA) composed of the viral protein p24. This electron dense conical core is a distinctive structural feature of HIV and can be observed by electron microscopy. The p24 protein can be detected by an antigen capture enzyme-linked immunosorbent assay (ELISA), which is one diagnostic method for primary HIV-1 infection. The single-stranded RNA is tightly bound to nucleocapsid proteins (p7, NC) and enzymes needed for the infection process of the

virion, such as reverse transcriptase (p64 and p51, RT), protease (p10, PR), and integrase (p32, IN). A matrix protein (p17, MA) surrounds the capsid, ensuring the integrity of the virion particle. In turn, the matrix is surrounded by the viral envelope, which is comprised of double-layered phospholipids taken from the cellular membrane when a newly formed virus particle buds from the human host cell. Embedded in the viral envelope are 72 copies of HIV-1 envelope glycoprotein (Env). Env is composed of surface glycoprotein (gp120, SU), which assembles into a trimer that is able to bind to cellular receptors, and transmembrane glycoprotein (gp41, TM), which also assembles into a trimer that anchors Env into the viral membrane.^{11,12} This envelope glycoprotein complex enables the virus to attach to and fuse into target cells, thereby initiating the infectious cycle (Figure 1-2).

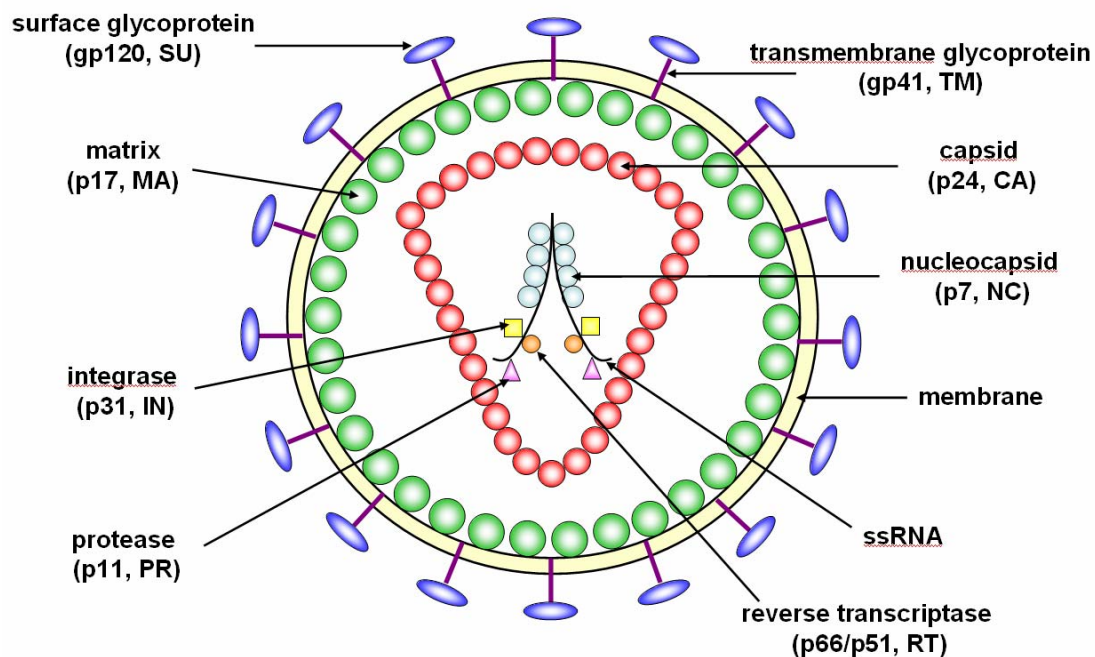


Figure 1-2. Schematic diagram of HIV virion structure

Table 1-1. HIV genes and gene products

Gene	Protein Product	Function of encoded proteins
<i>gag</i>	53kDa precursor	<i>Gag polyprotein precursor</i>
	p17	Matrix, forms outer core layer, important for virion stability
	p24	Capsid, forms inner conical core layer, important for virion maturation
	p7	Nucleocapsid, is tightly bound to ssRNA, important for RNA packaging
	p6	Related to virion assembly and release
<i>env</i>	160kDa precursor	<i>Envelope glycoproteins</i>
	gp120	Surface protein, a cap mediates receptor binding, important determinant of cell tropism
	gp41	Transmembrane protein, a stem anchors the Env into membrane, mediates fusion
<i>pol</i>	Precursor	<i>Enzymes</i>
	p66/p51	Reverse transcriptase, with DNA polymerase and RNase activities
	p10	Protease, mediates <i>gag</i> and <i>gag/pol</i> polyprotein cleavage
	p32	Integrase, catalyzes proviral integration
<i>tat</i>	p14	Transcriptional and posttranscriptional regulator, strongly activates transcription of proviral DNA
<i>rev</i>	p19	Posttranscriptional regulator, facilitates nuclear export, stability, and translation
<i>nef</i>	p27	Early regulatory proteins, increases viral replication; down-regulates host-cell CD4
<i>vif</i>	p23	Virus infectivity factor, promotes infectivity and efficient transmission of viral particle
<i>vpu</i> *	p16	Facilitates viral maturation and release
<i>vpx</i> *	p14	Facilitates viral replication and nuclear entry of the pre-integration complex in macrophages
<i>vpr</i>	p15	Weakly activates transcription of proviral DNA

* *vpu* is found only in HIV-1; *vpx* is found only in HIV-2 and SIV

The RNA genome of HIV contains 9,747 nucleotides and is the most complex among all retroviruses studied so far (Figure 1-3).^{13,14} Of the nine genes that are encoded within the RNA genome, three provide genetic information for HIV's structural components. Each of these three genes encodes a large polyprotein precursor, which will be cleaved during the infection process to provide the final functional proteins. They are *gag*, which encodes a 55kDa polyprotein (Pr55^{Gag}) that will be cleaved into viral core proteins including MA, CA, NC and p6 (function is currently unclear); *pol*, which encodes the three vital enzymes (RT, PR, and IN) required for viral replication; and *env*, which encodes the 160kDa envelope glycoprotein (gp160) that will be broken down by a host-cell protease to form gp120 and gp41. The six remaining genes [*tat*, *rev*, *nef*, *vif*, *vpr*, and *vpu* (or *vpx* in the case of HIV-2 and SIV)] are regulatory genes that modulate the ability of HIV to infect cells, produce new copies of virus (replicate), or cause disease.¹⁵⁻¹⁷ *Tat* and *rev* are splitted genes, and are essential for viral replication. Their exons are spliced together during RNA processing. The other four genes are dispensable under certain circumstances and, consequently, have been named accessory genes. However, the existence of these gene encoded proteins is still important for the life cycle of HIV. For example, *nef* is necessary for the virus to replicate efficiently¹⁷, and *vpu* influences the release of new HIV-1 particles from infected cells¹⁸. Table 1-1 summarizes the functions of these HIV proteins. Both ends of the viral RNA strand contain an RNA sequence called the long terminal repeat (LTR). LTRs act as switches to control production of new viruses. The LTRs are not genes, but rather are direct

host cell enzymes that transcribe the biological information in proviral DNA into RNA during viral replication.¹⁹ They can be triggered by proteins from either HIV or the host cell.

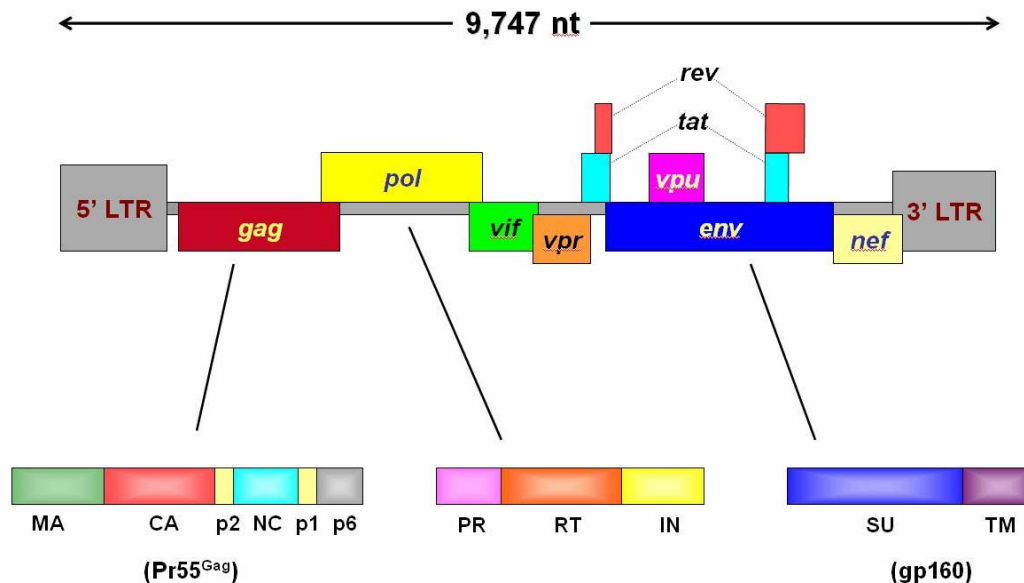


Figure 1-3. Genome of HIV-1

4. Life Cycle of HIV and Possible Anti-HIV Drug Targets

The life cycle of HIV has been and continues to be well studied in order to identify potential antiretroviral targets. The infection proceeds as described below. HIV entry into host cells is a complicated process mediated by the envelope glycoprotein (Env). The process involves at least three steps: (1) an initial attachment step in which cellular CD4 receptors bind with viral gp120 and cause a conformational change that allows the next step of co-receptor binding; (2) CCR5 and/or CXCR4 co-receptor binding with gp120, which results in a further conformational rearrangement and exposes the hydrophobic fusion domain of gp41;

and (3) a fusion process mediated by gp41.²⁰ Reportedly, some HIV strains can bypass CD4 binding and enter target cells via direct interactions with a co-receptor molecule *in vitro*.^{21,22} This CD4-independent infection route was possibly developed as an escape mechanism from inhibitors targeting CD4-binding.²³ However, CD4-independent infection is usually less efficient and more susceptible to neutralization.^{22,24} Numerous entry inhibitors targeting each of these three steps are in clinical and preclinical trials and will be reviewed in Chapter 2.

Once gp41 causes virus and cell membranes to fuse together, the viral capsid is released into the target cell. Within the cytoplasm, the capsid undergoes uncoating; a process that is largely unknown. During uncoating, the HIV RNA genome and various enzymes, including RT, IN, and PR, are injected into the cytoplasm.

Reverse transcription of the viral genomic RNA into the viral cDNA then occurs. This process is catalyzed by reverse transcriptase (RT). RT first mediates a RNA-dependent DNA polymerization reaction to transcribe the viral RNA into RNA-DNA hybrid molecules. The ribonuclease H (RNase H) domain of RT then degrades the RNA portion of the RNA-DNA hybrids. A subsequent RT-catalyzed DNA-dependent DNA polymerization reaction yields the viral double-strand DNA copy that is ready to be integrated into the target cell genome.²⁵ The first FDA-licensed anti-HIV drugs, such as AZT, inhibit RT and are still a critical part of AIDS treatment.

The viral double-strand cDNA produced by the reverse transcription step is translocated to the host cell nucleus where integration of the viral cDNA into the host

DNA genome takes place. The critical cutting and joining events leading to provirus formation are carried out by the viral integrase (IN).²⁶ IN catalyzes two distinct processes known as 3'-end processing and strand transfer. In detail, IN cleaves the 3'-end of the viral DNA to leave “sticky ends”. It also makes a cut in the host cell's DNA. At this cut, the HIV and cellular DNA can be stuck together as part of the cell's genome.²⁶ Because IN has no known homologues in human cells, it represents a valuable drug target for AIDS therapy. After the viral DNA is integrated into the genetic material of the host, HIV may persist in a latent state for many years, which is the major barrier to eradication or cure of HIV. Therefore, based on our current knowledge, patients must remain on antiviral therapy for life.

Following HIV integration, provirus gene expression is tightly controlled via the interplay of viral and multiple cellular factors. Viral proteins *tat* and *rev* are two regulatory proteins essential for HIV replication and have been widely investigated as potential targets.²⁵ However, inhibition of HIV gene expression may lead to significant host cell toxicity and may force the virus into a latent state.

After viral DNA is transcribed into viral messenger RNA (mRNA), mRNA is transported to the cytoplasm, where it is further translated into viral proteins by the cell's machinery. Once the Gag polyprotein precursors (Pr55^{Gag}) and Gag-Pol polyprotein precursors (Pr160^{Gag-Pol}) are translated, they recruit two copies of viral RNA and assemble with accessory proteins (*vif*, *vpr*, *nef*) to form the core virion near the inner face of the cell membrane.²⁷ The modified cell membrane containing envelope glycoproteins (Env) then surrounds the core particle and buds from the host

cell. This process leads to the production of immature non-infectious particles.

During or right after budding, the Gag and Gag-Pol polyproteins are cleaved. This cleavage is catalyzed by the third product of the *pol* gene – protease (PR). PR recognizes and cleaves Gag and Gag-Pol polyproteins at several specific sites to produce viral structural proteins [matrix (MA), capsid (CA), nucleocapsid (NC) and p6 proteins, as well as three *pol* products RT, IN and PR itself], which leads to the formation of a mature infectious HIV virion that can infect another target cell.²⁵ PR is one of the most exploited targets for the rational design of anti-HIV drugs. A novel recently discovered class of maturation inhibitors also focuses on blocking this step.

5. Approved Antiretroviral Therapy (ART)

Since the development of a safe and effective HIV vaccine has not yet been successful,²⁸ research on antiretroviral therapy (ART) continues to focus on chemical anti-HIV agents. Although all of the steps in the HIV life cycle can potentially serve as drug targets, current AIDS drugs fall mainly into three general categories: nucleoside/nucleotide RT inhibitors (NRTIs), non-nucleoside RT inhibitors (NNRTIs), and protease inhibitors (PIs). Current available HIV entry inhibitors include Fuzeon (enfuvirtide), which is a fusion inhibitor (FI) approved by the FDA in March 2003,²⁹ and Selzentry (maraviroc), which is a CCR5 co-receptor antagonist just approved in August 2007.³⁰ Lastly, the integrase strand transfer inhibitor Isentress (raltegravir) was approved in October 2007.³¹ (Table 1-2)

Table 1-2. US FDA approved anti-HIV drugs (brand names, generic names and abbreviation) *

NRTIs	NNRTIs	PIs	Entry Inhibitors	Integrase Inhibitors
Emtriva (emtricitabine, FTC)	Rescriptor (delavirdine, DLV)	Agenerase (amprenavir, APV)	Fuzeon (enfuvirtide, ENF, T20)	Isentress (raltegravir)
Epivir (lamivudine, 3TC)	Sustiva (efavirenz, EFV)	Aptivus (tipranavir, TPV)	Selzentry (maraviroc)	
Hivid (zalcitabine, ddC)	Viramune (nevirapine, NVP)	Crixivan (indinavir, IDV)		
Videx (didanosine, ddI)	Intelence (etravirine)	Invirase (saquinavir mesylate, SQV)		
Viread (tenofovir, TDF)		Lexiva (fosamprenavir, FPV)		
Zerit (stavudine, d4T)		Norvir (ritonavir, RTV)		
Ziagen (abacavir, ABC)		Prezista (darunavir)		
Retrovir (zidovudine, AZT + azidothymidine, ZDV)		Kaletra (lopinavir, LPV + ritonavir, RTV)		
Combivir (AZT+3TC)		Reyataz (atazanavir, ATV)		
Epzicom (ABC+ 3TC)		Viracept (nelfinavir, NFV)		
Trizivir (ABC+AZT+3TC)				
Truvada (TDF+FTC)				

* Until January 2008

5-1. NRTIs

NRTIs (Figure 1-4) mimic the structures of the base substrates for DNA synthesis. They interact at the substrate-binding site of RT and act as chain terminators.³² For example, AZT, a deoxythymidine analog, was the first successful NRTI for the treatment of HIV infection. It is phosphorylated by cellular enzymes to AZT-triphosphate (AZT-TP), which is recognized by RT in place of the normal deoxyribonucleoside triphosphates, dNTPs, and competitively incorporated into the DNA strand. Because the 3'-hydroxy is replaced by an azide moiety, AZT-TP cannot form the normal 3' to 5' phosphodiester bond. Therefore, elongation of the growing DNA chain is interrupted and viral replication is inhibited.

Viread (tenofovir disoproxil fumarate, TDF) represents the first nucleotide analog approved for HIV-1 treatment.³³ TDF is hydrolyzed to tenofovir *in vivo*, and then phosphorylated by cellular kinases to its active metabolite tenofovir diphosphate. It then competes for incorporation into viral DNA and acts as a chain elongation terminator because it lacks a ribose ring.³³

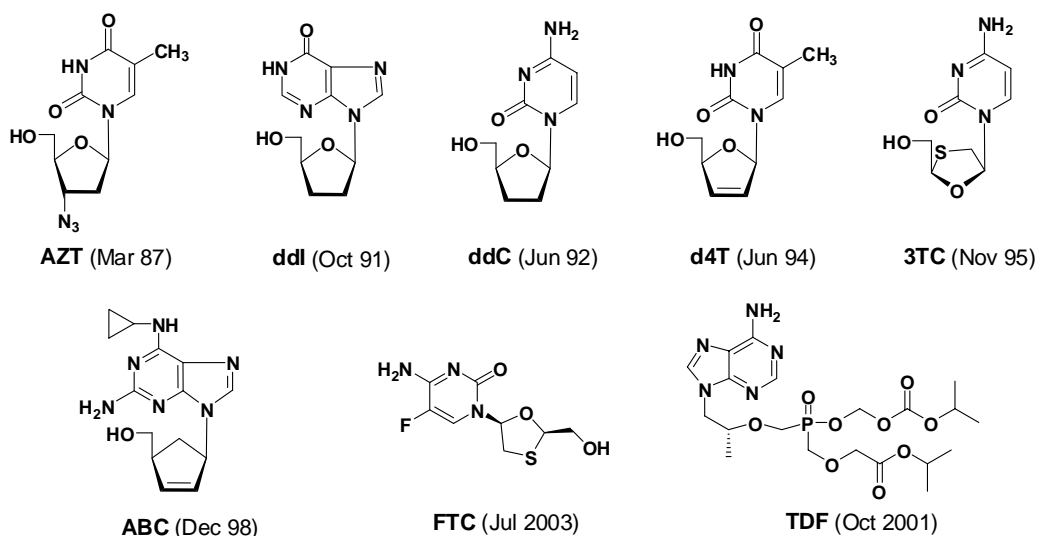


Figure 1-4. US-FDA approved NRTIs (date of approval)

5-2. NNRTIs

NNRTIs (Figure 1-5) inactivate RT by non-competitive interaction with an allosteric site of the enzyme. This highly hydrophobic binding pocket of NNRTIs is near to, but distinct from, the polymerase active site in the p66 subunit of RT.²⁵ The binding of NNRTIs does not interfere with RT binding of dNTPs, but does rearrange the enzyme into an inactive conformation that slows down the rate of incorporation of dNTPs into the DNA product.³⁴ NNRTIs preferentially inhibit RNA-dependent DNA polymerization. An obvious disadvantage of NNRTIs is that drug resistance can emerge quickly due to rapid mutation of the RT amino acid residues surrounding the NNRTI-binding site.³⁵

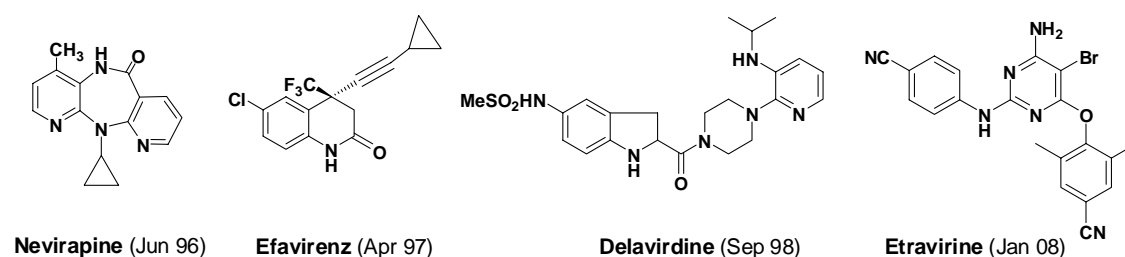


Figure 1-5. US-FDA approved NNRTIs (date of approval)

5-3. PIs

HIV-1 and HIV-2 proteases display similar structural features and belong to the aspartic protease group of enzymes. The HIV-1 protease is a homodimer stabilized by non-covalent interactions; each monomer has a 99-amino acid residue subunit. Each subunit contributes a conserved triad (Asp-Thr-Gly), which contains the catalytically active Asp25.²⁵ These active aspartates are located at the dimer interface.

PIs (Figure 1-6) bind tightly to the protease surface by mimicking the structures of the proteolysis sites of Gag and Gag-Pol polyproteins. By binding to the active sites, PIs prevent protease from cleaving the viral polyprotein precursors into mature viral structural proteins and functional enzymes, resulting in the suppression of viral replication and production of immature noninfectious virions.³⁶

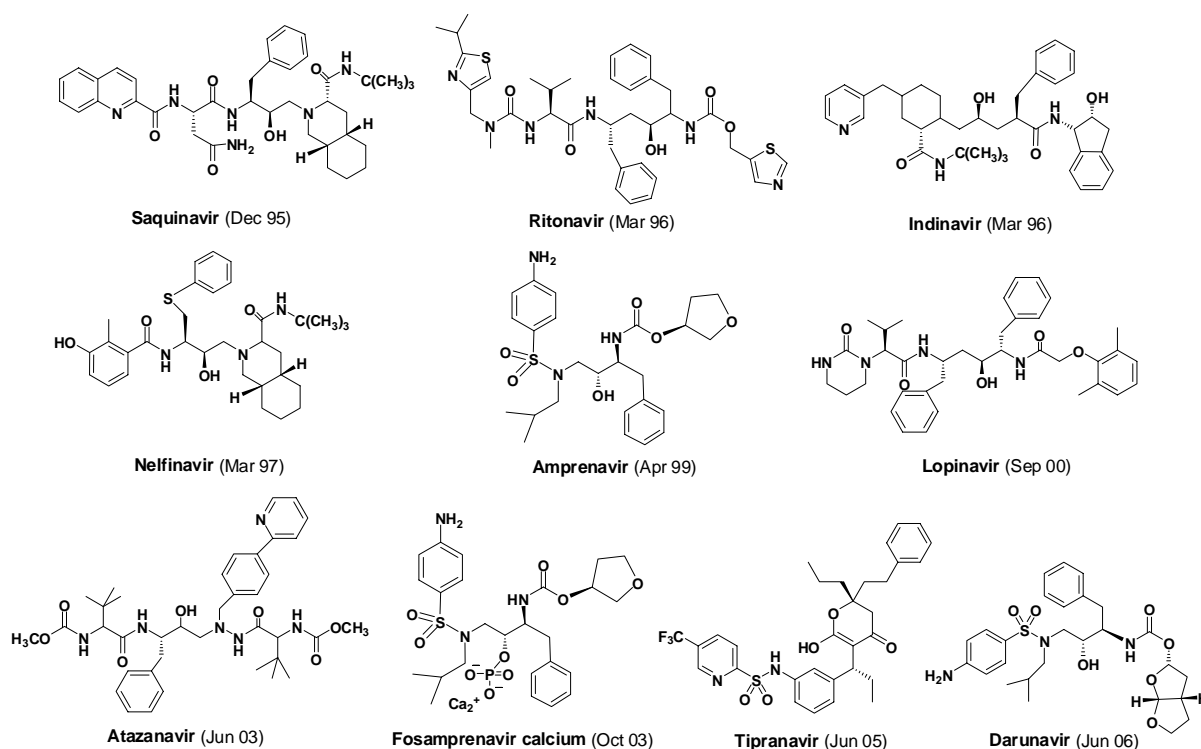
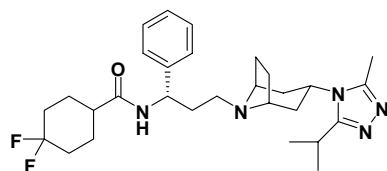


Figure 1-6. US-FDA approved PIs (date of approval)

5-4. Entry Inhibitors

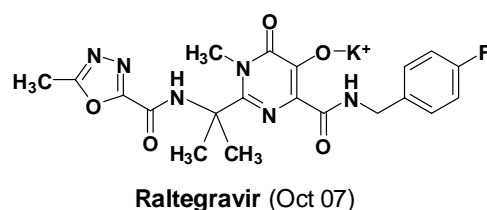


Maraviroc (Aug 07)

As previously described, viral entry is a complicated multi-step process. Inhibitors that target one or more of these steps can potently affect viral replication. Currently, there are two FDA approved HIV entry inhibitors. Fuzeon (enfuvirtide,

ENF, T20) is a synthetic peptide with 36 amino acid residues. It functions as a fusion inhibitor (FI).²⁹ Selzentry (maraviroc, MVC, UK-427,857) is an orally bioavailable CCR5 co-receptor antagonist.³⁰ Their detailed mechanisms will be reviewed in Chapter 2.

5-5. Integrase Inhibitors



Isentress (Raltegravir, MK-0518, Merck. Inc) is the first in a new class of orally administered HIV-1 integrase (IN) inhibitors. This compound selectively inhibits the strand transfer activity of IN and consequently inhibits viral cDNA integration into human DNA.³¹ It was approved by the US FDA in October 2007 for treatment of antiretroviral-resistant HIV-1 infected individuals with 400 mg twice daily dosing via oral administration.³¹

6. HAART and Associated Problems

Significant progress has been made in the development of antiretroviral therapy (ART). ART can successfully delay destruction of the immune system, reduce severity and frequency of opportunistic infections, and consequently delay AIDS progression. Introduction of highly active antiretroviral therapy (HAART), which employs a combinational use of drugs with different mechanisms, can reduce viral load to below detectable levels in patient plasma, resulting in improved patient health

and life span.³⁷⁻³⁹ However, the virus is suppressed rather than eradicated by HAART.⁴⁰⁻⁴² On HAART regimens, multiple drug therapies can lead to increased adverse effects and toxicities due to long-term use and drug-drug interactions.^{43,44} Moreover, inadequate clinical viral suppression of HIV-1, due to various reasons, and the high error rate of the reverse transcriptase can lead to the emergence of drug-resistant and multi-drug-resistant viral strains.⁴⁵ Drug-resistant virus is then involved in HIV transmission, and more than 25% of newly infected individuals harbor HIV-1 isolates that are resistant to at least one ART.^{46,47} Therefore, novel potent antiretroviral agents, which have simplified treatment regimens (fewer pills and less-frequent administration) and target different steps of viral life cycle, may hold particular promise in addressing issues of current therapies.

Chapter 2. HIV Entry Inhibitors and Triterpene Derivatives as Anti-HIV Agents – A Review

1. Introduction

HIV entry into host cells is a complicated multi-step process. Virions can first attach to target cells in a relatively nonspecific manner, followed by specific binding of HIV gp120 to the CD4 receptor on the cellular membrane. This binding induces a conformational change in gp120 that opens up a high-affinity binding site located within the third variable loop (V3) and surrounding surfaces for the chemokine co-receptors (primarily CCR5 and CXCR4).⁴⁸ Co-receptor binding results in further conformational rearrangements of gp120 that expose the fusion-peptide domain of gp41. Insertion of this hydrophobic domain into the cell membrane leads to the formation of a hairpin-like fold in the gp41 subunits.²⁰ The heptad repeat (HR) regions, HR1 and HR2 of the three subunits of gp41, fold and pack into a six-helix bundle, which brings the viral and cell membranes into juxtaposition and creates pores in the target cell membrane, enabling the release of viral capsid into the cytoplasm.⁴⁹⁻⁵¹ Different entry inhibitors that target one or more of these steps are now in preclinical and clinical trials. Entry inhibitors, especially potent, orally bioavailable small molecules are very promising for development as therapeutic antiviral drugs. Herein, we review their development, mechanisms of action, and

possible role in anti-HIV therapy.

2. Attachment Inhibitors

2-1. Nonspecific Attachment Inhibitors

Before gp120 and CD4 receptor binding firmly attaches HIV onto the target cells, less specific adsorption and attachment occur between the virions and cell membrane due to the interaction of the positively charged regions of Env with oppositely charged proteoglycans of the cell surface.^{52,53} Studies have reported that soluble polyanions, such as dextran sulfate, cyclodextrin sulfate and heparin, can block this nonspecific attachment of HIV virions.⁵⁴

Cyanovirin-N (Cellegy Pharmaceuticals), an 11kDa protein isolated from the cyanobacterium (blue-green algae) *Nostoc ellipsosporum*, specifically binds to a conserved high-mannose carbohydrate region on gp120, which prevents the attachment of virus to target cells at low nanomolar concentrations.⁵⁵⁻⁵⁷ Another example is PRO 2000 (Indevus Pharmaceuticals), a naphthalene sulfonate polymer (**1**) (Figure 2-1), which binds nonspecifically to CD4 receptor. Vaginal PRO 2000 gel has been effective and well tolerated in Phase I/II clinical trials.^{58,59} However, because of their mechanism of action and polymer properties, these two compounds are mainly being developed as topical microbicides.

Glycyrrhizin (**2**) (Figure 2-1), a triterpenoid saponin isolated from licorice root inhibits HIV-1 replication by partially blocking viral adsorption to CD4+ cells.⁶⁰ Sulfation of glycyrrhizin (**3**), amphotericin B, and lentinan, as well as polysulfonates

[e.g., suramin (**4**)] and polyhydroxycarboxylates [e.g., aurintricarboxylic acid (**5**)] also interfere with the nonspecific viral attachment process (Figure 2-1).

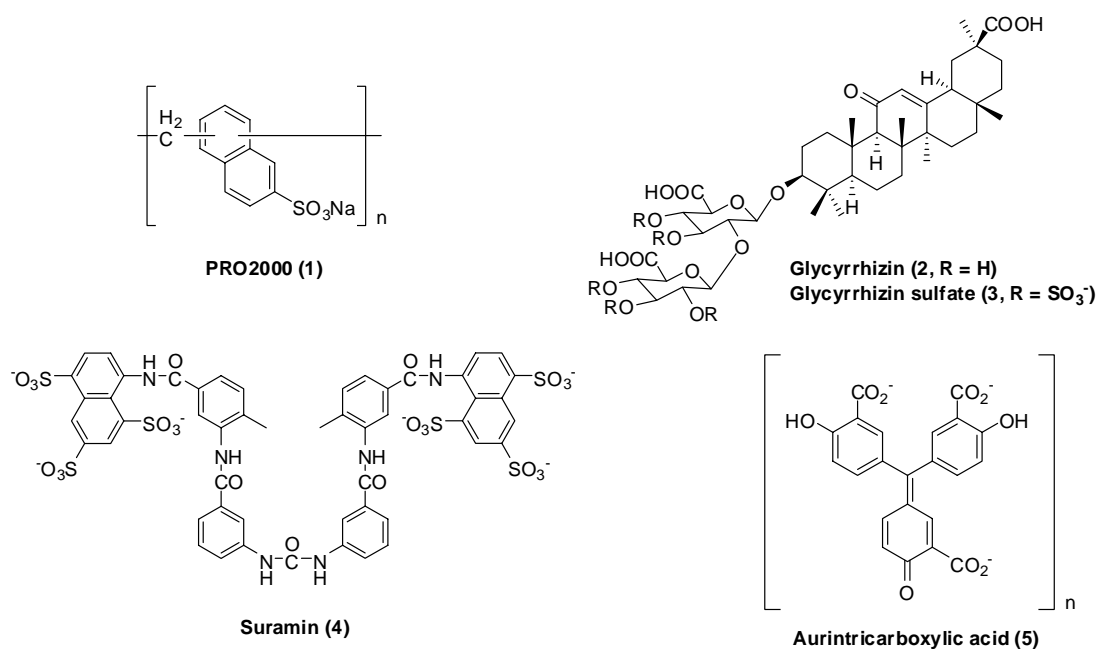


Figure 2-1. Structures of some selected sulfated compounds as HIV nonspecific attachment inhibitors

2-2. CD4-gp120 Binding Inhibitors

Many molecules can inhibit CD4 and gp120 binding via different modes of action, including inhibition of attachment by targeting Env gp120 or CD4 receptor, prevention of necessary conformational rearrangement, and down-regulation of CD4 expression.

PRO 542 (Progenics Pharmaceuticals) is a recombinant tetrameric CD4-IgG2 antibody-like fusion protein. It targets the CD4 binding site on gp120 by mimicking the CD4 receptor. In Phase I clinical trials, PRO 542 reduced viral load after a single intravenous dose and was well tolerated in infected adults and children.^{61,62}

TNX 355 (Tanox Inc.) is a humanized IgG4 monoclonal antibody against CD4,

which binds to the D2 domain of CD4 and inhibits CD4-induced post-binding conformational changes.⁶³ Phase I clinical studies concluded that TNX 355 reduced plasma HIV-1 RNA loads and increased CD4+ T-cells.⁶⁴ However, the need for infusion limits its clinical use.

BMS-378806 (**6**) and BMS-488043 (**7**) (Bristol-Myers Squibb) (Figure 2-2) are novel, small-molecule CD4-attachment inhibitors that specifically block HIV-1 entry by targeting Env gp120 with an EC₅₀ value of around 5 nM.^{65,66} Mechanism of action study revealed that both compounds selectively bind to gp120 and lead to conformational changes in gp120 at both the CD4 and CCR5 binding regions, which blocks CD4-gp120 interactions. Prior addition of soluble CD4 to the assay system before BMS-488043 treatment negates the inhibition activity of the compound, indicating that inhibition of CD4-gp120 binding is the primary mode of action.⁶⁷ An earlier report by Si *et al.* suggested that BMS analogs function by blocking conformational changes of gp120 after CD4 binding rather than by directly inhibiting CD4 binding;⁶⁸ however, a significantly altered Env structure and high concentrations of soluble CD4 may have led to this conclusion.⁶⁷ Drug development of BMS-378806 was discontinued after Phase I clinical study, because target exposure was not achieved. BMS-488043 is currently in Phase II clinical trials.⁶⁹ It is orally bioavailable with superior pharmacokinetic properties and good safety profiles. The New York Blood Center identified similar structures, NBD-556 (**8**) and NBD-557 (**9**) (Figure 2-2), which also contain an oxalamide moiety. These two compounds showed micromolar potency against HIV-1.⁷⁰ Compounds **10** and **11** (Figure 2-2) disclosed by

Pfizer Inc. in patents (WO-2005016344 and WO-2005121094) also share similar structures with BMS analogs and have nanomolar anti-HIV activity.⁶⁹

CADA analogs (cyclotriazadisulfonamide) (**12**) (Figure 2-2) reportedly inhibit HIV replication by down-regulating CD4 expression at a post-translational step.⁷¹⁻⁷³ This category of compounds showed anti-HIV entry activity at micromolar concentrations.⁷⁴

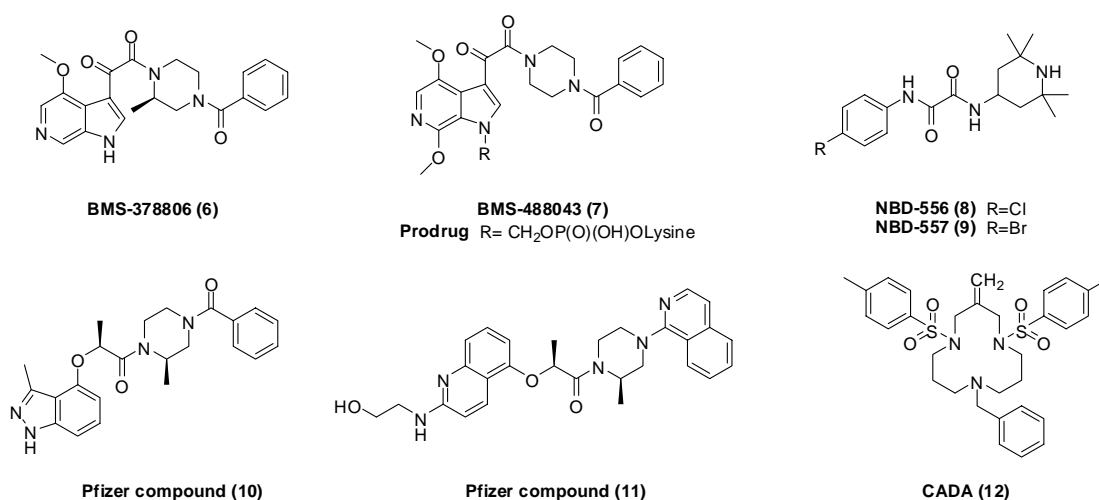


Figure 2-2. Selected structures of CD4-gp120 binding inhibitors

3. Co-receptor Binding Inhibitors

Chemokine receptors belong to the seven transmembrane G protein coupled receptor family. They are involved in the progression of many diseases, including rheumatoid arthritis, transplant rejection, asthma, cancer, HIV, and others. CCR5 and CXCR4 are the main chemokine receptors involved in the HIV entry process.⁷⁵ Based on their chemokine receptor usage, HIV isolates may be divided into R5, X4, and R5/X4 strains.⁷⁶ R5 isolates are the predominant virus strains, which are preferentially transmitted between HIV-infected patients.⁷⁷ However, R5 variants will eventually

develop into R5/X4 isolates in approximately 50% of HIV-1 positive individuals, resulting in increased viral replication rate, faster disease progression, and the onset of AIDS.⁷⁸

During the HIV entry process, the CD4-gp120 complex must further bind to chemokine co-receptors through the gp120 V3 region in order to enter the target cells.⁷⁹ V3 amino-acid sequences determine the usage of CCR5 or CXCR4.⁸⁰ Epidemiology data shows that individuals homozygous for $\delta 32$ CCR5 allele (no expression of CCR5 on cell surface) are highly resistant to HIV infection^{81,82} and apparently healthy. This fact highlights the merits of targeting co-receptor binding to inhibit HIV entry.

3-1. CCR5 Inhibitors

The CCR5 co-receptor binding site on HIV gp120 is concealed by V1, V2, and V3. The conformational change caused by the binding of gp120 with CD4 exposes this CCR5 binding site. When a CCR5 inhibitor is present, binding of the CCR5 N-terminus and ECL2 (second extracellular loop) with the V3 stem of gp120 is blocked, resulting in inhibition of viral entry⁵⁶ The strategies to block CCR5 co-receptor binding include modified non-agonistic CCR5 chemokine natural ligands, CCR5 small molecule antagonists, and CCR5 antibodies.

RANTES (**13**) was discovered as the natural β -chemokines ligand, which can compete with gp120 to bind the CCR5 co-receptor,⁸³ and thus, inhibit HIV infection. However, it also triggers CCR5-mediated down-stream signaling pathways, which

may lead to undesired side effects. Modification of **13** led to the discovery of PSC-RANTES (**14**), which is developed as a potential microbicide⁸⁴ (Figure 2-3).

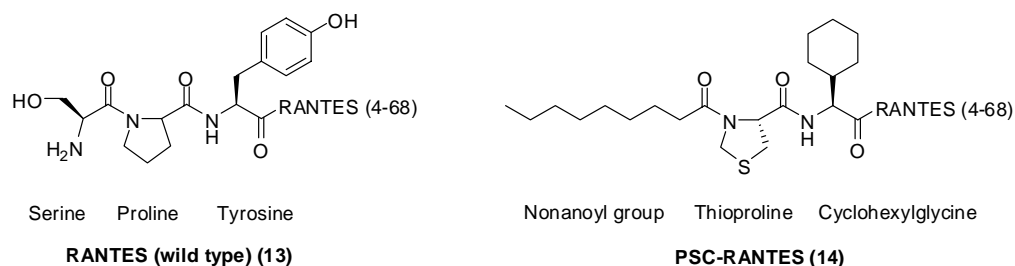


Figure 2-3. Structures of modified chemokine derivatives as HIV inhibitors

PRO 140 (Progenics Pharmaceuticals) is another promising large molecule CCR5 co-receptor binding inhibitor. It is a murine anti-CCR5 monoclonal antibody that binds a complex epitope spanning multiple extracellular domains on CCR5.⁸⁵ PRO 140 demonstrates a potent and genetic-subtype-independent anti-HIV-1 activity and is currently in Phase II clinical trials.

Because large molecules are often difficult to administer, their clinical application may be limited. Therefore, the search for orally bioavailable small molecule inhibitors remains of great interest. This search has led to the discovery of many small molecule CCR5 antagonists, which are very promising for development as therapeutic antiviral drugs.

TAK-799 (Takeda Chemical Industries) (**15**) (Figure 2-4) is the first reported nonpeptide small molecule that antagonizes the binding of RANTES to CCR5-expressing Chinese hamster ovary cells at nanomolar concentrations (1.6-3.7nM).⁸⁶ TAK-799 selectively inhibits CCR5 within the chemokine receptor family by binding inside a cavity formed by the transmembrane helices 1, 2, 3, and 7

of the CCR5 receptor.⁸⁷ Although it showed no cytotoxicity to the host cells, lack of oral bioavailability limits its further development. Clinical trials of an injectable quaternary ammonium salt TAK-799 were discontinued due to local reactions at injection sites. Modification of TAK-799 by replacing the quaternary ammonium moiety with a polar sulfoxide moiety led to the discovery of TAK-652 (**16**)⁸⁸ (Figure 2-4). TAK-652 showed increased anti-HIV-1 activity against different clinical HIV subtypes with a mean EC₅₀ value of 0.25 nM. More importantly, it has oral bioavailability and is well absorbed after oral administration in different preclinical animal studies. TAK-652 is currently in Phase I/II clinical trials. Additional high throughput screening against CCR5 in the same company led to the discovery of a different compound skeleton exemplified by **17** (Figure 2-4), which exhibits nanomolar anti-HIV-1 activity. However, **17** was rapidly degraded in metabolic stability studies. Continuing modification resulted in the identification of TAK-220 (**18**)⁸⁹ (Figure 2-4), an orally bioavailable, metabolically stable piperidine-4-carboxamide derivative, which is also in clinical studies.

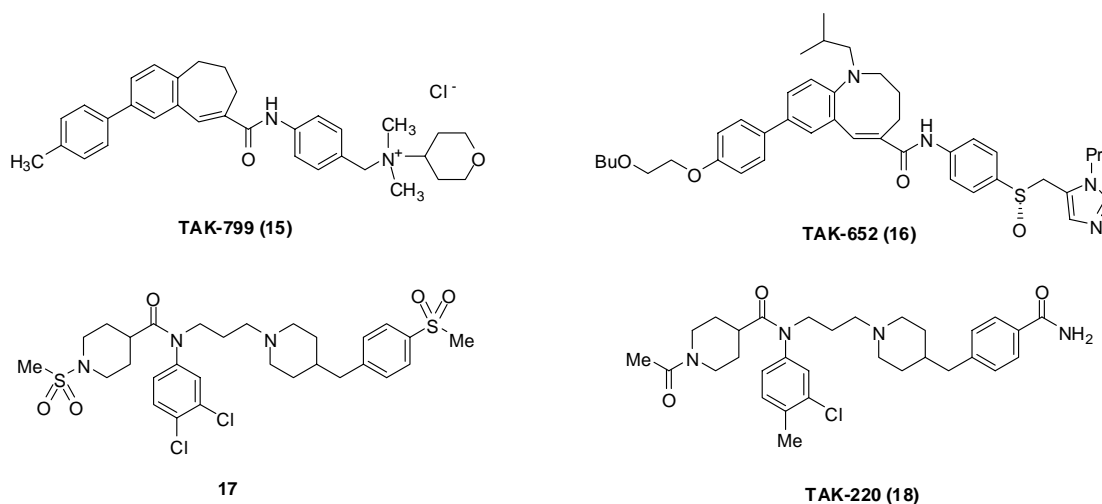


Figure 2-4. Structures of TAK analogs

Maraviroc (MVC, UK-427,857, Pfizer) (**19**) (Figure 2-5) is another selective CCR5 antagonist with potent antiviral activity against all CCR5-tropic HIV-1 viruses at low nanomolar concentrations (mean 90% inhibitory concentration of 2.0 nM)⁹⁰ It was obtained by medicinal chemistry optimization of a high throughput screening lead, the imidazopyridine derivative UK-107,543 (**20**)⁹⁰ (Figure 2-5). The initial modification of **20** by introducing an amide bond into the structure (**21**) (Figure 2-5) solved the high lipophilicity problem of the lead.⁹¹ Later study revealed that only the S enantiomer of **21** showed good potency. However, this type of piperidine-based CCR5 antagonist is also a potent CYP 2D6 inhibitor, which may create problems with drug-drug interactions in drug combinational use. Further development led to the discovery of tropane-based compound **22** (Figure 2-5), which does not inhibit CYP 2D6 liabilities, but retains high potency towards CCR5⁹². Unfortunately, **22** is also a potent inhibitor of the hERG ion channel. This undesired side effect was successfully conquered by replacing the benzimidazole group with a triazole moiety and replacing the cyclobutyl group with a difluorocyclohexane moiety, which resulted in the identification of Maraviroc (**19**).⁹³ Mechanism of action study revealed that **19** binds to the cavity formed by the transmembrane helices 2, 3, 6, and 7 of CCR5 receptor, which is different with the binding site of TAK-799⁹⁴. Thus, **19** does not compete with chemokine binding and does not affect associated intracellular signaling.⁹⁰ In clinical trials, it was administered orally with twice-daily dosing. In August 2007, **19** was approved by the US FDA as a CCR5 antagonist HIV entry inhibitor under the brand name Selzentry.

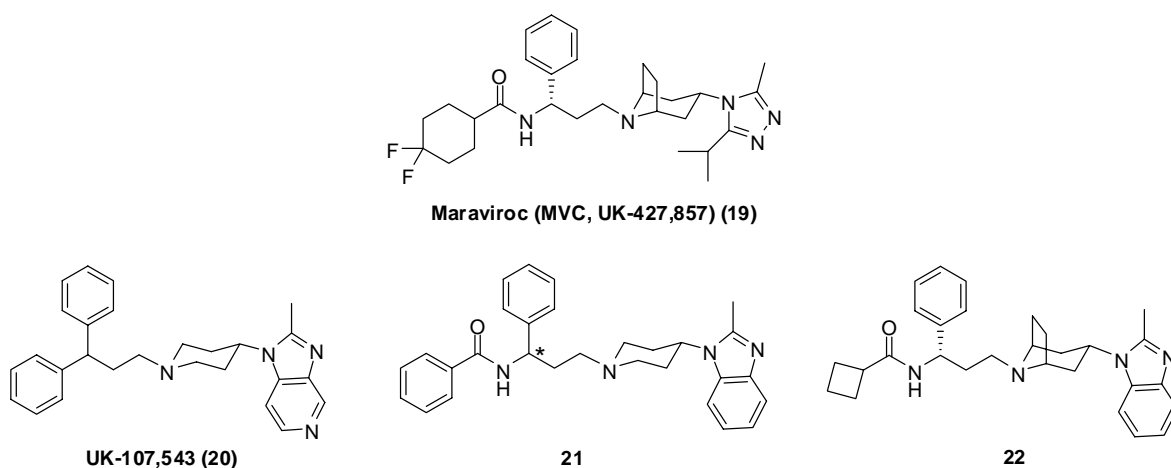


Figure 2-5. Lead optimization and identification of Maraviroc

Vicriviroc (SCH-D, SCH-417,690, Schering-Plough) (**23**) (Figure 2-6), a piperazine-based CCR5 antagonist, is also currently in Phase III clinical study. It is a second-generation compound with improved anti-HIV activity and pharmacokinetic profile compared with the first-generation Ancriviroc (SCH-C, SCH-351,125, Schering-Plough) (**24**) (Figure 2-6), a piperidino-piperidine derivative.^{95,96} Both compounds are orally bioavailable and interact within the cavity formed by CCR5 transmembrane regions, resulting in inhibition of HIV gp120 binding.⁹⁷ Compound **24** was discovered first by modification of a high throughput screening lead. However, later study revealed that high doses of **24** led to CNS side effects and acute CV [prolongations in the QT cardiac interval (time between depolarization and repolarization of the heart muscle adjusted for heart rate)].⁹⁶ The clinical studies of **24** were then discontinued. Within the piperazino-piperidine series, replacing the N-oxide of **25** by 4,6-dimethylpyrimidine carboxamide as in **26** (Figure 2-6) resulted in better CV profiles.⁹⁵ Further optimization of **26** led to the discovery of Vicriviroc (**23**),

which has potent, broad-spectrum antiviral activity against diverse HIV-1 subtypes and synergistic anti-HIV activity in combinational use with drugs from other classes. Another promising candidate in the piperazino-piperidine family is AD101 (SCH-350,581) (**27**) (Figure 2-6), which also shows potent anti-HIV-1 activity by blocking gp120/CD4 complex and CCR5 interaction. AD101 is currently in preclinical study.⁹⁸

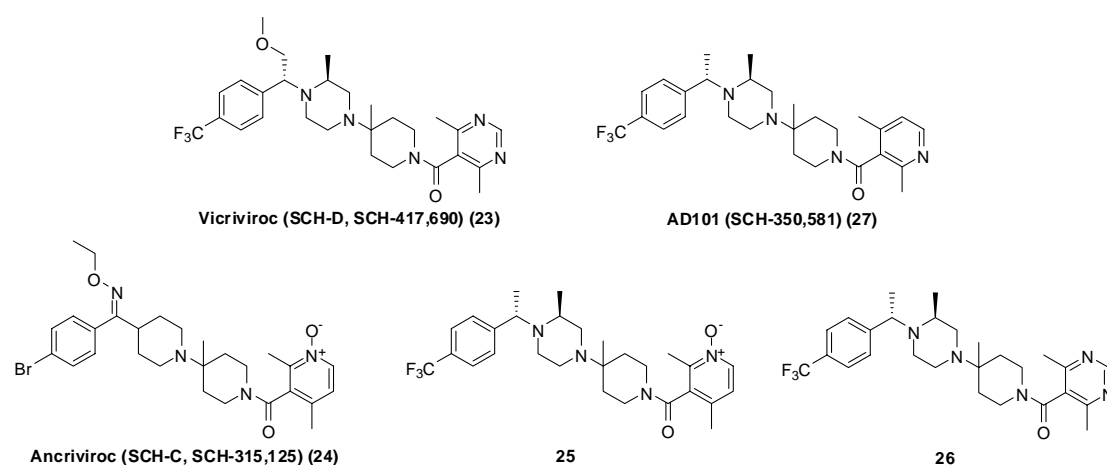


Figure 2-6. Structures of Vicriviroc and Ancriviroc analogs

INCB9471 (Incyte Corporation) (**28**) (Figure 2-7) is another promising candidate in Phase II clinical trials. It also belongs to the piperazino-piperidine family. The similar structures of INCB9471 and Vicriviroc suggest that they might share the same mechanism of action. INCB9471 is an orally bioavailable CCR5 antagonist with very potent antiviral activity against a wide range of HIV-1 strains, including drug resistant isolates.⁹⁹

Aplaviroc (GW873140, formerly ONO4128, AK602, GlaxoSmithKline) (**29**) (Figure 2-7) failed in Phase II clinical trials in October 2005, due to unexpected serious hepatotoxicity. It belongs to the spirodiketopiperazine family and exhibits

potent antiviral activity with EC₅₀ values around 0.1-0.6 nM.¹⁰⁰ Aplaviroc exerts its antiviral function by interacting with CCR5 ECL2 rather than binding to the CCR5 transmembrane cavity, which is distinct from other CCR5 antagonists.^{100,101}

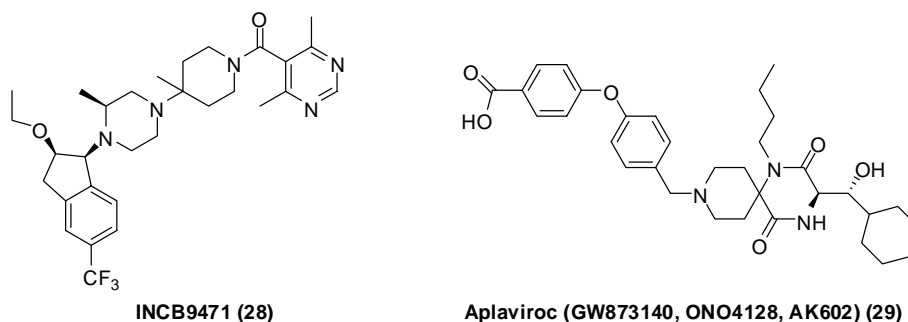


Figure 2-7. Structures of INCB9471 and Aplaviroc

Other classes of compounds have also been reported to be CCR5 antagonists. GlaxoSmithKline filed a patent (WO2004054974) describing some newly discovered anti-HIV-1 CCR5 antagonists. Among these compounds, GSK 163929 (**30**) (Figure 2-8) showed nanomolar level inhibition activity towards HIV replication and successfully completed preclinical studies.¹⁰² NSC651016 (**31**) (Figure 2-8) inhibits chemokine binding of CCR5, CXCR4, CCR1 and CCR3, but does not interact with CXCR2 or CCR2b. It inhibits a wide range of HIV-1 variants and HIV-2 isolates, and could be developed as a topical microbicide.¹⁰³ Shikonin (**32**) (Figure 2-8), a major component of purple gromwell (zicao, dried root of *Lithospermum erythrorhizon*) is a CCR5 chemokine antagonist with sub-micromolar level antiviral activity.¹⁰⁴ Merck reported the discovery of several compounds (**33-37**) (Figure 2-9) with potent CCR5 binding affinity. However, the anti-HIV activities of these compounds are only moderate.¹⁰⁵⁻¹⁰⁸

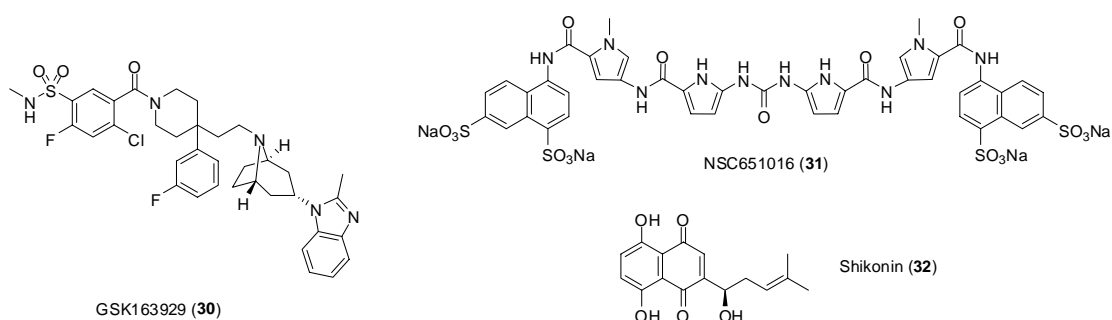


Figure 2-8. Selected promising CCR5 antagonists as anti-HIV agents

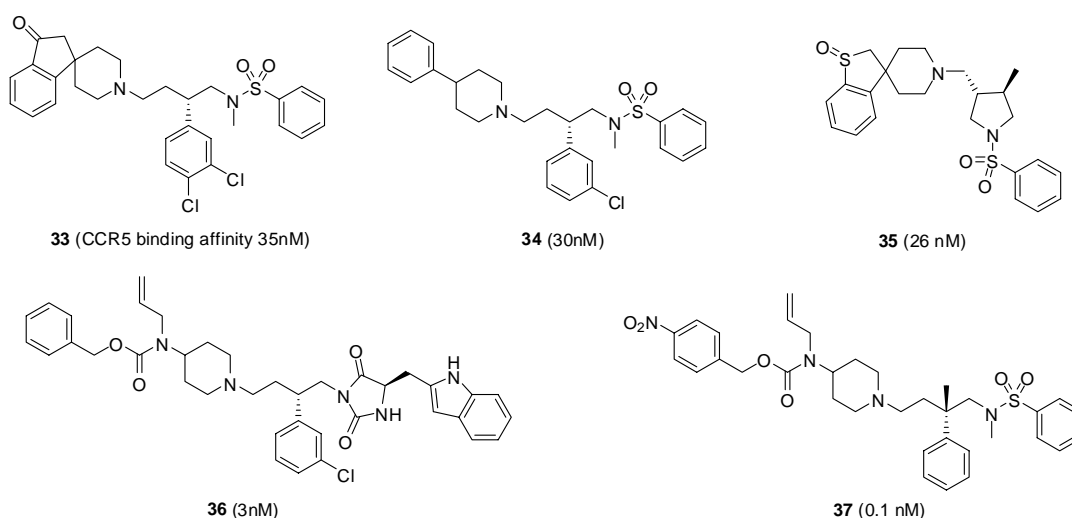


Figure 2-9. Merck analogs showing potent CCR5 binding affinity

3-2. CXCR4 Inhibitors

Although the deletion of CCR5 has little impact on an individual's health, CXCR4 is involved in a number of physiological processes. In a mice knockout study, knocking out either CXCR4 or its only known natural ligand SDF-1 (stromal cell-derived factor) resulted in abnormal cerebral development and was embryonically lethal.^{109,110} Whether CXCR4/SDF-1 is vital only in embryonic development needs to be further determined. Deletion of SDF-1 also caused defects in B-cell lymphopoiesis and bone marrow myelopoiesis in mice.¹¹¹ These findings make CXCR4 antagonists

less feasible. However, although R5 variants are dominant in initial HIV transmission, a switch in co-receptor use occurs after transmission, and the virus gains ability to use both R5 and X4 during AIDS progression.⁷⁸ Therefore, CXCR4 antagonists are still necessary. The ideal CXCR4 antagonist should block HIV entry without affecting CXCR4 down-stream signaling pathways or causing CXCR4 internalization.

The initial strategy for developing CXCR4 antagonists also focused on mimics of the CXCR4 natural ligand SDF-1. In addition to large molecule polypeptides, several small molecule CXCR4 antagonists are also under development. AMD3100 (AnorMED Inc., now Genzyme Corporation) (**38**) (Figure 2-10) is a low molecular weight bicyclam analog with potent anti-X4 HIV variant activity ($EC_{50} \sim 1.4$ nM).¹¹² Its development was terminated when abnormal cardiac activity was observed in Phase II clinical studies. The second generation cyclam analog AMD3465 (**39**) (Figure 2-10) has only one cyclam unit; the other is replaced by N-pyridinylmethylene.¹¹³ However, although the antiviral activity of **39** is slightly better than that of **38**, it still lacks oral bioavailability. The mechanism of action of cyclam analogs is related to the multiple positive charges associated with the basic nitrogen atoms,¹¹⁴ which interact with negatively charged acidic residues in CXCR4. Studies showed that residues D171, D262, and E288 are important in CXCR4 binding by **38**.¹¹⁴ The third generation AMD070 (AMD11070) (**40**) (Figure 2-10) is structurally different from the prior analogs and is also orally bioavailable.¹¹⁵ It is highly specific for the CXCR4 receptor. Compounds **38** and **40** have similar binding sites¹¹⁴ and exhibits similar antiviral activity against a broad range of X4 and R5X4

isolates, but are not active against R5 strains. Compound **40** is currently in Phase II clinical trials.

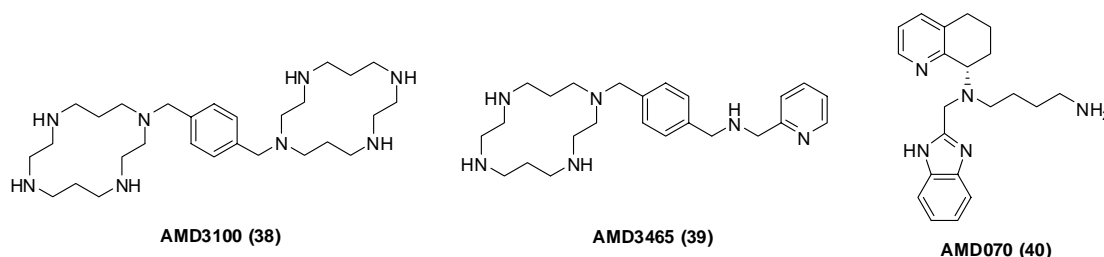
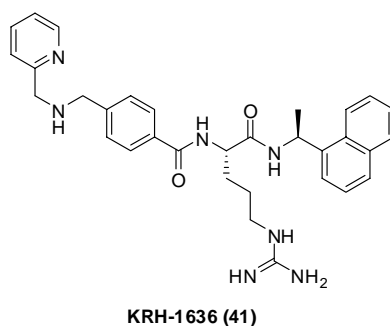


Figure 2-10. Structures of AMD analogs

KRH-1636 (Kureha Chemical Industries) (**41**) is an arginine-based CXCR4 antagonist with good anti-HIV-1 activity ($EC_{50} \sim 42\text{nM}$).¹¹⁶ It was obtained from optimization of a high throughput screening lead. It can be absorbed after intraduodenal administration to rats, suggesting that it may be orally bioavailable.¹¹⁶ Further modification led to the discovery of KRH-2731·5HCl (structure has not been released), which is a **41**-analog with improved antiviral potency ($EC_{50} = 1.0\text{nM}$) against X4 and R5X4 HIV isolates.¹¹⁷ KRH-2731·5HCl is orally bioavailable. Mechanism of action study revealed that it binds to ECL2 and ECL3 (second and third extracellular loops) of the CXCR4 receptor.⁸⁰



4. Fusion Inhibitors

As previously mentioned, the binding of CD4/gp120 complex with a

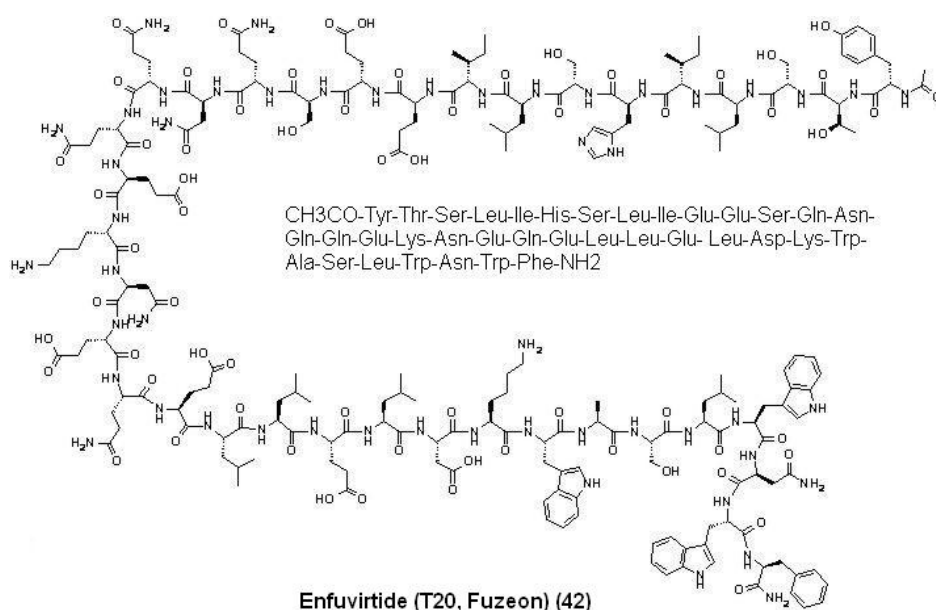
chemokine co-receptor leads to a conformational rearrangement in gp120 that enables gp41 to reorient parallel to viral and cellular membranes and expose a highly hydrophobic fusion-peptide (FP) region of trimeric gp41, which will later insert into the cell membrane. FP is located at the N-terminus of gp41, adjacent to two heptad repeats (HRs). During the fusion process, HR1 and HR2 form a thermostable, six-helix bundle structure.⁵¹ The change in free energy associated with this critical step provides the force needed for formation of the fusion pore, through which the viral capsid is released into the target cell.⁵¹

4-1. Large Molecule Fusion Inhibitors

As early as the 1990s, researchers realized that synthetic peptides based on the HR1 and HR2 sequences of gp41 have anti-HIV properties.^{118,119} The mechanism of action of this oligopeptide class is believed to be competitive binding of the synthetic peptides with the corresponding HR regions, which is also called the “dominant-negative inhibition model”.¹²⁰

Until now, fusion inhibitors have been the most successful class of HIV entry inhibitors. Enfuvirtide (T20, Fuzeon, Trimeris/Roche) (**42**) was approved for use in combination with other ARTs in treatment-experienced patients in March 2003 by the US FDA.^{121,122} It is a 36-amino acid synthetic peptide that mimics the HR2 region (residues 127 to 162 in C-terminal) of gp41.¹²² By competitively binding to the HR1 region of gp41, **42** prevents the formation of the six-helix bundle structure that is critical as the energy source for the fusion process.¹²³ Compound **42** shows good

antiviral potency and long-term safety in clinical use. A synergistic effect has also been observed in its combinational use with other ARTs. However, it is administered by subcutaneous injection of 90 mg twice daily, which is highly inconvenient. Moreover, inhibitor-naïve primary HIV-1 isolates exhibited wide ranging susceptibilities to **42**, and the compound has a relatively low genetic barrier for resistance.¹²⁴ Thus, enfuvirtide is considered only a second-line antiretroviral agent.

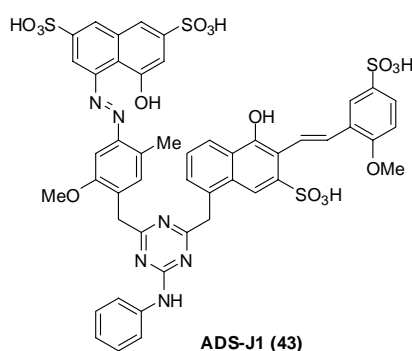


The second-generation fusion inhibitor Tifuvirtide (T-1249) shows tenfold more potent antiviral activity compared with **42**.¹²⁵ It preserves antiviral efficacy to **42**-resistant HIV-1 isolates as well as HIV-2 and SIV variants,¹²⁵ and is a 39-amino acid peptide mimicking a different region of HR2.¹²⁶ However, its clinical development was halted due to formulation challenges.¹²⁷

4-2. Small Molecule Fusion Inhibitors – Recent Progress with Triterpene Derivatives as HIV Inhibitors

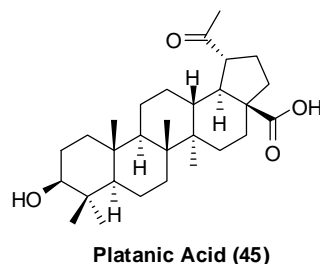
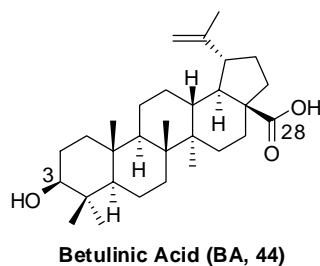
Until now, most reported fusion inhibitors have been large polypeptides,

which lack oral bioavailability and are relatively costly. The azo dye ADS-J1 (**43**) was originally defined as a fusion inhibitor;¹²⁸ however, recent study discovered that it acts before the gp41-dependent fusion step.¹²⁹ Small molecules that can be easily purified during manufacture and are more likely to be orally administered hold better potential to be developed into clinical drugs.



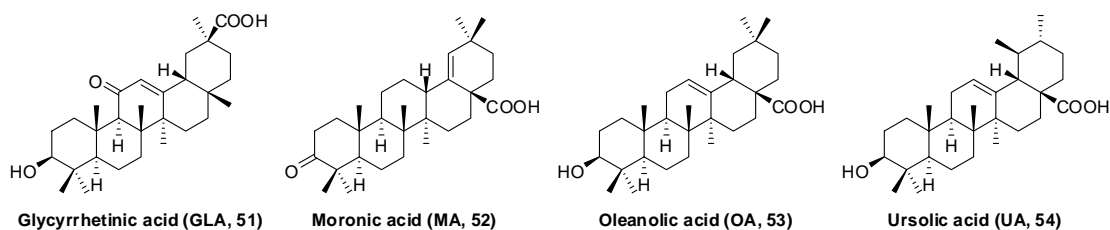
4-2-1. Discovery of RPR103611 and IC9564

Certain triterpene derivatives represent promising small molecule fusion inhibitors (exact binding site is currently unknown, but it has been demonstrated that this compound class functions at a post-binding, envelope-dependent step involved in fusion of the virus to the cell membrane, as discussed below). Betulinic acid (BA, 3 β -hydroxy-lup-20(29)-en-28-oic acid, **44**) and platanic acid (**45**), both of which are pentacyclic triterpenes extracted from *Syzigium claviflorum*, were first reported in 1994 to suppress HIV-1_{IIIB} replication *in vitro*, with EC₅₀ values of 1.4 μ M and 6.5 μ M, respectively.¹³⁰ Because of its promising anti-HIV activity and ready availability from various natural sources, including white birch trees, BA was selected as a lead in an anti-HIV drug discovery program.



C-28 ω -aminoalkanoic acid derivatives of BA were then synthesized and evaluated for antiviral activity by De Clercq *et al.*¹³¹ Initially, the chain length between the C-28 amide bond moiety and the terminal carboxylic acid group (**46a-l**, $m = 1-12$) (Figure 2-11) was explored, and incremental chain lengthening significantly influenced the anti-HIV-1 potency of the derivatives. Compounds with amide side chains between amino-octanoic acid and amino-dodecanoic acid (**46g-k**, $m = 7-11$) showed increased antiviral potency, with amino-undecanoic acid (**46j**, $m = 10$) being optimal. Condensation of these C-28 ω -aminoalkanoic acid derivatives with a second aminoalkanoic acid produced compounds with two amide moieties at different positions of the C-28 side chain. It was then discovered that small peptide amide derivatives of the parent octanoic acid analog **46g** were more potent than both the parent compound and **46j**. The presence of a small lipophilic space between the two amide moieties increased the anti-HIV-1 activity of **46g** by around tenfold, and substituents on this second aminoalkanoic acid moiety also modulated the antiviral potency. This effort led to the discovery of RPR103611 (**47**) (Figure 2-11), a statine derivative, which inhibits the infectivity of several HIV-1 strains in a 10 nM concentration range.^{131,132}

Research in the authors' laboratories on BA derivatives as HIV entry inhibitors focused on the modifications in the isopropylene and C-28 side chains. The study



4-2-2. Mechanism of Action Study of RPR103611 and IC9564

RPR103611 does not inhibit RT, integrase, or protease. A time-of-addition assay indicated that postponing the addition time of RPR103611 for 2 h cancelled its inhibitory potency on HIV-1 replication, suggesting that this compound functions at an early stage of the virus life cycle.¹³² A virus binding assay using recombinant soluble CD4 ruled out the possibilities that attachment of virus to target cells or CD4-gp120 binding were inhibited. RPR103611 does blockage syncytium formation, which indicates that it functions at a post-binding step necessary for virus-membrane fusion. Thus, this compound is the first nonpeptidic small molecule found to act as a fusion inhibitor.¹³²

A sequence analysis of RPR103611-resistant mutants indicated that a single amino acid change, I84S, in the HIV-1 gp41 region is sufficient to confer drug resistance.¹³⁵ The I84 residue is highly conserved and is only rarely replaced by another hydrophobic residue (e.g., phenylalanine). However, I84 is also found in gp41 of some naturally RPR103611-resistant HIV-1 strains, such as NDK or ELI.¹³⁵ Thus, although the drug-resistant mutants occur on gp41, it would be imprudent to conclude that gp41 is the direct target for RPR103611. It is possible that the mutation of I84 to a polar amino acid may alter the gp41 conformation so that the stability of the

gp120-gp41 complex is affected.¹³⁵ The mutation could also modify access of a compound to a target on gp120. Indeed, a later study from the same group reported that the antiviral efficacy of RPR103611 depends on both the sequence of the gp41 loop region (I84, L91) and the stability of the gp120-gp41 complex.¹³⁶ Virus with a decreased affinity between gp120 and gp41 is more susceptible to RPR103611.¹³⁶

A mechanism of action study on IC9564 by Chen et al. revealed that mutations in gp120 are responsible for resistance to the compound.¹³⁷ No mutations on gp41 were found to significantly affect the antiviral activity of the compound.¹³⁷ However, this discovery does not rule out the possibility that IC9564 and RPR103611 share the same mechanism of action, since IC9564-resistant viral strains carry mutations of G237R and R252K, which locate in the inner domain of gp120 core. The inner domain of gp120 is believed to interact with gp41, indicating that these mutations on gp120 may also affect the affinity between gp120 and gp41.¹³⁷ In this particular study, no mutations were found in the regions of gp120 that are well defined for CD4 binding or chemokine co-receptor binding. In continuing studies, a conformational change in gp120 induced by IC9564 was observed by using conformational monoclonal antibody.^{138,139} It was discovered that IC9564 induces a nonproductive gp120 conformation that is not able to trigger a conformational rearrangement in gp41 for membrane fusion.¹³⁹ This discovery supports the previous speculation that triterpenes in this class function as nonpeptidic small molecule fusion inhibitors.

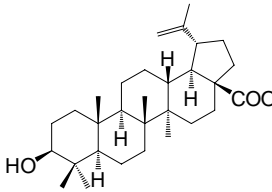
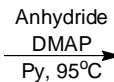
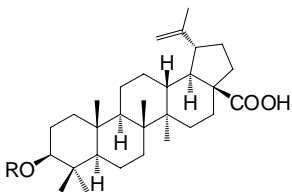
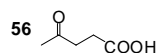
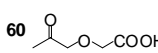
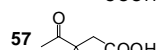
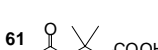

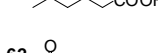
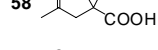
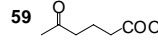



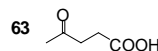
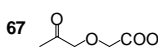
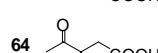


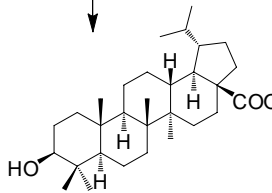
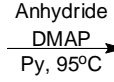
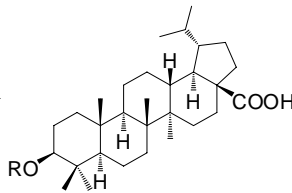
In their most recent publication, Dr. Chen's group reported that IC9564 can increase the antiviral activity of TAK-779 by more than 100-fold.¹⁴⁰ Mutations near

the tip of the V3 loop were found among IC9564 escaping viruses. Moreover, IC9564 can compete with the binding of V3 loop monoclonal antibodies and with the binding of CD4-gp120 complex to chemokine receptors.¹⁴⁰ These results suggested that IC9564 may also function by targeting the V3 loop of gp120, a domain involved in chemokine receptor binding.^{140,141} The exact binding target of triterpene derivatives is still under investigation.

4-2-3. Current Status of Triterpene Derivatives as Potent HIV-1 Inhibitors

Interestingly, the anti-HIV-1 targets of triterpene analogs can vary depending on the side chain modification positions. C-28 modified BA analogs are potent HIV entry inhibitors, while C-3 modified BA derivatives function by blocking virus maturation.¹⁴² As shown in Table 2-1, reacting **44** and **55** with an acid anhydride and DMAP in pyridine afforded 3-*O*-acyl-BA and dihydro-3-*O*-acyl-BA derivatives. BA analogues with 3,3-dimethylsuccinyl (DSB, **58**), and 3,3-dimethylglutaryl (**61**) side chains exhibited dramatically enhanced anti-HIV activity with EC₅₀ values in the nanomolar range. The corresponding substituted dihydro-BA derivatives [**65** (DSD) and **68**] showed comparable potency. Compounds **69** and **70**, which have an isovaleryl domain but lack a terminal carboxylic acid, were less potent, and compound **62**, which lack both features, exhibited no activity. In addition, BA analogues with C-3 ester groups containing no substitutions on the side chain (**56**, **59**, **63**, **66**) also showed reduced or no activities. These data suggested that, within the C-3 side chain, a terminal carboxylic acid and an isovaleryl domain contribute to anti-HIV activity.

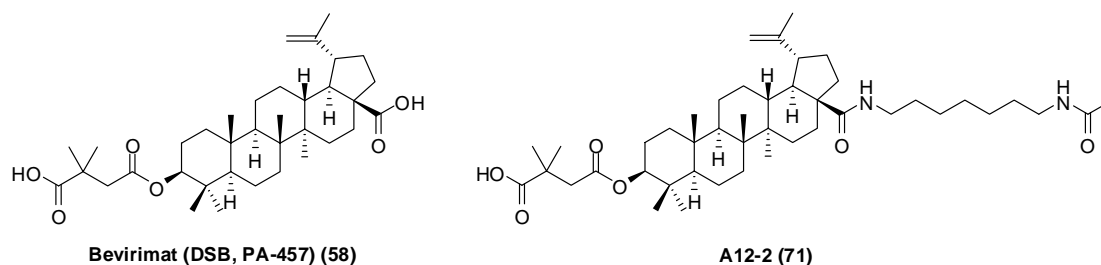
Table 2-1. Structures of 3-*O*-acyl-BA and dihydro-3-*O*-acyl-BA derivatives and their anti-HIV-1 activities in acutely infected H9 lymphocytes

 44		 56-62	 56	 60			
 57	 61						
 58	 62						
 59							
 63	 67						
 64	 68						
 65	 69						
 66	 70						
							
 55		 63-70					
Compd	IC ₅₀ (μM)	EC ₅₀ (μM)	TI	Compd	IC ₅₀ (μM)	EC ₅₀ (μM)	TI
44	13.0	1.4	9.3	55	12.6	0.9	14
56	16	4.0	4	63	13.4	1.8	7.5
57	15.9	2.7	6.7	64	7.7	0.56	13.8
58 (DSB)	7	0.00035	20,000	65 (DSD)	4.9	0.00035	14,000
59	12.8	0.044	292	66	7.9	0.9	9
60	11.7	0.01	1,170	67	5.8	0.0057	1,000
61	4.5	0.0023	2,000	68	13.1	0.0056	2,344
62	48	19	2.5	69	83	1.5	56
				70		NS	

NS: No suppression.

Compound **58** (DSB, PA-457, bevirimat), which exhibits remarkable anti-HIV-1 activity with a mean EC₅₀ value of <10 nM against primary and drug-resistant HIV-1 isolates,^{143,144} was chosen to do further mechanism of action study. It was discovered that **58** blocks the cleavage of CA-SP1 in the Gag polyprotein precursor, resulting in production of morphologically defective, non-infectious HIV-1 virions.¹⁴⁵ Thus, bevirimat (DSB, PA-457, Panacos Pharmaceuticals) (**58**) represents the first in a class known as HIV-1 maturation

inhibitors. It is orally bioavailable and shows good safety and pharmacokinetic profiles in Phase IIa clinical trials.^{146,147} It is encouraging that triterpene analogs can be safely and efficiently used in humans.



Recent progress in this research area has included the development of bi-functional BA analogs, which contain both the C-3 and C-28 side chains, such as A12-2 (**71**), with EC_{50} value of 2.6 nM.¹⁴⁸ This category of compounds preserves the anti-entry and anti-maturation activities of the parent compounds, and shows a synergistic effect on antiviral potency.

5. Conclusion

With increasing knowledge of the HIV entry process, various targets involved in different stages of viral entry have emerged. Inhibitors of these novel targets hold great potential to supplement current HAART, especially to treat individuals harboring multidrug-resistant virus. The success of enfuvirtide and maraviroc validates the clinical application of viral entry inhibitors as a new class of antiretroviral drugs. Many more HIV entry inhibitors are currently in clinical trials, and some have already advanced to Phase III clinical studies.

Triterpenes represent one of these promising compound classes. Within

different triterpenoid skeletons, betulinic acid (BA, **44**) is of particular interests due to its promising anti-HIV-1 activity and ready availability. Modifications of BA at different positions can render the compound with enhanced anti-HIV-1 activity with different mechanisms of action. Further modification on this compound should provide us more SAR information and may lead us to discover novel promising anti-HIV agents. With the emergence of HIV virus resistant to different current ARTs, the development of new antiviral drugs is still the focus of much research.

Chapter 3. Design, Synthesis and Anti-HIV-1 Activity of 3-*O*-Acyl-Betulinic Acid Derivatives as Maturation Inhibitors

1. Introduction

As introduced in Chapter 2, our modification study on betulinic acid (BA, **44**) resulted in the discovery of 3-*O*-(3',3'-dimethylsuccinyl)-betulinic acid (bevirimat, DSB, PA-457, **58**).¹⁴³ Bevirimat exhibits extremely potent antiviral activity against HIV-1 primary isolates and drug-resistant virus, and represents a unique first in a class of anti-HIV compounds termed maturation inhibitors (MIs).^{144,145} It has recently succeeded in Phase IIa clinical trials and is currently in Phase IIb clinical trials.^{146,147,149}

Our prior structure-activity relationship (SAR) study of **58** and other 3-*O*-acyl-betulinic acid derivatives suggested that both the BA triterpenoid skeleton itself and C-3 ester substitution are critical to enhanced anti-HIV-1 activity.^{142,143} Within the C-3 side chain, the proper length, a terminal carboxylic acid, and C-3' dimethyl substitution contribute to antiviral potency. However, the C-3 ester groups of prior **44**-analogs have mainly contained freely rotatable alkyl chains with a terminal carboxylic acid group. Therefore, five C-3 conformationally restricted **44**-analogs were synthesized in order to explore the conformational space of the C-3 ester

substitution. Moreover, four 3-*O*-monomethylsuccinyl betulinic acid (MSB) derivatives as well as two additional C-3 modified **44**-analogs were designed and synthesized to investigate how the methyl substituents on the C-3 side chain impact the antiviral potency and further establish SAR of the C-3 modification. This chapter reports their design, syntheses, isolation, structural assignment, and SAR study.

2. Design

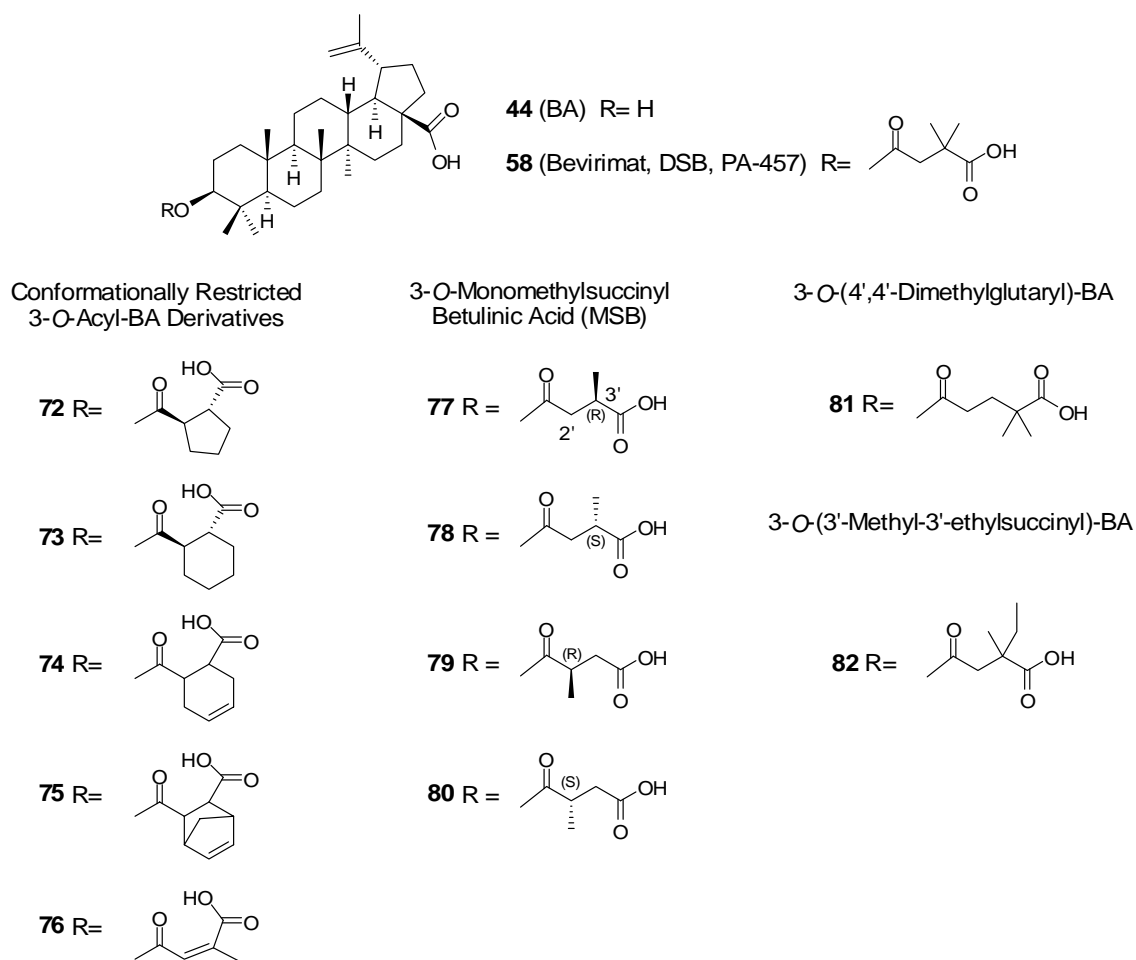


Figure 3-1. Structures of four MSB analogs and other 3-*O*-acyl BA analogs

Because the presence of C-3 substitution is critical to the anti-HIV-1 activity

of **44**-derivatives, five conformationally restricted 3-*O*-acyl-BA analogs (**72-76**) (Figure 3-1) were synthesized and evaluated in HIV-1 infected MT-2 cell lines, in order to further explore the conformational space of this pharmacophore. The C-3' dimethyl group was also moved towards the 4'-position of a C-3 glutaryl-substituted compound (**81**) to study the influence of a different positioning of the methyl groups. In addition, although we know that the presence of the C-3' dimethyl within the C-3 side chain is vital to anti-HIV-1 activity, it is still unclear which, if either, C-3' methyl group of **58** contributes more toward activity. Therefore, 3-*O*-monomethylsuccinyl betulinic acid (MSB) derivatives (**77-80**) (Figure 3-1) were designed and synthesized. Their antiviral activities were also evaluated *in vitro* against HIV-1 replication in MT-2 cell lines. After reviewing the initial promising bioassay results (data listed in Table 3-1), compound **82** (Figure 3-1) was designed to further study the impact of the substituents within the C-3 side chain and try to improve the antiviral potency of **58**.

3. Chemistry

Compounds **72** and **73** were synthesized by reaction of the corresponding cycloalkanedicarboxylic acid with the C-3 β -hydroxyl group of **44** in the presence of EDCI and DMAP, resulting in yields of 26% and 35%, respectively (Scheme 3-1). Compounds **74-76** and **81** were synthesized according to Scheme 3-2. Reaction of the corresponding acid anhydride with **44** furnished the target compounds in yields of 35-55%.

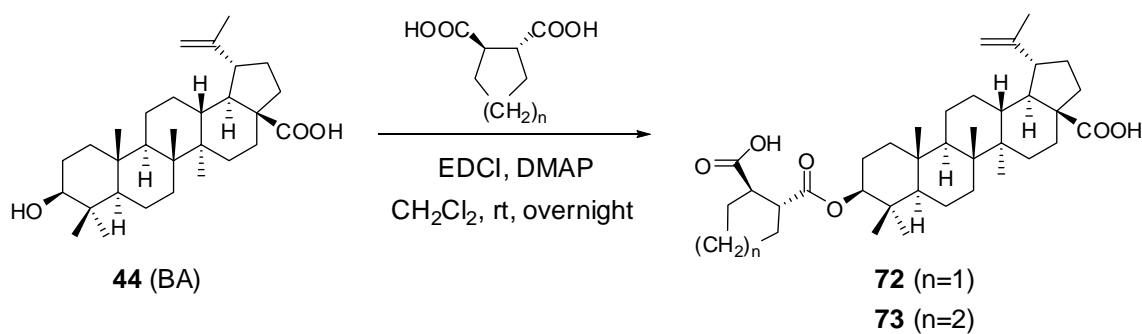
To obtain MSB analogs, **44** was treated with 2-methylsuccinic anhydride and

DMAP in pyridine at reflux to furnish the racemic 3'-MSB isomers, as well as the undesired 2'-MSB isomers. Separation of the four compounds (**77-80**) was challenging, because they differ only by the presence of a 2' or 3' (*R* or *S*) methyl group, but was successfully achieved by using recycle preparative HPLC (Figure 3-2). The purities of **77-80** were ascertained by analytical HPLC (Figure 3-3). By comparing the ¹H-NMR spectra of the purified isomers with those of **58** and 3-*O*-(2',2'-dimethylsuccinyl)-BA (**57**), peaks 1 and 2 were assigned as the 3'-MSBs, and peaks 3 and 4 as the 2'-MSBs. However, the stereochemistries of the C-3' and C-2' chiral centers were still not determined. Therefore, the 3'*R* and 3'*S* isomers were also prepared through total synthesis as described below.

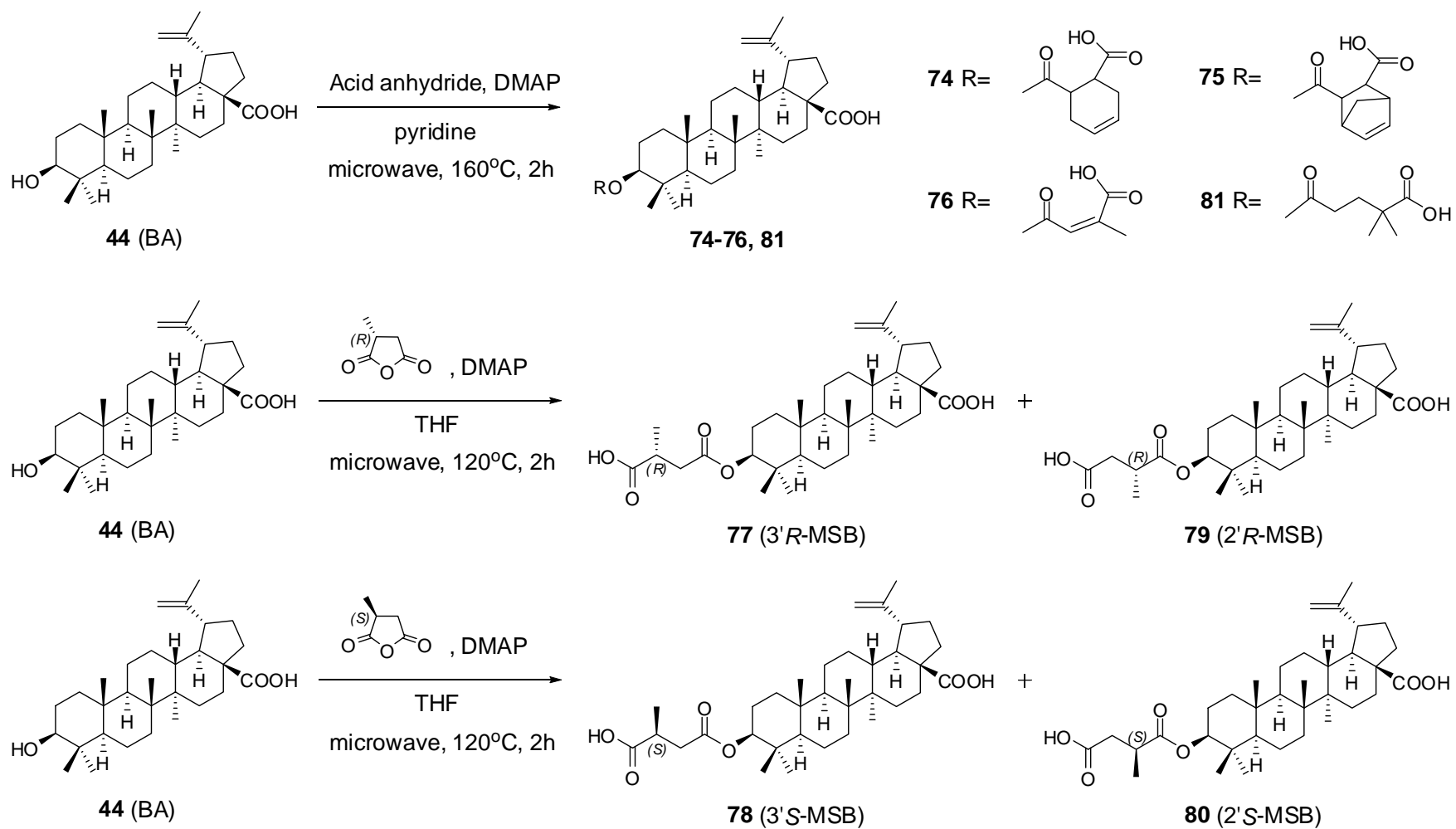
As shown in Scheme 3-3, the hydroxyl of 3*R*-bromo-2-methylpropanol (**83a**) was first protected by reaction with TBDPSCl in DMF to yield **84a** quantitatively. The bromide group was then replaced with a cyano group by reaction with sodium cyanide in DMSO to furnish **85a** in 93% yield. The cyano group was reduced to an aldehyde moiety (**86a**) by using DIBALH, with a yield of 95%.¹⁵⁰ The aldehyde was then oxidized to a carboxylic acid quantitatively in the presence of NaClO₂ and NaH₂PO₄ in DMSO to yield **87a**. Reaction of **44** with **87a** in the presence of EDCI and DMAP led to esterification of the 3β-hydroxy group of **44** with the carboxylic acid of **87a** to provide **88a** in yields of 25-48%. After cleavage of the TBDPS group with TBAF in THF, the primary hydroxy group of **89** was oxidized to a carboxylic acid in the presence of TEMPO, PhI(OAc)₂ in a solution of H₂O-CH₂Cl₂ to give 3-*O*-(3'*R*-methylsuccinyl)-betulinic acid (3'*R*-MSB, **77**).¹⁵¹ The 3'*S*-MSB isomer (**78**)

was synthesized using the same method starting with 3*S*-bromo-2-methylpropanol (**83b**). By comparing the HPLC retention times and ¹H-NMR spectra of these compounds, we determined that peak 1 is the 3'*S* diastereoisomer (**78**) and peak 2 is the 3'*R* diastereoisomer (**77**). Furthermore, the reaction of 2*R*-methylsuccinic anhydride with **44** in THF yielded the 3'*R*-MSB (**77**) and 2'*R*-MSB (**79**) isomers (Scheme 3-1). The HPLC retention times indicated that peak 4 is the 2'*R* isomer (**79**). Similarly, peak 3 was confirmed as the 2'*S* isomer (**80**) (Scheme 3-1). Thus, the stereochemistries of the 3' or 2' chiral center in **77–80** were fully determined.

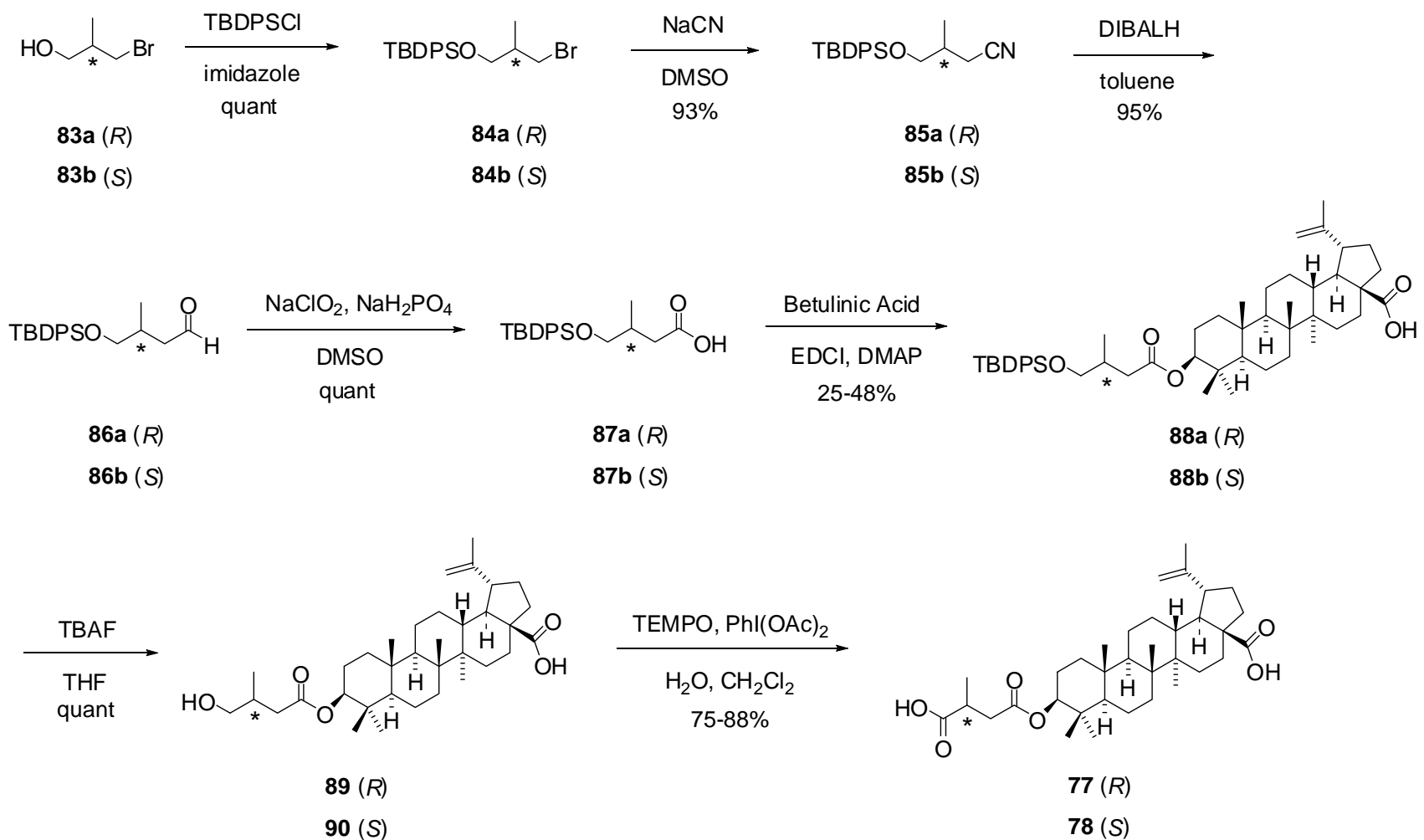
The synthesis of **82** started from the commercially available 2-ethyl-2-methylsuccinic acid (**91**), which was stirred in TFAA to form 2-ethyl-2-methylsuccinic anhydride (**92**). The reaction of **92** with **44** furnished 3-*O*-(3'-ethyl-3'-methylsuccinyl) betulinic acid (**82**) in 55% yield (Scheme 3-4).



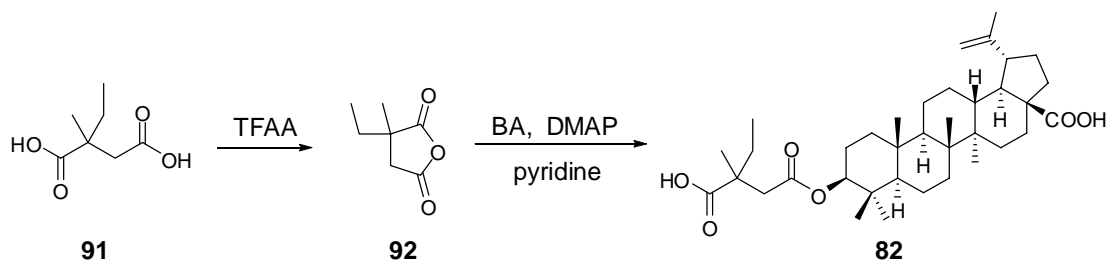
Scheme 3-1. Synthesis of compounds 72 and 73



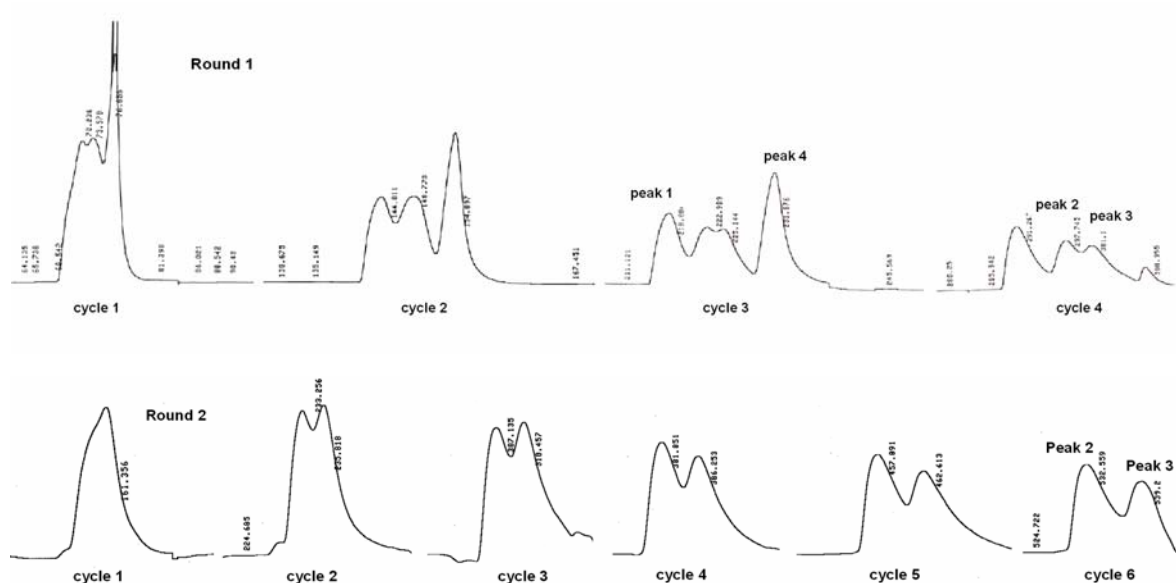
Scheme 3-2. Syntheses of compounds 74-81



Scheme 3-3. Total syntheses of compounds **77** and **78**



Scheme 3-4. Synthesis of compound 82



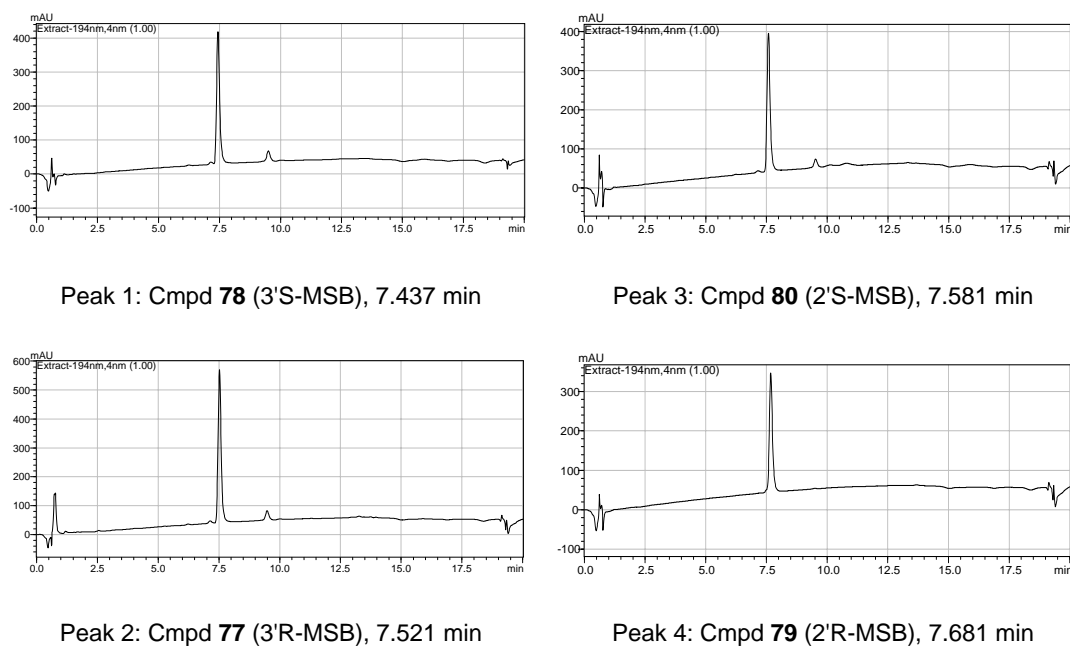


Figure 3-3. Purity confirmation of the four MSB (77-80) isomers by Shimadzu LC-20AT. Column: Alltima C18 5 μ m 150mm x 2.1mm.

4. Results and Discussion

The newly synthesized conformationally restricted 3-*O*-acyl-BA analogs (**72-76**) were first tested in acutely HIV-1 infected MT-2 cell lines and compared to **58** and AZT. The data are listed in Table 3-1. Only the 2-methylmaleic acid substituted BA derivative (**76**) showed moderate anti-HIV-1 activity with a TI of 1.4×10^2 and EC₅₀ of 0.18 μ M. A pendant cyclopentyl or cyclohexyl ring within the C-3 side chain reduced the antiviral potency of the derivatives (**72-75**) significantly. One possible reason for the reduced or abolished activity of these compounds is that the pendant ring moieties are locked into a conformation that is not the bioactive one. Alternatively, steric hindrance at the 2'-position [as was seen with 3-*O*-(2',2'-dimethylsuccinyl) BA (**57**), which had an EC₅₀ of only 2.7 μ M] may be a

contributing factor to the loss in potency. This hindrance may impart an unfavorable interaction with either the binding site, resulting in reduced affinity, or the triterpene template, leading to an unfavorable C-3 side chain conformation.

Table 3-1. Anti-HIV-1 activities for compounds 72-82, 90 and 93 in acutely infected MT-2 cell lines ^a

Compd	EC₅₀ (μM)	IC₅₀ (μM)	Therapeutic Index
AZT	0.034	1,870	55,000
58	0.0013	42.78	32,907
72	2.2	41.89	19
73	17.3	40.93	2.4
74	NS	41.06	—
75	NS	40.27	—
76	0.18	42.51	236.2
77	0.12	43.83	365.3
78	0.0087	32.78	3,768
79	NS	43.83	—
80	0.44	43.83	100
81	0.048	41.75	869.8
82	0.0006	36.41	60,683
90	NS	44.93	—
93	0.016	44.93	2,808
(77+78)			

^a All data presented are averages of at least two separate experiments performed by Panacos Pharmaceutical Inc. EC₅₀: concentration that inhibits HIV-1 replication by 50%. IC₅₀: concentration that inhibits mock-infected MT-2 cell growth by 50%. TI = IC₅₀/EC₅₀. NS: no suppression at the testing concentration.

In contrast, 3-*O*-(4',4'-dimethylglutaryl)-betulinic acid (**81**) had an antiviral EC₅₀ of 0.048 μM and TI of 8.7×10². This result confirms that the dimethyl moiety is essential to the anti-HIV-1 potency of 3-*O*-acyl-BA analogs. Although moving the dimethyl substitution to the 2'-position, as in **57**, was highly detrimental, moving the dimethyl group to the 4'-position of the C-3 side chain was well tolerated and significantly increased the antiviral activity, compared with that of the unesterified triterpene (**44**). However, the anti-HIV-1 activity of **81** was still 20-fold less than that of **58**, indicating that the 3'-position, rather than 4'-position, of the C-3 side chain remains the optimal substitution position. Overall, results of the conformationally restricted compounds (**72-76**) and **81** stimulated our interest in further study of the importance of the C-3' dimethyl moiety and the exact contribution of both groups to the anti-HIV-1 potency of **58**.

The MSB analogs (**77-80**) were then synthesized and evaluated in parallel with **58** and AZT against viral replication in HIV-1 infected MT-2 cell lines. The synthetic intermediate **90** and a 1:1 mixture (**93**) of the 3'*R*- and 3'*S*-MSB isomers (**77** and **78**) were also tested. The anti-HIV-1 activity data of these derivatives are also listed in Table 3-1.

Among the MSB derivatives, the 3'*S*-MSB isomer (**78**) showed very potent antiviral activity with a TI of 3.8×10³ and EC₅₀ of 0.0087 μM, which is comparable to that of **58** (EC₅₀: 0.0013 μM) and slightly better than that of AZT (EC₅₀: 0.034 μM) in this assay system. The 3'*R*-MSB isomer (**77**) exhibited only moderate anti-HIV-1 activity with a TI of 3.7×10² and EC₅₀ of 0.12 μM. The antiviral activity (EC₅₀: 0.016

μM) of the mixture (**93**) of the two stereoisomers fell in between those of **77** and **78**. This result indicates that the two C-3' methyl groups in the C-3 ester side chain contribute differently to the extremely potent anti-HIV-1 activity of this compound class. We postulate that interaction of the 3'*S*-methyl group with the viral target might be essential to the anti-HIV-1 activity of **58**. The interaction of the 3'*R*-methyl group within the target is less significant, but still necessary, since **58**, with dimethyl substitution at C-3' position, is slightly more potent than **78**, which has 3'*S*-monomethyl substitution. In comparison with **77** and **78**, both 2'-MSBs (**79**, **80**) exhibited no or little activity in the same assay. These results agree with those of our previous SAR study, indicating that methyl substitution at C-2' position is not favored and does not improve the antiviral activity significantly. In addition, compound **90**, which differs structurally from **78** only in the presence of a primary hydroxyl rather than carboxylic acid at the terminus of the 3-*O*-acyl side chain, had no activity. This result is also consistent with our findings in prior studies that the terminal carboxylic acid is essential for enhanced antiviral activity.

In order to further elucidate the mechanism of action, the production of virus from 3'*S*-MSB (**78**)-treated HIV-1_{NL4-3} or resistant variants infected Hela cells were subjected to characterization. Radioimmunoprecipitation analyses revealed that, like **58**, **78** also functions as a maturation inhibitor. In detail, **78** specifically inhibited the conversion of p25 (CA-SP1) to p24 (CA) in both cell and virion lysates (Figure 3-4), resulting in defective Gag processing and production of morphologically abnormal, non-infectious virion particles.

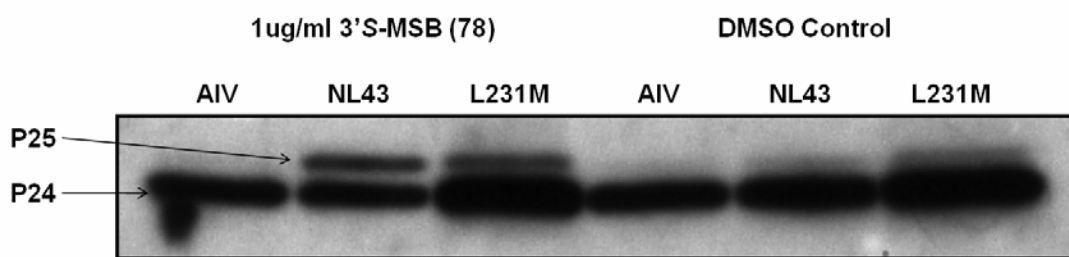


Figure 3-4. Effect of 3'S-MSB (78) on virus particle production and Gag processing. Note the accumulation of p25 in the presence of **78**. AIV is CA-SP1 mutants resistant to bevirimat (**58**). L231M is PI-resistant viral mutants.

As stated above, our investigation of the C-3' chiral center of the anti-HIV-1 clinical trials agent **58** showed that the 3'S-methyl group is the major contributor to enhanced anti-HIV-1 activity, while the 3'R methyl group is less important but still necessary. Accordingly, we postulated that the latter effect may be due to insufficient interaction of the 3'R substituent within the binding pocket or a slightly different positioning of the 3'S-methyl group when a 3'R-moiety is not present. To confirm our hypothesis, one of the methyl groups was further enlarged to an ethyl group to give the 3'-ethyl-3'-methyl substitution found in **82**, which is a mixture of 3'R and 3'S isomers. Compound **82** was evaluated and compared with **58** and AZT in the same assay system. It showed extremely potent antiviral activity with a TI of 6.1×10^4 and EC_{50} of 0.0006 μM , which was more active than AZT and the mixture (**93**) of 3'R-MSB and 3'S-MSB (**77** and **78**). Indeed, its potency was slightly better than that of the pure 3'S-MSB isomer (**78**) and that of **58**. This result confirms our hypothesis that enlarging the C-3' moiety will further increase the antiviral potency of this

compound class. Because the activity of a racemic mixture usually falls between those of the two pure isomers (for example, as was seen with **93** compared to **77** and **78**), whether the 3'*R* isomer or the 3'*S* isomer of **82** is more potent needs to be further determined. The separation of the two isomers also used recycling preparative HPLC (JAI LC-918). This information may help us to better understand the SAR of this critical pharmacophore and further improve the anti-HIV-1 activity of this compound class.

To conclude our SAR investigation of the C-3 modification, we found that no conformationally restricted 3-*O*-acyl BA analog (**72-76**) showed significant antiviral activity, indicating that C-3' dimethyl substitution of the succinyl side chain is crucial to the high potency of **58**. Further SAR study of the C-3' chiral center of the newly designed MSB analogs (**77-80**) revealed that the 3'*S*-methyl group of **58** is the major contributor to the compound's enhanced anti-HIV-1 activity. This result led us to design and synthesize 3-*O*-acyl-BA derivative **82** with an enlarged C-3' substituent. As we anticipated, **82** showed extremely potent antiviral activity, and was slightly better than **58**. Because **82** is a mixture of the 3'*R* and 3'*S* isomers, separation of these two isomers may provide us with better SAR information to further design the next generation of potent **44**-derived HIV-1 maturation inhibitors.

5. Experimental Section

5-1. Chemistry

The melting points were measured with a Fisher Johns melting apparatus without correction. ^1H NMR spectra were measured on a 300MHz Varian Gemini 2000 spectrometer using Me_4Si (TMS) as internal standard. The solvent used was CDCl_3 unless otherwise indicated. Mass spectra were measured on Shimadzu LCMS-2010 (ESI-MS). Optical rotations were measured with a Jasco Dip-2000 digital polarimeter at 20 °C at the sodium D line. Thin-layer chromatography (TLC) and preparative thin-layer chromatography (PTLC) were performed on Merck precoated silica gel 60 F-254 plates. Flash+TM and CombiFlash systems were used as medium pressure column chromatography. Silica gel (200-400 mesh) from Aldrich, Inc., was used for column chromatography. All other chemicals were obtained from Aldrich, Inc.

Synthesis of BA derivatives (72 and 73). A solution of betulinic acid (1 eq), *N*-(3-Dimethylaminopropyl)-*N'*-ethylcarbodiimide hydrochloride (EDCI, 8 eq), 4-(dimethylamino)pyridine (DMAP, 2 eq) and the proper cycloalkanedicarboxylic acid (5 eq) in anhydrous CH_2Cl_2 (8 mL) was stirred at room temperature overnight until the starting material was not observed by TLC. The solution was diluted with CH_2Cl_2 (20 mL) and washed three times with brine and distilled water. The organic layer was dried over anhydrous sodium sulfate (Na_2SO_4) and concentrated to dryness under reduced pressure. The residue was chromatographed using a silica gel column to yield the pure target compounds.

3 β -O-[(2'*R*, 3'*R*)-3'-Carboxycyclopentanecarbonyl]-betulinic acid (72):

26% yield (starting with 150 mg of **44**); white amorphous powder. Mp 228-230 °C. MS (ESI-) *m/z*: 595.4 (*M*⁻ - H) for C₃₇H₅₆O₆. ¹H NMR (300 MHz, CDCl₃): δ 4.70, 4.57 (1H each, s, H-29), 4.45 (1H, dd, *J* = 7.8, 5.7 Hz, H-3), 3.20 (1H, m, H-19), 3.01, 2.88 (1H each, m, H-3', H-2'), 1.85-2.06 (6H, m, 3 \times CH₂, H-4', 5', 6'), 1.65 (3H, s, H-30), 0.94 (6H, s, 2 \times CH₃), 0.85, 0.81, 0.75 (3H each, s, 3 \times CH₃). [α]_D²⁰ -15.29 ° (c = 0.17, MeOH).

3 β -O-[(2'*R*, 3'*R*)-3'-Carboxycyclohexanecarbonyl]-betulinic acid (73):

35% yield (starting with 150 mg of **44**); white amorphous powder. Mp 233-235 °C. MS (ESI-) *m/z*: 609.4 (*M*⁻ - H) for C₃₈H₅₈O₆. ¹H NMR (300 MHz, CDCl₃): δ 4.71, 4.59 (1H each, s, H-29), 4.46 (1H, dd, *J* = 10.2, 5.1 Hz, H-3), 2.98 (1H, m, H-19), 2.89, 2.71 (1H each, m, H-3', H-2'), 1.84-2.16 (8H, m, 4 \times CH₂, H-4', 5', 6', 7'), 1.66 (3H, s, H-30), 0.94 (9H, s, 3 \times CH₃), 0.81, 0.79 (3H each, s, 2 \times CH₃). [α]_D²⁰ -27.00 ° (c = 0.20, MeOH).

Synthesis of BA derivatives (74-76, 79, 80 and 81). A solution of betulinic acid (1 eq), DMAP (2 eq) and the proper acid anhydride (5 eq) in anhydrous pyridine (1.5 mL) was stirred at 160 °C for 2 h using microwave. The reaction mixture was diluted with EtOAc (20 mL) and washed three times with 20% HCl solution and distilled water. The organic layer was dried over anhydrous Na₂SO₄ and concentrated to dryness under reduced pressure. The residue was chromatographed using a silica gel column to yield the pure target compounds.

3 β -O-(3'-Carboxycyclohex-5'-enecarbonyl)-betulinic acid (74): 40% yield

(starting with 100 mg of **44**); white amorphous powder. Mp 178-180 °C. MS (ESI-) m/z : 607.4 ($M^- - H$) for $C_{38}H_{56}O_6$. 1H NMR (300 MHz, $CDCl_3$): δ 5.70 (2H, m, H-5', 6'), 4.72, 4.60 (1H each, s, H-29), 4.48 (1H, m, H-3), 3.02 (1H, m, H-19), 2.83, 2.72 (1H each, m, H-3', H-2'), 2.32-2.27 (4H, m, $2 \times CH_2$, H-4', 7'), 1.68 (3H, s, H-30), 1.01, 0.97 (3H each, s, $2 \times CH_3$), 0.89, 0.83, 0.81 (3H each, s, $3 \times CH_3$). $[\alpha]_D^{20} +14.17^\circ$ ($c = 0.18$, MeOH).

3 β -O-[3'-Carboxybicyclo[2.2.1]hept-5'-enecarbonyl]-betulinic acid (75): 35% yield (starting with 100 mg of **44**); white amorphous powder. Mp 165-167 °C. MS (ESI-) m/z : 619.4 ($M^- - H$) for $C_{39}H_{56}O_6$. 1H NMR (300 MHz, $CDCl_3$): δ 5.73 (2H, m, H-5', 6') 4.71, 4.59 (1H each, s, H-29), 4.45 (1H, m, H-3), 3.01 (1H, m, H-19), 2.95, 2.76 (1H each, m, H-3', H-2'), 2.52-2.39 (4H, m, $2 \times CH_2$, H-4', 7'), 1.67 (3H, s, H-30), 0.96 (6H, s, $2 \times CH_3$), 0.91, 0.85, 0.82 (3H each, s, $3 \times CH_3$). $[\alpha]_D^{20} +24.00^\circ$ ($c = 0.10$, MeOH).

3 β -O-[(Z)-3'-Carboxybut-2-enoyl]-betulinic acid (76): 55% yield (starting with 150 mg of **44**); red amorphous powder. Mp 169-171 °C. MS (ESI-) m/z : 567.4 ($M^- - H$) for $C_{35}H_{52}O_6$. 1H NMR (300 MHz, $CDCl_3$): δ 5.89 (1H, s, H-2'), 4.70, 4.58 (1H each, s, H-29), 4.46 (1H, m, H-3), 2.96 (1H, m, H-19), 1.93 (3H, s, CH_3 -3'), 1.66 (3H, s, H-30), 0.94, 0.93, 0.90 (3H each, s, $3 \times CH_3$), 0.80, 0.79 (3H each, s, $2 \times CH_3$). $[\alpha]_D^{20} +9.41^\circ$ ($c = 0.17$, MeOH).

3 β -O-(2'R-Methylsuccinyl)-betulinic acid (79): 8% (after HPLC separation); white amorphous powder. Mp 250–252 °C. MS (ESI-) m/z : 569.38 ($M^- - H$) for $C_{35}H_{54}O_6$. 1H NMR (300 MHz, $CDCl_3$): δ 4.73, 4.60 (1H each, s, H-29), 4.52 (1H, t, J

= 7.8 Hz, H-3), 2.90-3.10 (2H, m, H-19, H-2'), 2.67, 2.42 (1H each, dd, $J = 16.8, 9.6$, 4.2, H-3'), 2.13-2.20 (1H, m, H-13), 1.68 (3H, s, H-30), 1.26, 1.23 (3H, d, $J = 7.2$ Hz, CH₃-2'), 0.97 (6H, s, 2 × CH₃), 0.86, 0.83, 0.81 (3H each, s, 3 × CH₃). $[\alpha]_{\text{D}}^{20} +12.94^\circ$ ($c = 0.17$, MeOH).

3 β -O-(2'S-Methylsuccinyl)-betulinic acid (80): 15% (after HPLC separation); white amorphous powder. Mp 256–259 °C. MS (ESI-) m/z : 569.38 ($M^- - H$) for C₃₅H₅₄O₆. ¹H NMR (300 MHz, CDCl₃): δ 4.74, 4.61 (1H each, s, H-29), 4.48 (1H, dd, $J = 10.8, 4.8$ Hz, H-3), 2.80-3.01 (2H, m, H-19, H-2'), 2.76, 2.46 (1H each, dd, $J = 16.9, 9.5, 4.7$, H-3'), 2.10-2.18 (1H, m, H-13), 1.69 (3H, s, H-30), 1.25, 1.23 (3H, d, $J = 6$ Hz, CH₃-2'), 0.97, 0.92 (3H each, s, 2 × CH₃), 0.84-0.86 (9H, m, 3 × CH₃). $[\alpha]_{\text{D}}^{20} -11.00^\circ$ ($c = 0.10$, MeOH).

3 β -O-(4',4'-Dimethylglutaryl)-betulinic acid (81): 53% yield (starting with 100 mg of **44**); white amorphous powder. Mp 228-230 °C. MS (ESI-) m/z : 597.4 ($M^- - H$) for C₃₇H₅₈O₆. ¹H NMR (300 MHz, CDCl₃): δ 4.73, 4.61 (1H each, s, H-29), 4.45 (1H, dd, $J = 9.0, 5.2$ Hz, H-3), 3.00 (1H, m, H-19), 2.32 (2H, dd, $J = 6.6, 5.4$ Hz, H-2'), 2.16 (1H, m, H-13), 1.69 (3H, s, H-30), 1.22, 1.21 (3H each, d, $J = 6$ Hz, 2 × CH₃-4'), 0.97, 0.91 (3H each, s, CH₃-23, 24), 0.86, 0.85, 0.83 (3H each, s, CH₃-25, 26, 27). $[\alpha]_{\text{D}}^{20} -0.77^\circ$ ($c = 0.13$, MeOH).

Synthesis of 84a and 84b. A solution of **83a** or **83b** (1 eq), imidazole (1.1 eq) and TBDPSCl (1.1 eq) in dry DMF was stirred at room temperature, until the starting material was not observed by TLC. The reaction mixture was diluted with EtOAc and washed with 20% HCl solution and distilled water. The organic layer was dried over

anhydrous Na₂SO₄ and concentrated to dryness under reduced pressure. The residue was chromatographed using a silica gel column to yield the pure target compounds.

(3*R*-Bromo-2-methylpropoxy)(tert-butyl)diphenylsilane (84a): 2.03 g (100%) yielded from **83a**; colorless oil. MS (ESI+) *m/z*: 391.2 (M⁺ + H), 413.2 (M⁺ + Na) for C₂₀H₂₇BrOSi.

(3*S*-Bromo-2-methylpropoxy)(tert-butyl)diphenylsilane (84b): 1.44 g (100%) yielded from **83b**; colorless oil. MS (ESI+) *m/z*: 391.1 (M⁺ + H), 413.1 (M⁺ + Na) for C₂₀H₂₇BrOSi.

Synthesis of 85a and 85b. To a solution of **84a** or **84b** (1 eq) in dry DMSO (10 mL) was added sodium cyanide (3 eq). The mixture was stirred at 120 °C for 2 h until the starting material was not observed. After cooling to room temperature, the reaction was diluted with ether (30 mL) and washed with distilled water. The organic layer was dried over anhydrous Na₂SO₄ and concentrated to dryness under reduced pressure. The residue was chromatographed using a silica gel column to yield the pure target compounds.

4-(tert-Butyldiphenylsilyloxy)-3*R*-methylbutanenitrile (85a): 1.70g (93%) yield starting with **84a**; colorless oil. MS (ESI+) *m/z*: 338.2 (M⁺ + H) for C₂₁H₂₇NOSi.

4-(tert-Butyldiphenylsilyloxy)-3*S*-methylbutanenitrile (85b): 1.163 g (93%) yield starting with **84b**; colorless oil. MS (ESI+) *m/z*: 338.2 (M⁺ + H) for C₂₁H₂₇NOSi.

Synthesis of 86a and 86b. To a solution of **85a** or **85b** (1 eq) in anhydrous

toluene (10 mL) was added diisobutylaluminium hydride (DIBALH, 1.1 eq) dropwise at 0 °C under argon. After stirring for 30 min, ice water was added slowly followed by 10% HCl and aqueous saturated potassium tartrate. Stirring was continued for 15 min at 0 °C and then the aqueous layer was extracted three times with CH₂Cl₂. The organic layer was dried over anhydrous Na₂SO₄ and concentrated to dryness under reduced pressure. The residue was chromatographed using a silica gel column to yield the pure target compounds.

4-(tert-Butyldiphenylsilyloxy)-3R-methylbutanal (86a): 1.02 g (95%) yield starting with **85a**; colorless oil. MS (ESI+) *m/z*: 341.2 (M⁺ + H) for C₂₁H₂₈O₂Si.

4-(tert-Butyldiphenylsilyloxy)-3S-methylbutanal (86b): 1.047 g (90%) yield starting with **85a**; colorless oil. MS (ESI+) *m/z*: 341.2 (M⁺ + H) for C₂₁H₂₈O₂Si.

Synthesis of 87a and 87b. To a solution of **86a** or **86b** (1 eq) in dry DMSO (1.0 mL) was added NaH₂PO₄·H₂O (0.8 eq in 2.0 mL H₂O) and 80% NaClO₂ (1.5 eq in 2.0 mL H₂O) dropwise over 5min. The mixture was stirred overnight. The reaction was quenched with saturated NH₄Cl solution and extracted with EtOAc. The organic layer was washed with brine, dried over anhydrous Na₂SO₄ and concentrated to dryness under reduced pressure. The residue was chromatographed using a silica gel column to yield the pure target compounds.

4-(tert-Butyldiphenylsilyloxy)-3R-methylbutanoic acid (87a): 700 mg (100%) yield starting with **86a**; colorless oil. MS (ESI-) *m/z*: 355.2 (M⁻ - H) for C₂₁H₂₈O₃Si. ¹H NMR (300 MHz, CDCl₃): δ 7.68-7.62 (4H, m, H ar-2'), 7.45-7.33 (6H, m, H ar-3', 4'), 3.59, 3.43 (2H, dd, *J* = 7.6, 1.5 Hz, H-4), 2.61-2.30 (3H, m, H-2,

H-3), 1.05 (9H, s, SiC(CH₃)₃), 0.95 (3H, d, *J* = 10 Hz, H-5).

4-(tert-Butyldiphenylsilyloxy)-3*S*-methylbutanoic acid (87b): 830 mg (76%) yield starting with **86b**; colorless oil. MS (ESI-) *m/z*: 355.2 (*M*⁻ - H) for C₂₁H₂₈O₃Si. ¹H NMR (300 MHz, CDCl₃): δ 7.68-7.62 (4H, m, H ar-2'), 7.45-7.33 (6H, m, H ar-3', 4'), 3.58, 3.42 (2H, dd, *J* = 7.6, 1.5 Hz, H-4), 2.60-2.30 (3H, m, H-2, H-3), 1.05 (9H, s, SiC(CH₃)₃), 0.95 (3H, d, *J* = 10 Hz, H-5).

Synthesis of 88a and 88b. A solution of betulinic acid (1 eq), EDCI (8 eq), DMAP (2 eq) and **87a** or **87b** (5 eq) in anhydrous CH₂Cl₂ (5 mL) was stirred at room temperature overnight, until the starting material was not observed by TLC. The solution was diluted with CH₂Cl₂ (15 mL) and washed three times with brine and distilled water. The organic layer was dried over anhydrous Na₂SO₄ and concentrated to dryness under reduced pressure. The residue was chromatographed using a silica gel column to yield the pure target compounds.

3β-*O*-[4'-(tert-Butyldiphenylsilyloxy)-3'*R*-methylbutanoyl]-betulinic acid (88a): 32% yield starting with 340 mg BA, white powder. Mp 179-181 °C. MS (ESI-) *m/z*: 793.5 (*M*⁻ - H) for C₅₁H₇₄O₅Si. ¹H NMR (300 MHz, CDCl₃): δ 7.68-7.62 (4H, m, H ar-2'), 7.45-7.33 (6H, m, H ar-3', 4'), 4.72, 4.60 (1H each, s, H-29), 4.45 (1H, m, H-3), 3.58, 3.42 (2H, m, H-4'), 2.87-2.95 (2H, m, H-19, H-3'), 2.64-2.42 (2H, m, H-2'), 1.69 (3H, s, H-30), 1.28, 1.26 (3H, d, *J* = 6 Hz, CH₃-3'), 1.01 (9H, s, SiC(CH₃)₃), 0.96 (6H, s, 2 × CH₃), 0.89, 0.85, 0.82 (3H each, s, 3 × CH₃).

3β-*O*-[4'-(tert-Butyldiphenylsilyloxy)-3'*S*-methylbutanoyl]-betulinic acid (88b): 48% yield starting with 170 mg BA, white powder. Mp 186-187 °C. MS (ESI-)

m/z : 793.5 ($M^+ - H$) for $C_{51}H_{74}O_5Si$. 1H NMR (300 MHz, $CDCl_3$): δ 7.68-7.62 (4H, m, H ar-2'), 7.45-7.33 (6H, m, H ar-3', 4'), 4.73, 4.60 (1H each, s, H-29), 4.51 (1H, dd, $J = 11.1, 4.8$ Hz, H-3), 3.60-3.42 (2H, m, H-4'), 2.96-3.03 (1H, m, H-19), 2.86-2.93 (1H, m, H-3'), 2.73, 2.69 (1H each, dd, $J = 11.2, 5.7, 4.8$ Hz, H-2'), 1.69 (3H, s, H-30), 1.27, 1.25 (3H, d, $J = 6$ Hz, CH_3 -3'), 1.02 (9H, s, $SiC(CH_3)_3$), 0.97, 0.94, 0.86, 0.85, 0.81 (3H each, s, CH_3 -23, 24, 25, 26, 27).

Synthesis of 89 and 90. A solution of **88a** or **88b** (1 eq) and TBAF (1.0 M in THF, 3 eq) in anhydrous THF was stirred at 0 °C for 1.5 h. The mixture was then allowed to warm to room temperature and stirred until there was no starting material detected by TLC. The reaction was diluted with 15 mL of CH_2Cl_2 and washed with saturated NH_4Cl solution and brine. The organic layer was dried over anhydrous (Na_2SO_4 and concentrated to dryness under reduced pressure. The residue was chromatographed using a silica gel column to yield the pure target compounds.

3 β -O-(4'-Hydroxy-3'*R*-methylbutanoyl)-betulinic acid (89): 100% yield from **88a**, white powder. Mp 201-203 °C. MS (ESI-) m/z : 555.4 ($M^+ - H$) for $C_{35}H_{56}O_5$. 1H NMR (300 MHz, $CDCl_3$): δ 4.73, 4.60 (1H each, s, H-29), 4.54 (1H, dd, $J = 9.9, 5.7$ Hz, H-3), 3.55, 3.42 (2H, m, H-4'), 3.01 (1H, m, H-19), 2.87-2.95 (1H, m, H-3'), 2.70-2.42 (2H, m, H-2'), 1.68 (3H, s, H-30), 1.27, 1.25 (3H, d, $J = 6$ Hz, CH_3 -3'), 0.93 (6H, s, $2 \times CH_3$), 0.85, 0.84, 0.81 (3H each, s, $3 \times CH_3$). $[\alpha]_D^{20} +15.50^\circ$ ($c = 0.12$, MeOH).

3 β -O-(4'-Hydroxy-3'*S*-methylbutanoyl)-betulinic acid (90): 100% yield from **88b**, white powder. Mp 229-231 °C. MS (ESI-) m/z : 555.4 ($M^+ - H$) for $C_{35}H_{56}O_5$.

¹H NMR (300 MHz, CDCl₃): δ 4.73, 4.60 (1H each, s, H-29), 4.51 (1H, dd, *J* = 12.5, 5.6 Hz, H-3), 3.58, 3.43 (2H, m, H-4'), 2.97-3.01 (1H, m, H-19), 2.83-2.92 (1H, m, H-3'), 2.70, 2.62 (1H each, dd, *J* = 16.2, 6.3, 4.8 Hz, H-2'), 1.69 (3H, s, H-30), 1.27, 1.25 (3H, d, *J* = 6 Hz, CH₃-3'), 1.01, 0.96, 0.86, 0.85, 0.81 (3H each, s, CH₃-23, 24, 25, 26, 27). [α]_D²⁰ -16.10 ° (c = 0.11, MeOH).

Synthesis of 77 and 78. To a solution of **89** or **90** (1 eq) in CH₂Cl₂ (5 mL) was added TEMPO (0.1 eq), and PhI(OAc)₂ (1.5 eq). The mixture was stirred at room temperature until the starting material was not observed by TLC. The reaction was filtered through thin silica gel pad and eluted with CH₂Cl₂ and washed with saturated NH₄Cl solution and brine. The organic layer was dried over anhydrous Na₂SO₄ and concentrated to dryness under reduced pressure. The residue was chromatographed using a silica gel column to yield the pure target compounds.

3β-O-(3'R-Methylsuccinyl)-betulinic acid (77): 75% yield from **89**, white amorphous powder. Mp 268–271 °C. MS (ESI-) *m/z*: 569.38 (M⁺ - H) for C₃₅H₅₄O₆. ¹H NMR (300 MHz, CDCl₃): δ 4.73, 4.60 (1H each, s, H-29), 4.54 (1H, dd, *J* = 9.9, 5.7 Hz, H-3), 3.01 (1H, m, H-19), 2.87-2.95 (1H, m, H-3'), 2.84, 2.42 (1H each, dd, *J* = 15.9, 8.3, 5.6, H-2'), 2.10-2.20 (1H, m, H-13), 1.69 (3H, s, H-30), 1.28, 1.26 (3H, d, *J* = 6 Hz, CH₃-3'), 0.97 (6H, s, 2 × CH₃), 0.86, 0.83, 0.80 (3H each, s, 3 × CH₃). [α]_D²⁰ +13.00 ° (c = 0.05, MeOH).

3β-O-(3'S-Methylsuccinyl)-betulinic acid (78): 88% yield from **90**, white amorphous powder. Mp 279–281 °C. MS (ESI-) *m/z*: 569.38 (M⁺ - H) for C₃₅H₅₄O₆. ¹H NMR (300 MHz, CDCl₃): δ 4.73, 4.60 (1H each, s, H-29), 4.51 (1H, dd, *J* = 11.1,

4.8 Hz, H-3), 2.96-3.03 (1H, m, H-19), 2.86-2.93 (1H, m, H-3'), 2.70, 2.61 (1H each, dd, $J = 16.2, 6.3, 4.8$ Hz, H-2'), 2.06-2.16 (1H, m, H-13), 1.69 (3H, s, H-30), 1.27, 1.25 (3H, d, $J = 6$ Hz, CH₃-3'), 0.97, 0.94, 0.86, 0.85, 0.81 (3H each, s, CH₃-23, 24, 25, 26, 27). $[\alpha]_D^{20} -16.88^\circ$ ($c = 0.08$, MeOH).

3 β -O-(3'-Ethyl-3'-methylsuccinyl)-betulinic acid (82):

2-Ethyl-2-methylsuccinic acid (50 mg, 4 eq) was stirred in trifluoroacetic anhydride (TFAA) at room temperature for 3 h until the reaction mixture become homogenous. The solution was then concentrated to dryness under reduced pressure to yield 2-ethyl-2-methylsuccinic anhydride (**92**). Compound **92** was reacted without further purification with betulinic acid (36 mg, 1 eq) and DMAP (19 mg, 2 eq) in anhydrous pyridine (1.5 mL), stirring at 160 °C for 2 h in microwave. The reaction mixture was diluted with EtOAc (10 mL) and washed three times with 20% HCl solution and distilled water. The organic layer was dried over anhydrous Na₂SO₄ and concentrated to dryness under reduced pressure. The residue was chromatographed using a silica gel column to yield 30 mg (55%) of **82**; white amorphous powder. Mp 179-181 °C. MS (ESI-) m/z : 597.4 ($M^- - H$) for C₃₇H₅₈O₆. ¹H NMR (300 MHz, CDCl₃): δ 4.70, 4.58 (1H each, s, H-29), 4.475 (1H, dd, $J = 10.2, 5.6$ Hz, H-3), 2.99 (1H, m, H-19), 2.73, 2.55 (1H each, dd, $J = 11.9, 5.6$, H-2'), 1.66 (3H, s, H-30), 1.34-1.32 (2H, m, CH₂-3'), 1.23 (3H, s, CH₃-3'), 1.18 (2H, m, CH₃-3''), 0.94 (6H, s, 2 \times CH₃), 0.85, 0.84, 0.78 (3H each, s, 3 \times CH₃). $[\alpha]_D^{20} -3.00^\circ$ ($c = 0.10$, MeOH).

5-2. HIV-1 Replication Inhibition Assay in MT-2 Cell Lines^{134,152,153}

The evaluation of HIV-1 inhibition was carried out as follows using MT-2 lymphocytes. The human T-cell line, MT-2, was maintained in continuous culture with complete medium (RPMI 1640 with 10% fetal calf serum supplemented with L-glutamine at 5% CO₂ and 37°C. Test samples were first dissolved in dimethyl sulfoxide (DMSO) at a concentration of 10 mg/mL to generate master stocks with dilutions made into tissue culture media to generate working stocks. The following drug concentrations were routinely used for screening: 100, 20, 4 and 0.8 µg/mL. For agents found to be active, additional dilutions were prepared for subsequent testing so that an accurate EC₅₀ value could be determined. Test samples were prepared, and to each sample well, was added 90 µL of media containing MT-2 cells at 3×10⁵ cells/mL and 45 µL of virus inoculum (HIV-1_{IIIB} isolate) containing 125 TCID₅₀. Control wells containing virus and cells only (no drug) and cells only (no virus or drug) were also prepared. A second identical set of samples were added to cells under the same conditions without virus (mock infection) for toxicity determinations (IC₅₀ defined below). In addition, AZT and bevirimat (DSB, PA-457) were also assayed during each experiment as a positive drug control. On day 4 PI, the assay was terminated and culture supernatants were harvested for p24 antigen ELISA analysis. The p24 antigen is the core protein of HIV and, therefore, it was an indirect measure of virus present in the supernatants. The p24 antigen assay used a HIV-1 anti-p24 specific monoclonal antibody as the capture antibody coated on 96-well plates. Following a sample incubation period, rabbit serum containing antibodies for HIV-1 p24 was used to tag

any p24 ‘captured’ onto the microtiter well surface. Peroxidase conjugated goat anti-rabbit serum was then used to tag HIV-1 p24 specific rabbit antibodies that have complexed with captured p24. The presence of p24 in test samples was revealed by addition of substrate to peroxidase. P24 in the culture medium was quantitated against a standard curve containing known amounts of p24. The compound toxicity was determined by XTT using the mock-infected sample wells. If a test sample inhibited virus replication and was not toxic, its effects were reported in the following terms: EC₅₀, the concentration of the test sample that was able to suppress HIV replication by 50%; IC₅₀, the concentration of test sample that was toxic to 50% of the mock-infected cells; and therapeutic index (TI), the ratio of the IC₅₀ to EC₅₀.

5-3. HIV-1 Maturation Inhibition Assay¹⁴⁵

Hela cells were transfected with pNL4-3 or mutated HIV-1 virus (A1V or L231M) and cultured in the absence or presence of **78**. Two days post-transfection, cells were metabolically labeled for 2h with ³⁵S-Met/Cys. Cell lysates were prepared, and virions were pelleted by ultracentrifugation. Cell and viral lysates were immunoprecipitated with HIV-Ig. Western blotting was then performed^{154,155} and p25 and p24 are indicated.

Chapter 4. Synthesis of 28,30-Disubstituted Betulinic Acid Derivatives as Novel HIV-1 Entry Inhibitors

1. Introduction

The betulinic acid (BA, **44**) triterpenoid skeleton contains three functional groups – C-3 hydroxyl group, C-28 carboxylic acid group and C-19 isopropenyl moiety (Figure 4-1). Structural modification of the first two groups resulted in identification of different anti-HIV-1 targets. C-3 esterification of BA led to the discovery of bevirimat (DSB, **58**), which is a maturation inhibitor (MI) that blocks cleavage of p25 (CA-sp1) to functional p24 (CA).^{142,143,145} On the other hand, the C-28 side chain was proven to be a necessary pharmacophore for anti-HIV-1 entry activity, as seen with RPR103611 (**47**), IC9564 (**48**) and A43-D (**94**) (Figure 4-1), which showed potent antiviral activity (EC_{50} 0.05-2 μ M) in different assay systems.^{131,133,136,148} Mechanism of action study revealed that C-28 modified BA derivatives function at a post-binding, envelope-dependent step involved in fusion of the virus to the cell membrane.¹³² Because most reported fusion inhibitors are large molecules that lack orally bioavailability and are relatively costly, analogs **47**, **48**, and **94** represent a promising class of small molecule fusion inhibitors. However, the clinical development of **47** by Rhone-Poulenc (now Sanofi-Aventis) was stopped due to poor “pharmacodynamic properties”,¹⁴¹ suggesting that further modification of this

compound class is still necessary. Because the C-19 isopropenyl group has been less investigated, modification was carried out on this moiety, as well as the C-28 side chain, in order to explore SAR and generate potent BA-derived HIV-1 entry inhibitors. This chapter reports their design, syntheses and bioassay data.

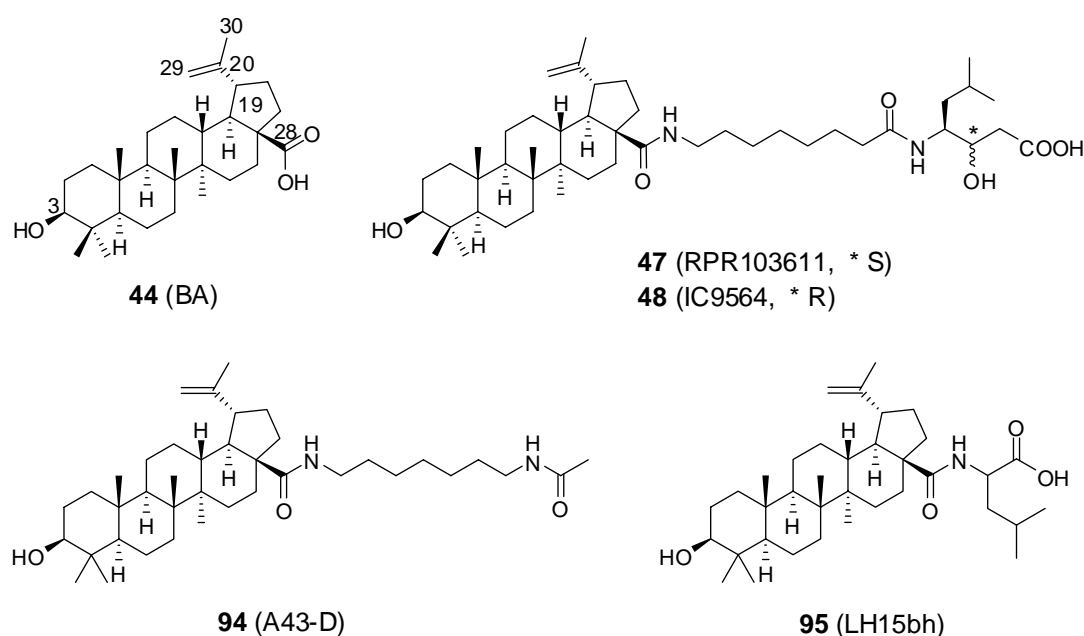


Figure 4-1. Structures of BA and selected C-28 modified BA derivatives

2. Design

The C-28 side chain of **44** and its contribution to HIV-1 entry inhibition activity has been extensively investigated, and these studies led to the identification of lead compounds **47**, **48** and **94** (Figure 4-1). However, less effort has been focused on the C-19 isopropenyl moiety and its effect on HIV replication. Limited SAR on C-19 modification suggested that 20(29) double bond saturated dihydro-BA (**55**) and its derivatives showed similar antiviral activity, but slightly increased cytotoxicity,

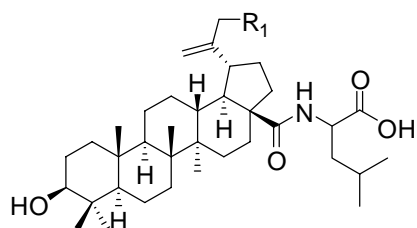
compared with **44** and its corresponding derivatives. Insertion of thioether-linked substitution on the C-30 allyl position slightly decreased anti-HIV-1 potency in the resulting BA analogs, while substitution through an amine bond abolished antiviral activity.

Because the available SAR is very limited, we carried out additional modification on the C-30 side chain in order to better explore its contribution towards anti-HIV-1 activity. In this study, diverse substituents were introduced into the C-30 allyl position (Figure 4-2), including a bromide group (**96**), methylene chains (**97-99**) and aromatic rings (**100-104**), which may facilitate hydrophobic interactions, as well as morpholine moieties (**105-106**) and a hydroxyl group (**107**), which may form hydrogen bonds with the binding target. Because analogs with a thioether moiety showed only slightly decreased anti-HIV-1 activity, we selected a bioisosteric oxygen ether bond as the primary linkage between the added C-30 substituents and the BA backbone. Moreover, leucine was incorporated into the C-28 side chain, because 28-leucine-BA (15bh, **95**) (Figure 4-1) showed moderate *in vitro* anti-HIV-1 entry activity (EC_{50} : $\sim 1\mu M$) in a luciferase-based envelope-induced fusion assay. The anti-HIV-1 replication activity of these newly synthesized 28,30-disubstituted BA analogs (Series I, **96-107**) were evaluated in both HIV-1_{IIIB} infected MT-2 and HIV-1_{NL4-3} infected MT-4 cell lines.

After reviewing bioassay data and attempting to explain the poor “pharmacodynamic properties” of **47**, the partition coefficient (Log P) value of several lead compounds including **47/48** (diastereoisomers), **94** and **95** were calculated by

ACD/LogP DB software. The calculated Log P values of **47/48**, **94** and **95** are 9.38 (\pm 0.63), 9.03 (\pm 0.54) and 9.57 (\pm 0.55), respectively. The hydrophobic effect may be related to poor tissue distribution profile, increased toxicity and low solubility, which may result in poor pharmacodynamic properties in the body. Therefore, several novel 28, 30-disubstituted BA derivatives (Series II, **108-112**) (Figure 4-2) were designed and synthesized to address these issues. In this new series, 8-aminooctanoic acid was attached at the BA C-28 side chain via an amide bond. Thus, this group replaced the shorter leucine moiety in **95** or the mono-acetate protected 1,7-heptanediamine in **94**. In addition, polar groups such as a hydroxyl group (**110**) and morpholine moiety (**111**) were incorporated into the C-30 substitution in order to increase the hydrophilicity and water solubility of the derivatives. Analog **111**, with a morpholine group in the C-30 side chain, proved to be a good antiviral hit. Accordingly, its terminal carboxylic acid was reacted with methylamine to form a second amide bond in the C-28 side chain (**112**) and modulate the Log P value.

In addition, the C-3 β -hydroxyl group of **96** was esterified with 2',2'-dimethylsuccinic anhydride to furnish **113** (Figure 4-2). This analog was designed to study how the presence of both C-28 and C-30 substitutions affected the activity of the C-3 modified BA derivative bevirimat (DSB, **58**).



Series I. 96-107

96 $R_1 = -\text{Br}$

97 $R_1 = -\text{OCH}_2\text{CH}_3$

98 $R_1 = -\text{O}(\text{CH}_2)_2\text{CH}_3$

99 $R_1 = -\text{O}(\text{CH}_2)_3\text{CH}_3$

100 $R_1 = -\text{O}(\text{CH}_2)_2-\text{C}_6\text{H}_5$

101 $R_1 = -\text{O}(\text{CH}_2)_2-\text{C}_6\text{H}_4\text{OMe}$

102 $R_1 = -\text{O}(\text{CH}_2)_2-\text{C}_6\text{H}_4\text{F}$

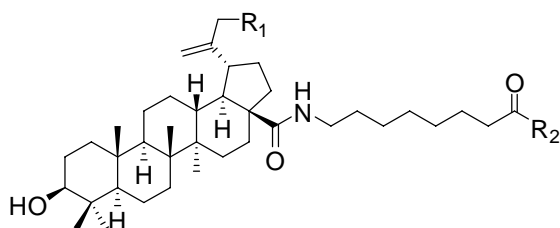
103 $R_1 = -\text{O}(\text{CH}_2)_2-\text{C}_6\text{H}_4\text{Br}$

104 $R_1 = -\text{O}(\text{CH}_2)_2-\text{C}_6\text{H}_4\text{Cl}$

105 $R_1 = -\text{N}(\text{CH}_2)_2\text{O}$

106 $R_1 = -\text{O}(\text{CH}_2)_2-\text{N}(\text{CH}_2)_2\text{O}$

107 $R_1 = -\text{OH}$



Series II. 108-112

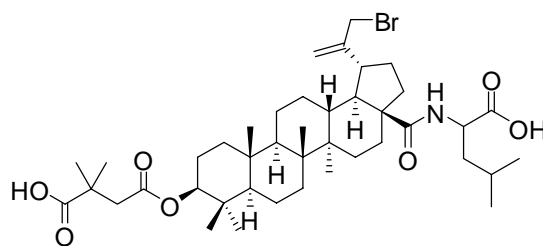
108 $R_1 = -\text{H}, R_2 = \text{OH}$

109 $R_1 = -\text{Br}, R_2 = \text{OH}$

110 $R_1 = -\text{OH}, R_2 = \text{OH}$

111 $R_1 = -\text{O}(\text{CH}_2)_2-\text{N}(\text{CH}_2)_2\text{O}, R_2 = \text{OH}$

112 $R_1 = -\text{O}(\text{CH}_2)_2-\text{N}(\text{CH}_2)_2\text{O}, R_2 = \text{NHCH}_3$



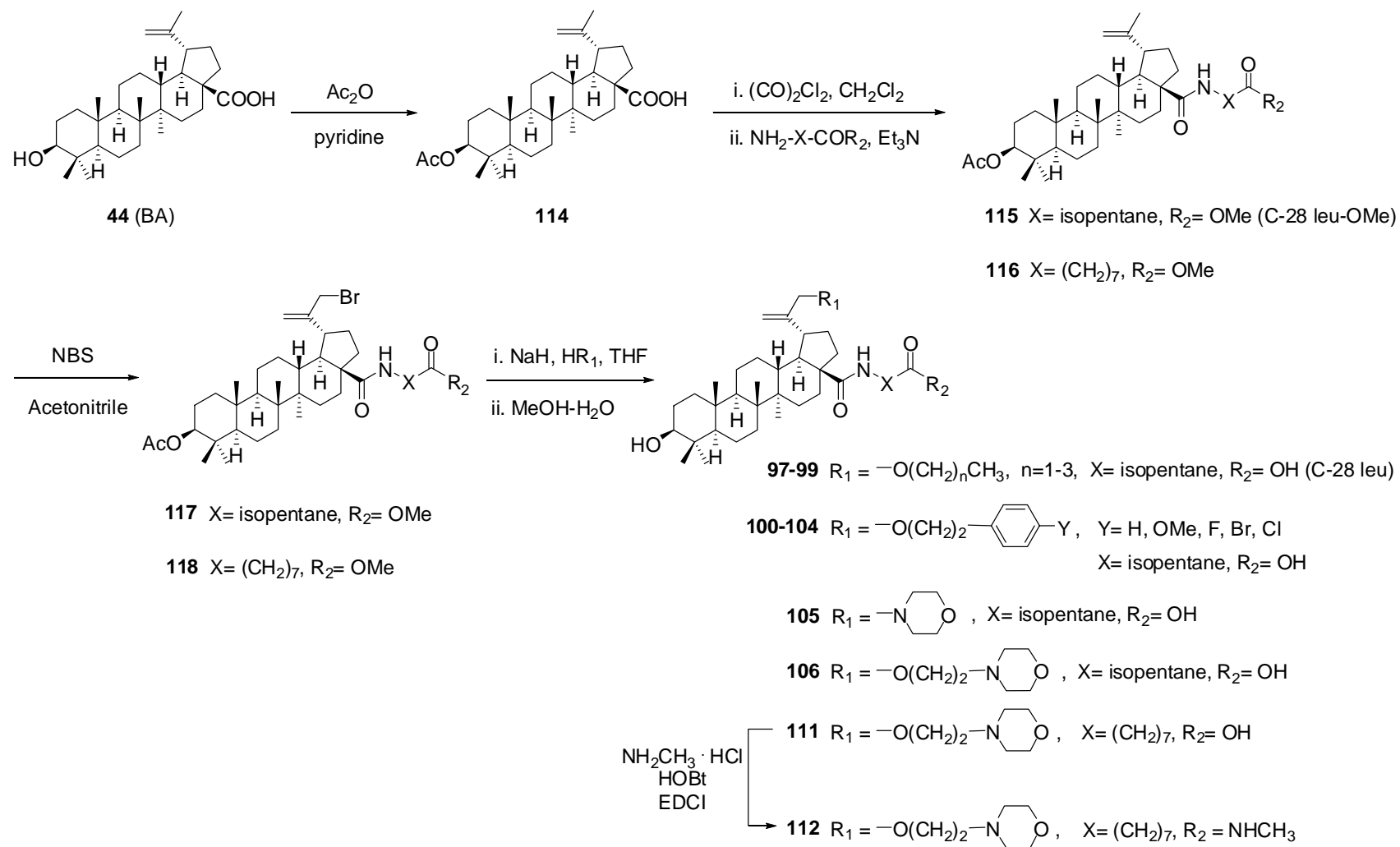
113

Figure 4-2. Structures of Series I (96-107), Series II (108-112) and 113

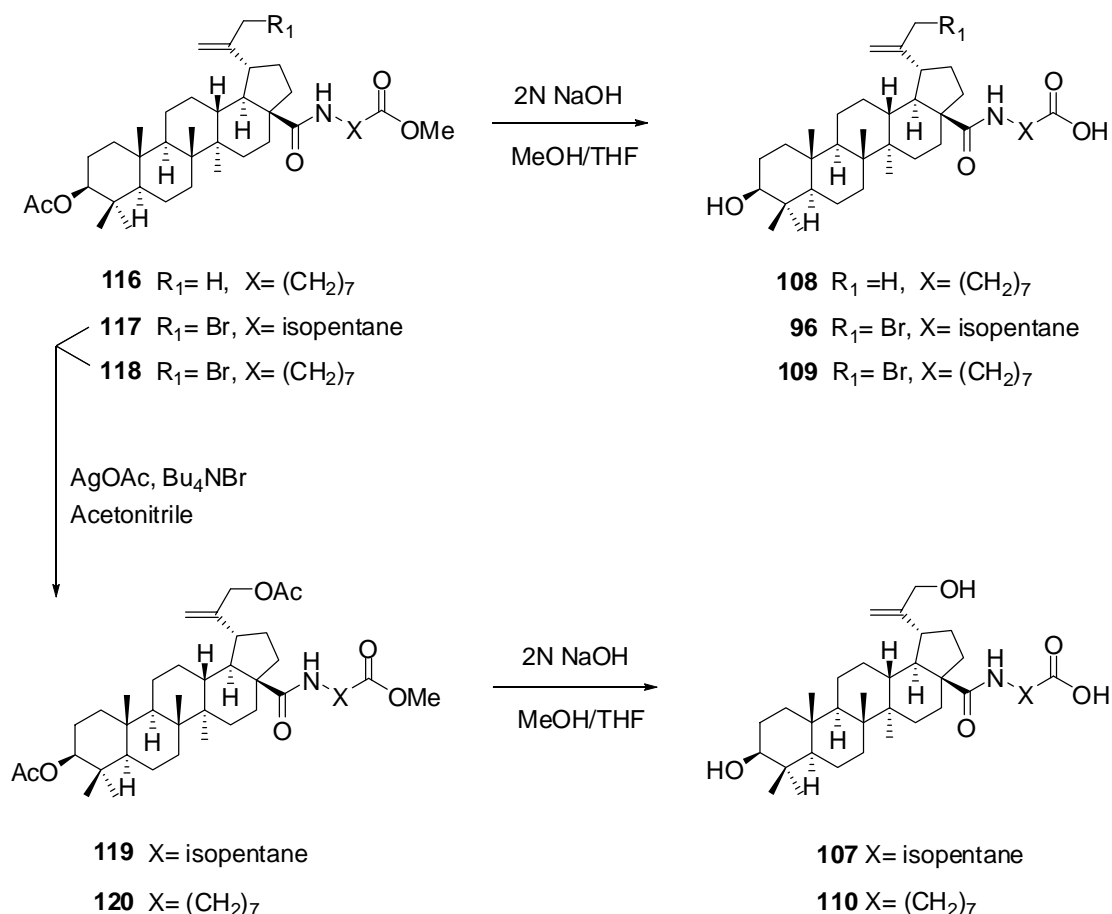
3. Chemistry

Scheme 4-1 depicts the syntheses of 28,30-disubstituted BA derivatives **97-16** and **111-112**. The C-3 β -hydroxyl group of BA was protected as the acetate ester by reaction with acetic anhydride to yield 3-OAc-BA (**114**). Compound **114** was treated with oxalyl chloride in dichloromethane to yield an intermediate acid chloride, which was then reacted with readily prepared leucine methyl ester and 8-aminooctanoic acid

methylester to furnish **115** and **116** in yields of 81% and 98%, respectively. Allylic bromination of **115** and **116** was carried out using *N*-bromosuccinimide (NBS) in dilute acetonitrile at room temperature to provide 30-bromo BA derivatives **117** and **118** in 66% and 72.5% yield, respectively. More concentrated solvent conditions or heating led to the formation of byproducts, which had close R_f values, resulting in difficult separation. We first attempted to use the Trost-Tsuji π -allylpalladium procedure¹⁵⁶ to replace the bromide group in **117** and **118** with different nucleophiles. In detail, palladium acetate and triphenylphosphine were stirred with triethylamine in THF at room temperature for 30 min. After a yellow-orange suspension was formed, the appropriate nucleophilic compound and 30-bromo BA derivative **117** were added, and the reaction was carried out at reflux for more than 144 h.¹⁵⁶ The whole process was conducted under dry nitrogen atmosphere. However, no product was detected. An alternative synthetic method was then applied. In this method, the desired nucleophilic compound was first treated with 10 equivalents of NaH under dry nitrogen gas in THF for 30 min. The 30-bromo BA derivative (**117** or **118**) was then added into the system. The reactions were carried out using a microwave apparatus at 120 °C for 30 min. After the reaction mixture was cooled to room temperature, 1 mL MeOH-H₂O was added to convert the intermediate esters to carboxylic acids by saponification, which furnished the target compounds **97-106** and **111** in 59-77% yields. Reaction of **111** with methylamine in the presence of HOBt/EDCI in dichloromethane led to **112** in a 69% yield.



Scheme 4-1. General synthetic route to 97-106, 111-112



Scheme 4-2. Synthesis of 96, 107-110

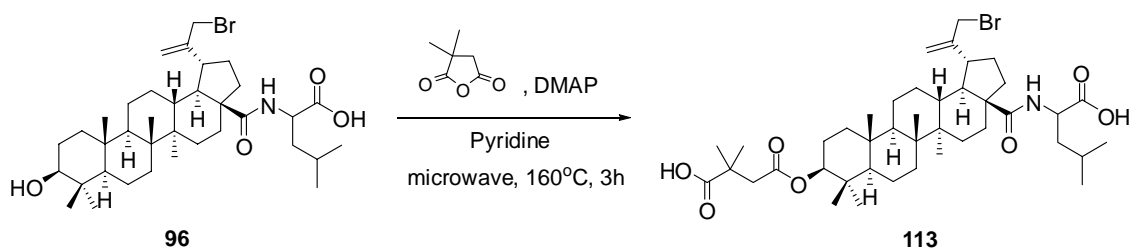


Figure 4-3. Synthesis of 113

Saponification of intermediate esters **116-118** with 2N sodium hydroxide in MeOH/THF yielded the corresponding carboxylic acids **108**, **96** and **109** quantitatively (Scheme 4-2). Reaction of silver acetate with the 30-bromo BA derivatives **117** and **118**, in the presence of a catalytic amount of the phase transfer

catalyst tetrabutylammonium bromide (Bu₄NBr) in acetonitrile, gave diacetoxy esters **119** and **120** in yields of 68% and 69.5%, respectively.¹⁵⁷ Saponification of these diacetoxy esters were then carried out with 2N sodium hydroxide in MeOH/THF to yield 30-hydroxyl BA derivatives **107** and **110** (Scheme 4-2).

The 3,28,30-trisubstituted BA analog **113** was synthesized according to Scheme 4-3. Compound **96** was reacted with 2',2'-dimethylsuccinic anhydride in the presence of DMAP in pyridine at 160 °C using microwave technology for 3h to furnish **113** in 32% yield. A longer reaction time was needed compared to corresponding esterification of BA.

4. Results and Discussion

The anti-HIV-1 replication activities of Series I (**96-107**), Series II (**108-112**), **113** and some intermediates (**115-120**) were assessed in HIV-1_{IIIB} infected MT-2 cells in parallel with AZT, bevirimat (DSB, **58**) and **95**. The results are summarized in Table 4-1. Selected compounds were further evaluated in HIV-1_{NL4-3} infected MT-4 cells using the prior best entry inhibitor hit **94** as the control, and the data are listed in Table 4-2.

Among Series I compounds, **104** and **106** showed very weak antiviral activity against HIV-1_{IIIB}, while the remaining 28,30-disubstituted BA derivatives from this series did not inhibit replication of either the HIV-1_{IIIB} or HIV-1_{NL4-3} variant. Surprisingly, **95**, which showed moderate anti-HIV-1 entry activity in an *in vitro* fusion assay, also did not exhibit antiviral replication activity in these general

screenings. This result indicates that the C-30 modification of **95** did not cause the resulting derivatives from Series I to lose antiviral potency. However, because neither the presence of different C-30 substitutions nor reduction of the 20(29) double bond increased anti-HIV-1 activity of BA derivatives, the C-19 isopropenyl moiety is unlikely to be an activity pharmacophore. Thus, C-30 modification may still be useful to influence pharmacological properties, such as hydrophilicity and solubility.

The conflicting results with **95** in the HIV replication and fusion assays and the poor “pharmacodynamic properties” of **47** led us to postulate that introduction of the critical C-28 lipophilic side chain may result in derivatives with poor physicochemical properties or stability problems. The calculated partition coefficient (Log P) values of **47/48**, **94** and **95** (average 9.33) support our postulate. Therefore, our next step in developing potent anti-HIV-1 entry inhibitors was to increase the derivatives’ antiviral potency as well as improve their physicochemical properties.

Accordingly, in analog **108** of Series II analogs, the C-28 amide side chain is 8-aminooctanoic acid rather than leucine as in **95**. Other groups, including bromide, hydroxyl and 2-morpholinoethoxy, were also introduced at C-30 to provide corresponding analogs **109–111**, respectively. While **95** showed no suppression of HIV-1_{IIIB} replication, **108**, **109** and **111** had EC₅₀ values ranging from 1.8 to 3.3 μ M (Table 4-1). However, the introduction of a free hydroxyl group at C-30 reduced the antiviral activity of **110** by several folds. Because prior studies showed that a primary amine substituent at C-30 is also unfavorable, it seems that a hydrogen bond donor is not tolerated near the C-19 isopropenyl moiety. Nevertheless, our results still confirm

that, except for hydroxyl and amine moieties, the C-30 position of BA can accommodate some diverse substituents without influencing the antiviral activity of C-28 modified BA derivatives (compare **108** and **111**). The introduction of the morpholinoethoxy moiety in **111** reduced the Log P value to 8.26 (\pm 0.69), resulting in a notable increase in the derivative's solubility. In addition, because prior studies have shown that a second amide bond near the end of the C-28 side chain is necessary for enhanced antiviral potency, the terminal carboxylic acid of **111** was reacted with methylamine to produce **112**. Interestingly, **112** differs from the prior best hit A43-D (**94**) only in the direction of the terminal amide linkage (-CONHCH₃ in **112** and -NHCOCH₃ in **94**). Analog **112** exhibited potent anti-HIV-1 activity with an EC₅₀ value of 0.09 μ M and TI of 250 against both HIV-1_{IIIB} and HIV-1_{NL4-3} variants, which were similar to those of **94** (EC₅₀: 0.10 μ M, TI > 150) and comparable to those of **58** (EC₅₀: 0.011 μ M, TI > 3.6 \times 10³). Moreover, **112** shows a significantly reduced Log P value of 7.50 (\pm 0.72) compared to those of **94** and **47/48**, resulting in greater water solubility. Since Compound **112** is also a C-28 modified BA derivative, we postulate that it also functions as a HIV-1 entry inhibitor.

Intermediates **115-118** as well as diacetoxo esters **119** and **120** did not inhibit HIV-1_{IIIB} replication at the tested concentrations. This result is consistent with our previous finding that a C-28 terminal carboxylic acid or amide moiety is necessary for antiviral potency. An ester group at the C-28 side chain terminus and acetyl protection of the C-3 β -hydroxyl group reduced anti-HIV-1 activity significantly.

Finally, the C-3 β -hydroxyl group of **96** was esterified with

2',2'-dimethylsuccinic anhydride to give **113**. This analog showed extremely potent antiviral activity with an EC₅₀ value of 0.009 μ M and TI of 3.5×10^3 , which are similar to those of bevirimat (DSB, **58**) and slightly better than those of AZT (Table 4-1). This result suggests that the presence of small substitutions on C-28 and C-30 of BA does not harm the high anti-HIV-1 potency of **58**. Thus, incorporation of polar groups into the C-30 position may also help to improve the hydrophobicity of bi-functional BA derivatives.

In conclusion, diverse 28,30-disubstituted BA analogs were synthesized in our study. We found that hydrogen bond donors such as a hydroxyl group and primary amine moieties are not tolerated near the C-19 isopropenyl moiety. Otherwise, C-30 substitution did not significantly influence the anti-HIV-1 activity of the C-28 modified BA derivative. Therefore, the C-30 position serves as a good place to incorporate water-solubilizing moieties to increase the hydrophilicity of C-28 modified BA derivatives. Accordingly, combination of a morpholinoethoxy group at C-30 together with aminooctanoic acid N-methylamide at C-28 led to the discovery of **112**, which showed potent anti-HIV-1 activity similar to that of **47**, **48** and **94**. Compared to **47/48** and **94**, **112** had a smaller calculated Log P value and significantly increased water solubility, suggesting that it may have a better tissue distribution profile. Moreover, a 3,28,30-trisubstituted BA analog **113** was synthesized in this study. The high potency of **113** suggests that combination of C-3 and C-28 modifications (for activity) and C-30 modification (for physicochemical properties) into one BA molecule is feasible.

Table 4-1. Anti-HIV-1 replication activities of 96-113, 115-120 in HIV-1_{IIIB} infected MT-2 cell lines ^a

	EC ₅₀ (μM)	IC ₅₀ (μM)	TI		EC ₅₀ (μM)	IC ₅₀ (μM)	TI
AZT	0.056	1,870	33,392	107	NS	30.72	–
58	0.011	40	3,636	108	3.3	> 33.44	> 10.1
95	NS	29.75	–	109	2.3	> 36.94	> 16.1
96	NS	26.77	–	110	14.8	> 40.72	> 2.8
97	NS	40.72	–	111	1.8	> 24.76	> 13.8
98	NS	25.32	–	112	0.09	22.31	249.9
99	NS	24.92	–	115	NS	39.94	–
100	NS	21.74	–	116	NS	38.23	–
101	NS	16.67	–	117	NS	35.47	–
102	NS	24.44	–	118	NS	34.11	–
103	NS	20.81	–	119	NS	36.55	–
104	27.8	> 34.55	> 1.2	120	28.5	> 35.11	> 1.2
105	NS	27.48	–	113	0.009	> 32.18	> 3,576
106	26.6	> 35.76	> 1.4				

^a All data presented are averages of at least two separate experiments performed by Panacos Pharmaceutical Inc., Gaithersburg, MD. EC₅₀: concentration that inhibits HIV-1_{IIIB} replication by 50%. IC₅₀: concentration that inhibits mock-infected MT-2 cell growth by 50%. TI = IC₅₀/EC₅₀. NS: no suppression at the testing concentration (10μg/mL).

Table 4-2. Anti-HIV-1 replication activities of 95-107 and 112 in HIV-1_{NL4-3} infected MT-4 cell lines ^b

	EC ₅₀ (μM)	IC ₅₀ (μM) ^c	TI		EC ₅₀ (μM)	IC ₅₀ (μM)	TI
94	0.10	> 10	> 150	102	NS	NT	–
95	NS	NT	–	103	NS	NT	–
96	NS	NT	–	104	NS	NT	–
97	NS	NT	–	105	NS	NT	–
98	NS	NT	–	106	NS	NT	–
99	NS	NT	–	107	NS	NT	–
100	NS	NT	–	112	0.09	> 10	> 138
101	NS	NT	–				

^b All data presented are averages of at least two separate experiments performed by Dr. Chin-Ho Chen, Duke University, NC. ^c IC₅₀ was not tested for inactive compounds. EC₅₀: concentration that inhibits HIV-1_{NL4-3} replication by 50%. IC₅₀: concentration that inhibits mock-infected MT-4 cell growth by 50%. TI = IC₅₀/EC₅₀. NS: no suppression at the testing concentration (10μg/mL).

5. Experimental Section

5-1. Chemistry

The melting points were measured with a Fisher Johns melting apparatus without correction. ¹H NMR spectra were measured on a 300MHz Varian Gemini 2000 spectrometer using Me₄Si (TMS) as internal standard. The solvent used was CDCl₃ unless otherwise indicated. Mass spectra were measured on Shimadzu LCMS-2010 (ESI-MS). Optical rotations were measured with a Jasco Dip-2000

digital polarimeter at 20 °C at the sodium D line. Thin-layer chromatography (TLC) and preparative thin-layer chromatography (PTLC) were performed on Merck precoated silica gel 60 F-254 plates. Flash+TM and CombiFlash systems were used as medium pressure column chromatography. Silica gel (200-400 mesh) from Aldrich, Inc., was used for column chromatography. All other chemicals were obtained from Aldrich, Inc.

3-*O*-Acetyl-betulinic acid (114): A mixture of betulinic acid (2.1 g), pyridine (1.5 mL) and acetic anhydride (Ac₂O, 20mL) was stirred at room temperature overnight until it became homogenous. The reaction was then poured into ice-cold water (30 mL) and stirred for 20 min. The crude product was filtered off and purified on a silica-gel column to yield 1.98 g (87% yield) of pure **114**; white amorphous powder. Mp 289-291 °C. MS (ESI-) *m/z*: 497.38 (M⁻ - H) for C₃₂H₅₀O₄. ¹H NMR (300 MHz, CDCl₃): δ 4.74, 4.61 (1H each, s, H-29), 4.47 (1H, dd, *J* = 9.9, 5.9 Hz, H-3), 3.01 (1H, m, H-19), 2.05 (3H, s, OCOCH₃), 1.69 (3H, s, H-30), 0.97, 0.93, 0.86, 0.84, 0.83 (3H each, s, 5 × CH₃).

Syntheses of BA derivatives 115 and 116. Oxalyl chloride solution (2M in CH₂Cl₂, 10 mL) was added to **114** (1 eq) in CH₂Cl₂ (10 mL) and stirred for 2 h. After concentration under vacuum, the residual mixture was treated with leucine methyl ester (1.6 eq), or 8-aminooctanoic acid methyl ester (1.6 eq) and triethylamine (Et₃N, 1.2 eq) in CH₂Cl₂. The mixture was stirred at room temperature overnight until no starting material was observed by TLC. The solution was then diluted with CH₂Cl₂ (20 mL) and washed three times with brine and distilled water. The organic layer was

dried over anhydrous Na₂SO₄ and concentrated to dryness under reduced pressure. The residue was chromatographed using a silica gel column to yield the pure target compounds.

Methyl *N*-[3 β -Acetoxy-lup-20(29)-en-28-oyl]-leucinate (115): 1.15 g (80.5% yield) starting from 1 g of **114**; white amorphous powder. Mp 230-232 °C. MS (ESI+) *m/z*: 626.48 (M⁺ + H), 648.47 (M⁺ + Na) for C₃₉H₆₃NO₅. ¹H NMR (300 MHz, CDCl₃): δ 5.87 (1H, d, *J* = 8 Hz, -CONH-), 4.72, 4.59 (1H each, s, H-29), 4.64 (1H, m, -NHCH-), 4.49 (1H, t, *J* = 8 Hz, H-3), 3.73 (3H, s, -COOCH₃), 3.05 (1H, m, H-19), 2.10-2.20 (1H, m, H-13), 2.04 (3H, s, OCOCH₃), 1.68 (3H, s, H-30), 1.01 (6H, s, leucine moiety -(CH₃)₂), 0.97 (6H, s, 2 \times CH₃), 0.89, 0.84, 0.83 (3H each, s, 3 \times CH₃).

Methyl *N*-[3 β -Acetoxy-lup-20(29)-en-28-oyl]-8-aminooctanoate (116): 643 mg (98% yield) starting from 500 mg of **114**; light yellow amorphous powder. Mp 104-105 °C. MS (ESI+) *m/z*: 654.5 (M⁺ + H) for C₄₁H₆₇NO₅. ¹H NMR (300 MHz, CDCl₃): δ 5.57 (1H, t, *J* = 6 Hz, -CONH-), 4.73, 4.60 (1H each, s, H-29), 4.45 (1H, m, H-3), 3.67 (3H, s, -COOCH₃), 3.30-3.08 (3H, m, H-19, -CONHCH₂-), 2.50 (1H, m, H-13), 2.31 (2H, t, *J* = 7 Hz, -CH₂COOCH₃), 2.05 (3H, s, OCOCH₃), 1.68 (3H, s, H-30), 0.97, 0.94 (3H each, s, 2 \times CH₃), 0.85, 0.84, 0.81 (3H each, s, 3 \times CH₃).

Syntheses of BA derivatives 117 and 118. A mixture of N-bromosuccinimide (1.1 eq) and **115** or **116** (1 eq) in acetonitrile (ACN, 30 mL) was stirred at room temperature until the starting material was not observed by TLC. The reaction was concentrated to dryness under reduced pressure and chromatographed over silica gel to yield pure target compounds.

Methyl *N*-[3 β -Acetoxy-30-bromo-lup-20(29)-en-28-oyl]-leucinate (117):

297 mg (66% yield) starting from 400 mg of **115**; light yellow amorphous powder. Mp 127-129 °C. MS (ESI+) m/z : 704.4 ($M^+ + H$), 706.4 ($M^+ + H$) for $C_{39}H_{62}BrNO_5$. 1H NMR (300 MHz, $CDCl_3$): δ 5.81 (1H, d, $J = 8$ Hz, -CONH-), 5.11, 5.05 (1H each, s, H-29), 4.65 (1H, m, -NHCH-), 4.45 (1H, t, $J = 8$ Hz, H-3), 4.00 (2H, s, H₂-30), 3.72 (3H, s, -COOCH₃), 3.10 (1H, m, H-19), 2.50-2.32 (1H, m, H-13), 2.05 (3H, s, OCOCH₃), 1.02 (6H, s, leucine moiety -(CH₃)₂), 0.99 (6H, s, 2 \times CH₃), 0.89, 0.86, 0.85 (3H each, s, 3 \times CH₃).

Methyl *N*-[3 β -Acetoxy-30-bromo-lup-20(29)-en-28-oyl]-8-aminooctanoate

(118): 402 mg (72.5% yield) starting from 360 mg of **116**; light yellow amorphous powder. Mp 99-101 °C. MS (ESI+) m/z : 732.4 ($M^+ + H$), 734.4 ($M^+ + H$) for $C_{41}H_{66}BrNO_5$. 1H NMR (300 MHz, $CDCl_3$): δ 5.59 (1H, t, $J = 6$ Hz, -CONH-), 5.13, 5.04 (1H each, s, H-29), 4.47 (1H, t, $J = 8.1$ Hz, H-3), 4.00 (2H, s, H₂-30), 3.67 (3H, s, -COOCH₃), 3.41-3.09 (3H, m, H-19, -CONHCH₂-), 2.46 (1H, m, H-13), 2.31 (2H, t, $J = 7.5$ Hz, -CH₂COOCH₃), 2.04 (3H, s, OCOCH₃), 0.97, 0.93 (3H each, s, 2 \times CH₃), 0.89, 0.84, 0.83 (3H each, s, 3 \times CH₃).

Syntheses of BA derivatives 97-106 and 111. NaH (60% in mineral oil) was washed three times with hexane. A solution of appropriate nucleophilic compound (8 eq) and NaH (10 eq) in anhydrous THF (1.5 mL) was stirred under dry nitrogen at room temperature for 30 min. The 30-bromo BA derivative **117** or **118** (1 eq) was then added into the system. The reaction was heated using microwave at 120 °C for 30 min. After cooling to room temperature, 1 mL MeOH-H₂O was added into the mixtures

and stirred to transform the intermediate esters to carboxylic acids by saponification. The reaction was neutralized with 10% HCl and dried under vacuum and reconstituted with EtOAc. The organic layer was washed with brine and dried over anhydrous Na₂SO₄ and concentrated to dryness under reduced pressure. The residue was chromatographed using a silica gel column to yield the pure target compounds.

***N*-[3 β -Hydroxy-30-ethoxy-lup-20(29)-en-28-oyl]-leucine (97):** 22 mg (59% yield) starting from 40 mg of **117**; white amorphous powder. Mp 128-130 °C. MS (ESI-) *m/z*: 612.4 (M⁻ - H) for C₃₈H₆₃NO₅. ¹H NMR (300 MHz, CDCl₃): δ 5.88 (1H, d, *J* = 8 Hz, -CONH-), 4.93, 4.92 (2H, *br s*, H-29), 4.63-4.58 (1H, m, -NHCH-), 3.90 (2H, s, H₂-30), 3.47 (2H, m, 30-OCH₂CH₃), 3.18 (1H, dd, *J* = 11.1, 5.4 Hz, H-3), 2.99 (1H, m, H-19), 2.50-2.32 (1H, m, H-13), 1.00 (9H, *br s*, 30-OCH₂CH₃, leucine moiety -(CH₃)₂), 0.96 (6H, s, 2 \times CH₃), 0.89, 0.86, 0.85 (3H each, s, 3 \times CH₃).

***N*-[3 β -Hydroxy-30-propoxy-lup-20(29)-en-28-oyl]-leucine (98):** 23 mg (60% yield) starting from 40 mg of **117**; white amorphous powder. Mp 116-117 °C. MS (ESI-) *m/z*: 626.5 (M⁻ - H) for C₃₉H₆₅NO₅. ¹H NMR (300 MHz, CDCl₃): δ 6.13 (1H, *br s*, -CONH-), 4.91, 4.90 (2H, *br s*, H-29), 4.52 (1H, m, -NHCH-), 3.90 (2H, s, H₂-30), 3.36 (2H, t, *J* = 6.9 Hz, 30-OCH₂CH₂CH₃), 3.18 (1H, dd, *J* = 11.1, 5.4 Hz, H-3), 2.99 (1H, m, H-19), 0.96, 0.94, 0.92, 0.89 (15H, m, 30-O(CH₂)₂CH₃, leucine moiety -(CH₃)₂, CH₃-23, 24), 0.82, 0.81, 0.79 (3H each, s, 3 \times CH₃).

***N*-[3 β -Hydroxy-30-butoxy-lup-20(29)-en-28-oyl]-leucine (99):** 10 mg (37% yield) starting from 30 mg of **117**; yellow amorphous powder. Mp 104-105 °C. MS (ESI-) *m/z*: 640.2 (M⁻ - H) for C₄₀H₆₇NO₅. ¹H NMR (300 MHz, CDCl₃): δ 6.01 (1H,

br s, -CONH-), 4.90, 4.88 (2H, *br s*, H-29), 4.58 (1H, *m*, -NHCH-), 3.89 (2H, *s*, H₂-30), 3.37 (2H, *m*, 30-OCH₂(CH₂)₂CH₃), 3.17 (1H, *m*, H-3), 3.01 (1H, *m*, H-19), 0.99 (9H, *br s*, 30-O(CH₂)₃CH₃, leucine moiety -(CH₃)₂), 0.96 (6H, *s*, 2 × CH₃), 0.86, 0.84, 0.81 (3H each, *s*, 3 × CH₃).

***N*-[3β-Hydroxy-30-phenethoxy-lup-20(29)-en-28-oyl]-leucine (100)**: 37 mg (77% yield) starting from 50 mg of **117**; light yellow amorphous powder. Mp 155-157 °C. MS (ESI-) *m/z*: 688.4 (M⁻ - H) for C₄₄H₆₇NO₅. ¹H NMR (300 MHz, CDCl₃): δ 7.68-7.62 (2H, *m*, H ar-3'), 7.28-7.20 (3H, *m*, H ar-2', 4'), 5.97 (1H, *br s*, -CONH-), 4.91, 4.90 (2H, *br s*, H-29), 4.44 (1H, *m*, -NHCH-), 3.93 (2H, *s*, H₂-30), 3.64 (2H, *t*, *J* = 7.2 Hz, 30-OCH₂CH₂ph), 3.17 (1H, *dd*, *J* = 11.1, 5.4 Hz, H-3), 2.91 (1H, *m*, H-19), 2.57 (2H, *m*, 30-OCH₂CH₂ph), 0.95 (12H, *s*, leucine moiety -(CH₃)₂, CH₃-23, 24), 0.89, 0.78, 0.74 (3H each, *s*, 3 × CH₃).

***N*-[3β-Hydroxy-30-(4'-methoxyphenethoxy)-lup-20(29)-en-28-oyl]-leucine (101)**: 46 mg (64% yield) starting from 70 mg of **117**; light yellow amorphous powder. Mp 128-129 °C. MS (ESI-) *m/z*: 718.5 (M⁻ - H) for C₄₅H₆₉NO₆. ¹H NMR (300 MHz, CDCl₃): δ 7.27, 7.16-7.13, 6.85-6.82 (5H, *m*, H ar-2', 3', 4'), 5.97 (1H, *br s*, -CONH-), 4.91, 4.89 (H each, *br s*, H-29), 4.48 (1H, *m*, -NHCH-), 3.93 (2H, *s*, H₂-30), 3.79 (3H, *s*, ar-OCH₃), 3.60 (2H, *t*, *J* = 7.2 Hz, 30-OCH₂CH₂ph(*p*-OCH₃)), 3.17 (1H, *dd*, *J* = 11.1, 5.4 Hz, H-3), 2.85 (1H, *t*, *J* = 7.5 Hz, H-19), 2.39 (3H, *m*, 30-OCH₂CH₂ph(*p*-OCH₃), H-13), 0.95, 0.93, 0.90 (15H, *s*, leucine moiety -(CH₃)₂, 3 × CH₃), 0.79, 0.75 (3H each, *s*, 2 × CH₃).

***N*-[3β-Hydroxy-30-(4'-fluorophenethoxy)-lup-20(29)-en-28-oyl]-leucine**

(102): 24 mg (40% yield) starting from 60 mg of **117**; light yellow amorphous powder. Mp 102–104 °C. MS (ESI-) *m/z*: 706.4 ($M^- - H$) for $C_{44}H_{66}FNO_6$. 1H NMR (300 MHz, $CDCl_3$): δ 7.16–6.80 (5H, m, H ar-2', 3', 4'), 5.96 (1H, *br s*, -CONH-), 4.90, 4.89 (2H, *br s*, H-29), 4.48 (1H, m, -NHCH-), 3.92 (2H, s, H₂-30), 3.61 (2H, t, $J = 7.2$ Hz, 30-OCH₂CH₂ph(*p*-F)), 3.17 (1H, m, H-3), 2.87 (1H, t, $J = 7.5$ Hz, H-19), 2.36–2.10 (3H, m, 30-OCH₂CH₂ph(*p*-F), H-13), 0.95, 0.88 (15H, s, leucine moiety -(CH₃)₂, 3 × CH₃), 0.75, 0.73 (3H each, s, 2 × CH₃).

***N*-[3 β -Hydroxy-30-(4'-bromophenethoxy)-lup-20(29)-en-28-oyl]-leucine**

(103): 18 mg (41% yield) starting from 40 mg of **117**; light yellow amorphous powder. Mp 127–129 °C. MS (ESI-) *m/z*: 706.4 ($M^- - H$) for $C_{44}H_{66}BrNO_6$. 1H NMR (300 MHz, $CDCl_3$): δ 7.56–7.28 (5H, m, H ar-2', 3', 4'), 5.96 (1H, *br s*, -CONH-), 4.91, 4.90 (2H, *br s*, H-29), 4.48 (1H, m, -NHCH-), 3.91 (2H, s, H₂-30), 3.60 (2H, t, $J = 7.0$ Hz, 30-OCH₂CH₂ph(*p*-Br)), 3.17 (1H, dd, $J = 11.0, 5.6$ Hz, H-3), 2.89 (1H, t, $J = 7.5$ Hz, H-19), 2.39 (1H, m, 30-OCH₂CH₂ph(*p*-Br)), 0.96 (12H, s, leucine moiety -(CH₃)₂, 2 × CH₃), 0.82, 0.79, 0.75 (3H each, s, 3 × CH₃).

***N*-[3 β -Hydroxy-30-(4'-chlorophenethoxy)-lup-20(29)-en-28-oyl]-leucine**

(104): 16 mg (38% yield) starting from 40 mg of **117**; light yellow amorphous powder. Mp 119–121 °C. MS (ESI-) *m/z*: 706.4 ($M^- - H$) for $C_{44}H_{66}ClNO_6$. 1H NMR (300 MHz, $CDCl_3$): δ 7.18–6.87 (5H, m, H ar-2', 3', 4'), 5.96 (1H, *br s*, -CONH-), 4.91, 4.90 (2H, *br s*, H-29), 4.48 (1H, m, -NHCH-), 3.91 (2H, s, H₂-30), 3.62 (2H, t, $J = 6.8$ Hz, 30-OCH₂CH₂ph(*p*-Cl)), 3.17 (1H, dd, $J = 11.0, 5.6$ Hz, H-3), 2.87 (1H, t, $J = 7.5$ Hz, H-19), 2.36–2.06 (3H, m, 30-OCH₂CH₂ph(*p*-Cl), H-13), 0.96 (15H, s, leucine moiety

-(CH₃)₂, 3 × CH₃), 0.81, 0.76 (3H each, s, 2 × CH₃).

***N*-[3β-Hydroxy-30-morpholino-lup-20(29)-en-28-oyl]-leucine (105)**: 22 mg (41% yield) starting from 60 mg of **117**; white amorphous powder. Mp 98-100 °C. MS (ESI-) *m/z*: 653.5 (M⁻ - H) for C₄₀H₆₆N₂O₅. ¹H NMR (300 MHz, CDCl₃): δ 5.61 (1H, d, *J* = 6 Hz, -CONH-), 4.92, 4.90 (H each, s, H-29), 4.63-4.58 (1H, m, -NHCH-), 3.72 (4H, m, 30-N(CH₂CH₂)₂O), 3.17 (1H, dd, *J* = 11.1, 5.4 Hz, H-3), 3.00 (3H, m, H-19, H₂-30), 2.53 (4H, m, 30-N(CH₂CH₂)₂O), 2.42 (1H, m, H-13), 0.96 (6H, s, leucine moiety -(CH₃)₂), 0.92 (6H, s, 2 × CH₃), 0.86, 0.81, 0.75 (3H each, s, 3 × CH₃).

***N*-[3β-Hydroxy-30-(2'-morpholinoethoxy)-lup-20(29)-en-28-oyl]-leucine (106)**: 26 mg (56% yield) starting from 50 mg of **117**; white amorphous powder. Mp 89-91 °C. MS (ESI-) *m/z*: 697.4 (M⁻ - H) for C₄₂H₇₀N₂O₆. ¹H NMR (300 MHz, CDCl₃): δ 5.61 (1H, d, *J* = 8 Hz, -CONH-), 4.92, 4.90 (H each, s, H-29), 4.59 (1H, m, -NHCH-), 3.94 (2H, s, H₂-30), 3.72 (4H, m, -N(CH₂CH₂)₂O), 3.58 (2H, t, *J* = 5.7 Hz, 30-OCH₂CH₂-morpholine), 3.18 (1H, dd, *J* = 11.4, 4.6 Hz, H-3), 3.01 (1H, m, H-19), 2.60 (2H, t, *J* = 5.4 Hz, 30-OCH₂CH₂-morpholine), 2.53 (4H, m, -N(CH₂CH₂)₂O), 1.00 (6H, s, leucine moiety -(CH₃)₂), 0.96 (6H, s, 2 × CH₃), 0.89, 0.85, 0.80 (3H each, s, 3 × CH₃).

***N*-[3β-Hydroxy-30-(2'-morpholinoethoxy)-lup-20(29)-en-28-oyl]-8-aminooctanoic acid (111)**: 51 mg (64% yield) starting from 80 mg **118**; white amorphous powder. Mp 111-112 °C. MS (ESI-) *m/z*: 725.5 (M⁻ - H) for C₄₄H₇₄N₂O₆. ¹H NMR (300 MHz, CDCl₃): δ 5.61 (1H, d, *J* = 8 Hz, -CONH-), 4.91, 4.90 (H each, s, H-29), 3.94 (2H, s, H₂-30), 3.72 (4H, m, -N(CH₂CH₂)₂O), 3.58 (2H, t, *J* = 5.7 Hz,

30-OCH₂CH₂-morpholine), 3.18 (3H, m, -CONHCH₂-, H-3), 3.01 (1H, m, H-19), 2.60 (2H, t, *J* = 5.4 Hz, 30-OCH₂CH₂-morpholine), 2.53 (4H, m, -N(CH₂CH₂)₂O), 2.28 (2H, t, *J* = 7.5 Hz, -CH₂COOH), 0.96 (6H, s, 2 × CH₃), 0.92, 0.81, 0.75 (3H each, s, 3 × CH₃).

***N'*-[*N*-[3β-Hydroxy-30-(2'-morpholinoethoxy)-lup-20(29)-en-28-oyl]-8-aminoctanoyl]-aminomethane (112):** A solution of **111** (30 mg, 1 eq), EDCI (2 eq), N-Hydroxybenzotriazole (HOBt, 1 eq), Et₃N (0.05 mL) and methylamine hydrochloride (2 eq) in anhydrous CH₂Cl₂ (8 mL) was stirred at room temperature overnight until the starting material was not observed by TLC. The solution was diluted with CH₂Cl₂ (20 mL) and washed three times with brine and distilled water. The organic layer was dried over anhydrous Na₂SO₄ and concentrated to dryness under reduced pressure. The residue was chromatographed using a silica gel column to yield 21 mg (69% yield) of pure **112**; white amorphous powder. Mp 106-107 °C. MS (ESI+) *m/z*: 740.5 (M⁺ + H) for C₄₅H₇₇ N₃O₅. ¹H NMR (300 MHz, CDCl₃): δ 5.61 (2H, m, 2 × -CONH-), 4.92, 4.90 (H each, s, H-29), 3.94 (2H, s, H₂-30), 3.72 (4H, m, -N(CH₂CH₂)₂O), 3.58 (2H, t, *J* = 5.7 Hz, 30-OCH₂CH₂-morpholine), 3.28-3.14 (3H, m, -CONHCH₂-, H-3), 3.01 (1H, m, H-19), 2.81 (3H, d, *J* = 4.8 Hz, -CONHCH₃), 2.60 (2H, t, *J* = 5.4 Hz, 30-OCH₂CH₂-morpholine), 2.53 (4H, m, -N(CH₂CH₂)₂O), 2.16 (2H, t, *J* = 7.5 Hz, -CH₂CONHCH₃), 0.96 (6H, s, 2 × CH₃), 0.92, 0.81, 0.75 (3H each, s, 3 × CH₃).

Syntheses of BA derivatives 119 and 120. A solution of 30-bromo BA derivative **117** or **118** (1 eq), silver acetate (AgOAc, 2 eq) and tetrabutylammonium

bromide (Bu_4NBr , 0.2 eq) in acetonitrile (1.5 mL) was heated using microwave at 100 °C for 25 min. The precipitant was filtered and the solution was concentrated to dryness under vacuum. The residue was chromatographed over a silica-gel column to yield the pure diacetoxyl intermediates **119** and **120**.

Methyl *N*-[3 β ,30-diacetoxy-lup-20(29)-en-28-oyl]-leucinate (119**):** 80 mg (68% yield) starting from 120 mg of **117**; off-white amorphous powder. Mp 201-203 °C. MS (ESI+) m/z : 684.5 ($\text{M}^+ + \text{H}$) for $\text{C}_{41}\text{H}_{65}\text{NO}_7$. ^1H NMR (300 MHz, CDCl_3): δ 5.69 (1H, *br s*, -CONH-), 4.97, 4.94 (2H, *d*, $J = 9$, H-29), 4.58-4.52 (3H, *m*, -NHCH-, H₂-30), 4.45 (1H, *t*, $J = 8$ Hz, H-3), 3.72 (3H, *s*, -COOCH₃), 3.10 (1H, *m*, H-19), 2.50-2.32 (1H, *m*, H-13), 2.08 (6H, *s*, $2 \times \text{OCOCH}_3$), 1.05 (6H, *s*, leucine moiety $-(\text{CH}_3)_2$), 0.96 (6H, *s*, $2 \times \text{CH}_3$), 0.89, 0.82, 0.81 (3H each, *s*, $3 \times \text{CH}_3$).

Methyl *N*-[3 β ,30-diacetoxy-lup-20(29)-en-28-oyl]-8-aminooctanoate (120**):** 77.8 mg (69.5% yield) starting from 80 mg of **118**; white amorphous powder. Mp 167-169 °C. MS (ESI+) m/z : 712.5 ($\text{M}^+ + \text{H}$) for $\text{C}_{43}\text{H}_{69}\text{NO}_7$. ^1H NMR (300 MHz, CDCl_3): δ 5.60 (1H, *t*, $J = 4.6$ Hz, -CONH-), 4.94, 4.90 (1H each, *s*, H-29), 4.56 (2H, *s*, H₂-30), 4.45 (1H, *t*, $J = 7$ Hz, H-3), 3.66 (3H, *s*, -COOCH₃), 3.41-3.09 (3H, *m*, H-19, -CONHCH₂-), 2.46 (1H, *m*, H-13), 2.31 (2H, *t*, $J = 7.5$ Hz, -CH₂COOCH₃), 2.05 (6H, *s*, $2 \times \text{OCOCH}_3$), 0.97, 0.96, 0.85, 0.81, 0.80 (3H each, *s*, $5 \times \text{CH}_3$).

Syntheses of BA derivatives 96, 107-110. To a solution of the appropriate ester intermediates **116-120** (1 eq) in MeOH (8 mL) and THF (4 mL) was added 2N NaOH (4 mL). The mixture was stirred overnight, then neutralized with 20% HCl. The solution was dried under vacuum and reconstituted with EtOAc. The organic

layer was washed with brine and dried over anhydrous Na₂SO₄ and concentrated to dryness under reduced pressure. The residue was chromatographed using a silica gel column to yield the pure target compounds.

***N*-[3 β -Hydroxy-30-bromo-lup-20(29)-en-28-oyl]-leucine (96):** 102 mg (100% yield) starting from 110 mg of **117**; white amorphous powder. Mp 102-104 °C. MS (ESI-) *m/z*: 646.41, 648.39 (*M*⁻ - H) for C₃₆H₅₈BrNO₄. ¹H NMR (300 MHz, CDCl₃): δ 5.86 (1H, d, *J* = 8 Hz, -CONH-), 5.11, 5.02 (1H each, s, H-29), 4.65 (1H, m, -NHCH-), 3.90 (2H, s, H₂-30), 3.17 (1H, dd, *J* = 9.7, 5.4 Hz, H-3), 3.10-3.03 (1H, m, H-19), 1.00 (6H, s, leucine moiety -(CH₃)₂), 0.96 (6H, s, 2 \times CH₃), 0.83, 0.80, 0.79 (3H each, s, 3 \times CH₃). [α]_D²⁵ -10.5 ° (*c* = 0.15, MeOH).

***N*-[3 β ,30-Dihydroxy-lup-20(29)-en-28-oyl]-leucine (107):** 24 mg (98% yield) starting from 30 mg of **119**; white amorphous powder. Mp 145-148 °C. MS (ESI-) *m/z*: 584.5 (*M*⁻ - H) for C₃₆H₅₉NO₅. ¹H NMR (300 MHz, CDCl₃): δ 5.89 (1H, *br* s, -CONH-), 4.91, 4.90 (1H each, s, H-29), 4.68 (1H, m, -NHCH-), 4.12 (2H, s, H₂-30), 3.17 (1H, dd, *J* = 11.2, 5.6 Hz, H-3), 3.01 (1H, m, H-19), 2.34 (1H, m, H-13), 1.10 (6H, s, leucine moiety -(CH₃)₂), 0.99 (6H, s, 2 \times CH₃), 0.86, 0.83, 0.80 (3H each, s, 3 \times CH₃). [α]_D²⁵ -39.3 ° (*c* = 0.35, MeOH).

***N*-[3 β -Hydroxy-lup-20(29)-en-28-oyl]-8-aminooctanoic acid (108):** 37 mg (100% yield) starting from 40 mg of **116**; white amorphous powder. Mp 110-112 °C. MS (ESI-) *m/z*: 596.5 (*M*⁻ - H) for C₃₈H₆₃NO₄. ¹H NMR (300 MHz, CDCl₃): δ 5.60 (1H, *br* s, -CONH-), 4.73, 4.60 (1H each, s, H-29), 3.21-3.09 (4H, m, H-3, H-19, -CONHCH₂-), 2.31 (2H, t, *J* = 6.9 Hz, -CH₂COOH), 2.10-2.20 (1H, m, H-13), 1.68

(3H, s, H-30), 0.97 (6H, s, $2 \times \text{CH}_3$), 0.85, 0.79, 0.75 (3H each, s, $3 \times \text{CH}_3$). $[\alpha]_D^{25}$ -3.6 ° (c = 0.19, CHCl_3). $[\alpha]_D^{25}$ -8.48 ° (c = 0.20, MeOH).

***N*-[3 β -Hydroxy-30-bromo-lup-20(29)-en-28-oyl]-8-aminooctanoic acid**

(109): 44 mg (95% yield) starting from 50 mg of **118**; white amorphous powder. Mp 119-122 °C. MS (ESI-) m/z : 674.4 ($\text{M}^- - \text{H}$) for $\text{C}_{38}\text{H}_{62}\text{BrNO}_4$. ^1H NMR (300 MHz, CDCl_3): δ 5.60 (1H, *br s*, -CONH-), 5.13, 5.04 (1H each, s, H-29), 4.00 (2H, s, H₂-30), 3.21-3.09 (4H, m, H-3, H-19, -CONHCH₂-), 2.34 (2H, m, -CH₂COOH), 0.96 (6H, s, $2 \times \text{CH}_3$), 0.92, 0.82, 0.81 (3H each, s, $3 \times \text{CH}_3$). $[\alpha]_D^{25}$ -16.5 ° (c = 0.22, MeOH).

***N*-[3 β ,30-Dihydroxy-lup-20(29)-en-28-oyl]-8-aminooctanoic acid (110):** 50

mg (80% yield) starting from 58 mg of **120**; white amorphous powder. Mp 135-137 °C. MS (ESI-) m/z : 612.5 ($\text{M}^- - \text{H}$) for $\text{C}_{38}\text{H}_{63}\text{NO}_5$. ^1H NMR (300 MHz, CDCl_3): δ 5.61 (1H, *br s*, -CONH-), 4.94, 4.90 (1H each, s, H-29), 4.12 (2H, s, H₂-30), 3.25-3.15 (3H, m, H-3, -CONHCH₂-), 3.01 (1H, m, H-19), 2.34 (2H, t, $J = 7.6$ Hz, -CH₂COOH), 2.06 (1H, m, H-13), 0.97, 0.96 (3H each, s, $2 \times \text{CH}_3$), 0.92, 0.82, 0.75 (3H each, s, $3 \times \text{CH}_3$). $[\alpha]_D^{25}$ -143.3 ° (c = 0.10, MeOH).

***N*-[3 β -O-(3',3'-Dimethylsuccinyl)-30-bromo-lup-20(29)-en-28-oyl]-leucine**

(113): A solution of **96** (50 mg, 1 eq), DMAP (1 eq) and 2',2'-dimethylsuccinic anhydride (5 eq) in anhydrous pyridine (1.5 mL) was stirred at 160 °C for 3 h using microwave. The reaction mixture was diluted with EtOAc (15 mL) and washed three times with 20% HCl solution and distilled water. The organic layer was dried over anhydrous Na_2SO_4 and concentrated to dryness under reduced pressure. The residue was chromatographed using a silica gel column to yield 20 mg (32% yield) of **113**;

light yellow amorphous powder. Mp 105-107 °C. MS (ESI-) m/z : 774.5 ($M^+ - H$) for $C_{42}H_{66}BrNO_7$. 1H NMR (300 MHz, $CDCl_3$): δ 5.86 (1H, d, $J = 8$ Hz, -CONH-), 5.11, 5.02 (1H each, s, H-29), 4.65 (1H, m, -NHCH-), 4.54 (1H, dd, $J = 11.2, 5.7$ Hz, H-3), 3.90 (2H, s, H₂-30), 2.99 (1H, m, H-19), 2.64-2.42 (2H, m, H-2'), 1.30, 1.26 (3H each, s, 2 \times CH₃-3'), 1.00 (6H, s, leucine moiety -(CH₃)₂), 0.96 (6H, s, 2 \times CH₃), 0.87, 0.86, 0.81 (3H each, s, 3 \times CH₃).

5-2. HIV-1_{IIIB} Replication Inhibition Assay in MT-2 Cell Lines^{152,153}

This screening was performed by Panacos Pharmaceutical Inc. The general procedure was described previously in Chapter 3, 5-2.

5-3. HIV-1_{NL4-3} Replication Inhibition Assay in MT-4 Cell Lines^{134,148}

A 96-well microtiter plate was used to set up the HIV-1_{NL4-3} replication screening assay. NL4-3 variants at a multiplicity of infection (MOI) of 0.01 were used to infect MT4 cells. Culture supernatants were collected on day 4 post-infection for the p24 antigen capture using an ELISA kit from ZeptoMetrix Corporation (Buffalo, New York).

5-4. Cell Fusion Assay^{133,148}

TZM cells that expressed luciferase upon fusion with envelop-expressing COS cells were used as fusion partners. The fusion assays were performed by transfecting monkey kidney cells (COS) with an expression vector pSRHS that contained the

HIV-1 NL4-3 envelope genes. Electroporation was performed to express the HIV-1 envelope on COS cells. Briefly, COS cells (10^6) in culture medium were incubated with 2 μ g of the envelop expression vector on ice for 10min. Electroporation was performed using a gene pulser (BioRad, Hercules, CA) with capacitance set at 950 μ F and voltage at 150 V. The transfected COS cells were cultured for 1 day before mixing with TZM cells. TZM cells (10×10^4) were incubated with COS cells (10^4) in 96-well flat-bottomed plates (Costar) in a 100 μ L culture medium. Compounds to be tested at various concentrations in 10 μ L of culture medium were incubated with cell mixtures at 37 °C for 24 h. Luciferase activity was quantified using a Biotek luminometer.

Chapter 5. Novel Designed 3,28-Disubstituted BA Analogs with Improved Metabolic Stability as Potent Anti-HIV-1 Inhibitors

1. Introduction

Although bevirimat (DSB, **58**), a C-3 modified BA derivative functioning as a HIV-1 maturation inhibitor, is now efficiently proceeding in clinical trials,^{146,147} clinical development of C-28 modified BA analog RPR103611 (**47**) has been less successful due to poor “pharmacodynamic properties”.¹⁴¹ This result led us to speculate that the C-28 long lipophilic side chain, which is critical for anti-HIV-1 entry activity, may cause the problems. In Chapter 4, we reported the synthesis of **112**, which has a similar C-28 side chain and comparable antiviral potency to those of **47**, IC9564 (**48**) and A43-D (**94**). Compound **112** also has a water solubilizing moiety introduced at the C-30 position, and consequently, showed increased hydrophilicity and better physicochemical properties than **47**, **48** and **94**.

Deficiency in ADME (absorption, distribution, metabolism, and excretion) properties can be a major cause of failure during drug development. Therefore, to optimize our BA-derived drug lead(s) and guide further structural modification, metabolic stabilities of current C-28 modified BA analogs were further evaluated *in vitro*. From these studies, we learned that these compounds have a relatively short half

life ($t_{1/2}$). Thus, a novel C-28 side chain was designed to investigate SAR, enhance antiviral potency, and increase metabolic stability. This chapter reports new analog design, syntheses, anti-HIV-1 activity and metabolic stability assessment.

In addition, we know that A12-2 (**71**) (Figure 5-1), which contains both the C-3 side chain of **58** and C-28 side chain of **94** in one BA molecule, is currently our best bi-functional inhibitor, preserving both anti-entry and anti-maturation activities.¹⁴⁸ However, like **94**, **71** also has metabolic problems, likely due to the C-28 side chain. Therefore, the newly designed C-28 side chain was also incorporated into the disubstituted BA derivatives. Their syntheses and bioassay data will also be discussed in this chapter.

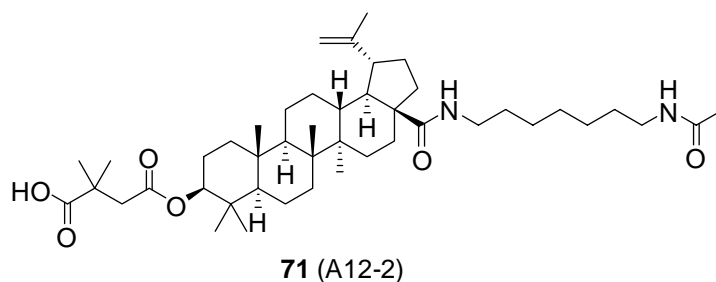


Figure 5-1. Structure of 71

2. Design

In vitro metabolic stability assessment of potential drug candidates in an early phase of drug discovery is a more cost-effective approach than *in vivo* studies to identify compounds with unfavorable ADME characteristics. Thus, a metabolic stability test of C-28 modified BA derivatives was performed. In this study, **108**, which has the common anti-entry C-28 side chain 8-aminooctanoic acid, was incubated with pooled human liver microsomes to assess its *in vitro* stability, because

cytochrome P450 enzymes are often the principal means of metabolism of many pharmaceuticals. Results from the study revealed that **108** exhibited a relatively short half life, suggesting that it carries some structural feature that is easily metabolized. To overcome this shortcoming, a cyclic secondary amine (from 4-piperidine butyric acid), rather than a primary amine, was used to form the critical amide bond with the C-28 carboxylic acid group, which yielded **121** (Figure 5-2). This design attempted to increase steric hindrance at the C-28 position, so that the amide bond would be less available to metabolic enzymes, while maintaining the general length and terminal carboxylic acid of the C-28 side chain in **108**. The metabolic stability of **121** was also evaluated in human liver microsomes and compared to that of **108**. Dimethylsuccinyl and dimethylglutaryl side chains were then introduced at the C-3 position of **121** to furnish **122** and **123** (Figure 5-2) and explore the impact of the newly designed C-28 side chain on anti HIV-1 activity of 3,28-disubstituted BAs. Antiviral activity was evaluated in HIV-1_{IIIB} infected MT-2 cell lines.

Because an amide is generally more stable *in vivo* than an ester moiety, we also synthesized 3,28-disubstituted BA analog **124**. Its C-3 side chain is similar to that of the potent **58**, except for a C-3 amide rather than ester bond (Figure 5-2). Analog **124** was also assayed against HIV-1_{IIIB} in MT-2 cell lines.

According to prior SAR conclusions, introduction of a second amide bond near the tail of the C-28 side chain is necessary for enhanced anti-HIV-1 entry activity.¹³¹ Therefore, four different amine moieties were introduced at the terminal carboxylic acid of **121** to yield **125-128** (Figure 5-2). Three analogs (**126-128**)

contained a water-solubilizing morpholine moiety in the introduced amide substitution to explore its impact on antiviral activities and physicochemical properties. A dimethylsuccinyl ester was then incorporated at the C-3 position of these four newly synthesized HIV-1 entry inhibitors to furnish a new generation of BA-derived bi-functional HIV-1 inhibitors (**129-132**) (Figure 5-2).

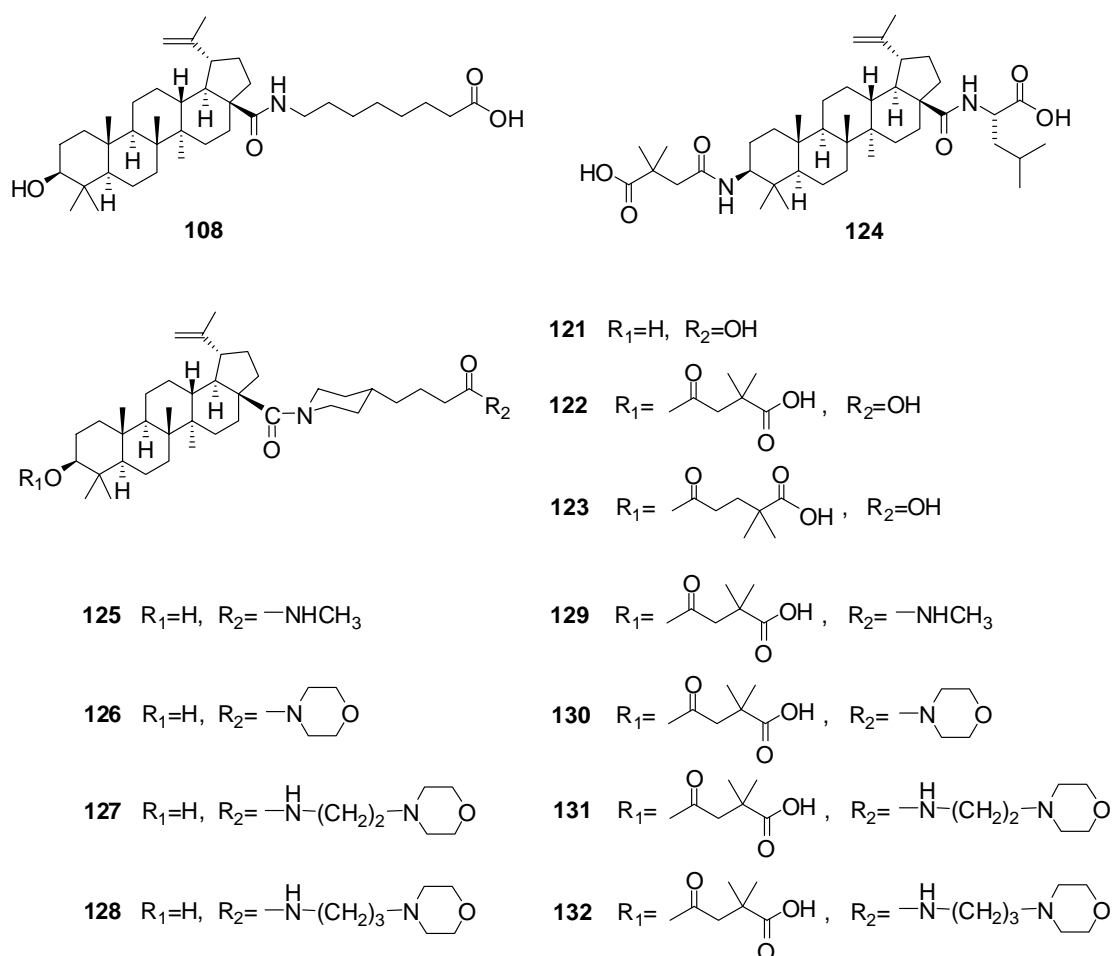


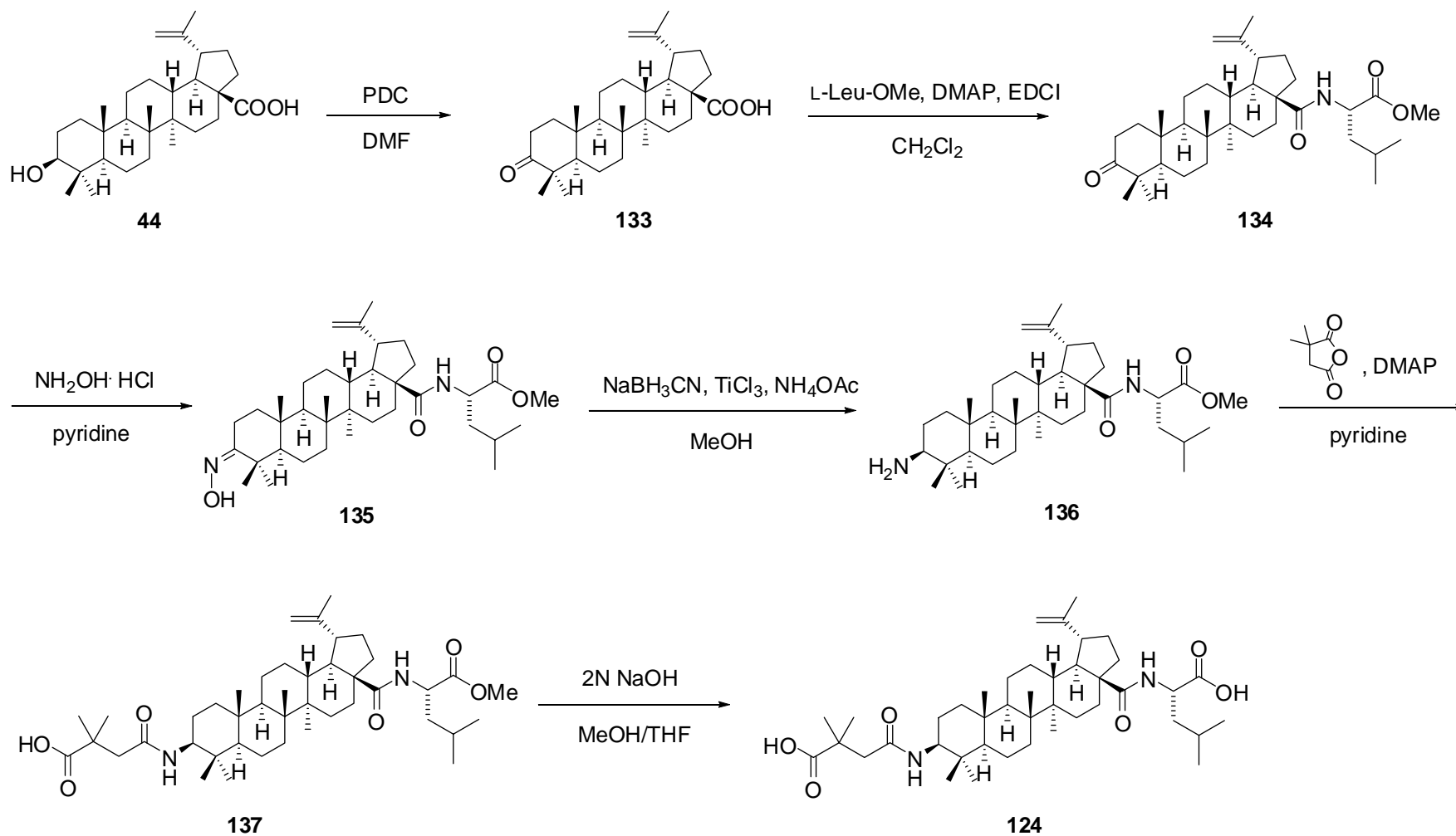
Figure 5-2. Structures of 108 and 121-132

3. Chemistry

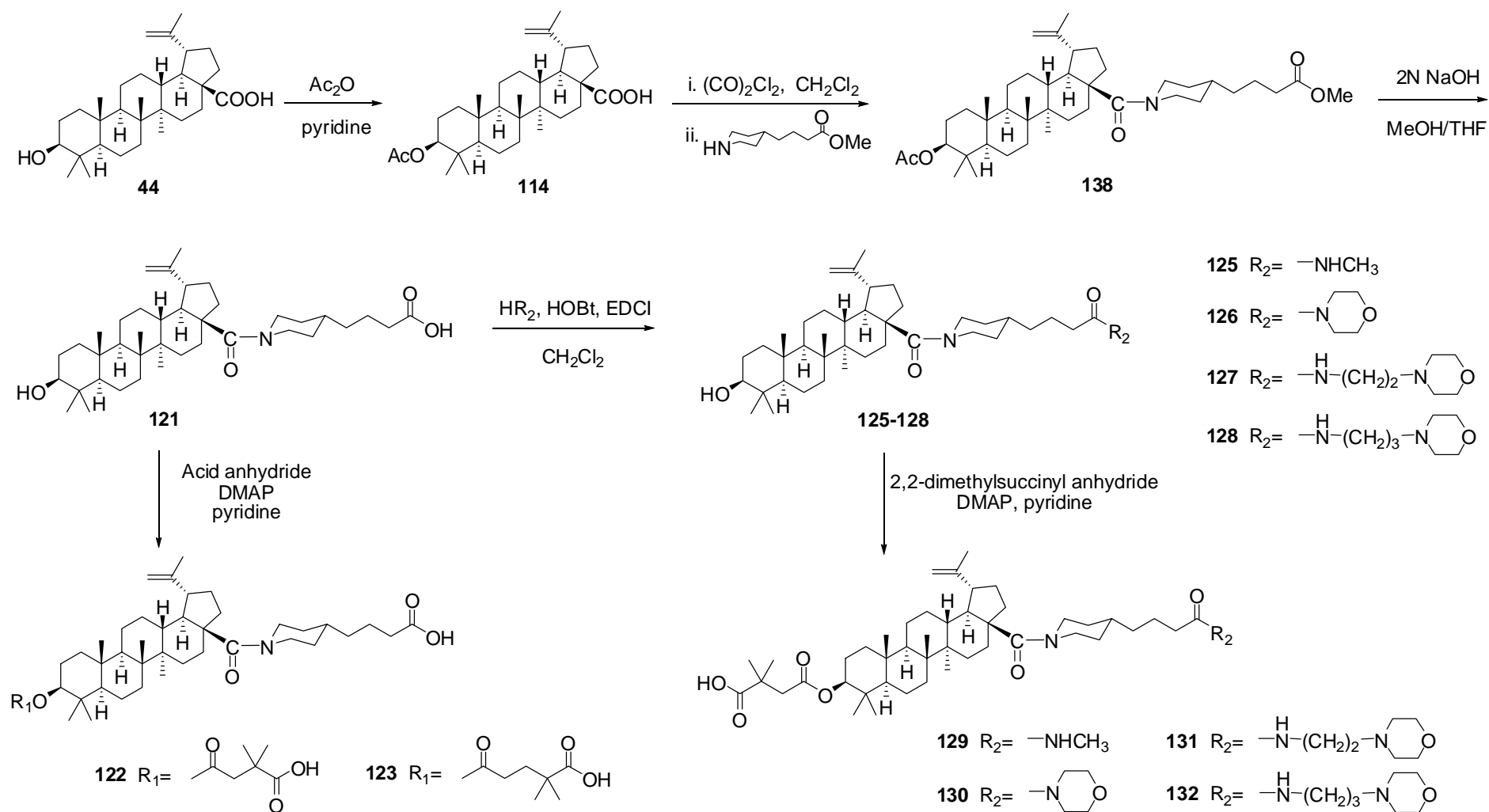
Scheme 5-1 depicts the synthesis of 3 β -amino BA analog **124**. Oxidation of **44** with 2 equivalents of PDC produced the 3-keto-BA **133** (87% yield). L-leucine methyl

ester was reacted with the C-28 carboxylic acid of **133** in the presence of DMAP and EDCI to furnish **134** (58% yield). The keto moiety of **134** was then converted to an oxime by treatment with hydroxylamine hydrochloride ($\text{NH}_2\text{OH}\cdot\text{HCl}$) in pyridine, which yielded **135** (90% yield). The 3 β -amine **136** was readily prepared in 82% yield from oxime **135** by enantioselective reduction of the Schiff base with TiCl_3 and NaCNBH_3 , as reported by Leeds and Kirst.¹⁵⁷ Treatment of **136** with 2,2-dimethylsuccinic anhydride under DMAP in pyridine yielded **137** (62% yield). Finally, hydrolysis of **137** with 2N sodium hydroxide furnished the desired 3, 28-disubstituted, 3 β -amino BA analog **124**.

The syntheses of **121-123**, **125-132** were carried out according to Scheme 5-2. First, the 3 β -hydroxyl group of **44** was protected with an acetyl moiety. Then, the 3-OAc-BA (**114**) was treated with oxalyl chloride in dichloromethane to yield the acid chloride intermediate, followed by reaction with the readily prepared 4-piperidine butyric acid methyl ester to provide **138** (94% yield). Saponification of **138** with 2N sodium hydroxide in MeOH/THF yielded the desired lead compound **121** quantitatively. Esterification of **121** with 2,2-dimethylsuccinic anhydride and 2,2-dimethylglutaric anhydride using DMAP in pyridine led to **122** and **123** in yields of 55% and 36%, respectively. The syntheses of **125-128** were carried out by reacting **121** with different amines in the presence of HOBt and EDCI, which yielded **125-128** (80-100% yields). Reaction of the 3 β -hydroxyl group of **125-128** with 2,2-dimethylsuccinic anhydride using DMAP in pyridine provided the 3,28-disubstituted target compounds **129-132** (58-81% yields).



Scheme 5-1. Synthesis of 124



Scheme 5-2. Synthesis of 121-123, 125-132

4. Results and Discussion

The newly synthesized BA derivatives **121-132** were evaluated *in vitro* for suppression of HIV-1_{IIIB} replication in MT-2 lymphocytes and compared to AZT and bevirimat (DSB, **58**). Compounds **129-132**, which showed potent antiviral activity in this first assay, were further tested against HIV-1_{NL4-3} in MT-4 cell lines, in parallel with the prior best BA-derived HIV-1 entry inhibitor A43-D (**94**) and IC9564 (**48**). All bioassay data are summarized in Table 5-1.

We discovered that bioisosteric replacement of the C-3 ester bond with an amide bond in 3,28-disubstituted BA analog **124** caused a significant decrease in antiviral activity (EC_{50} : 13.2 μ M), suggesting that an amide moiety is not tolerated at the BA C-3 position. This result is consistent with the previous finding that C-3 esterification is critical for high antiviral potency of BA-derived maturation inhibitors.

Changing the C-28 side chain from 8-aminooctanoic acid (**108**) to 4-piperidine butyric acid (**121**) significantly increased *in vitro* metabolic stability. Specifically, approximately 50% of parent lead compound **108** disappeared after around 35 minutes of incubation with pooled human liver microsomes, indicating that it was degraded quite easily in the assay system. Comparatively, it took about 110 min to lose 50% of **121**, suggesting a much longer half life (Figure 5-3). Thus, **121** represents a better lead for the development of C-28 modified BA-derived HIV-1 entry inhibitors and 3,28-disubstituted HIV inhibitors. Indeed, compound **122**, which resulted from esterifying **121** with the C-3 side chain of **58**, showed very potent anti-HIV-1 activity with a TI of 1.4×10^3 and an EC_{50} value of 0.015 μ M, which was similar to that of **58**

(EC₅₀: 0.012 μ M). This result proves that the presence of this novel C-28 side chain does not harm the antiviral potency of **58**. Compound **123**, with a 4',4'-dimethylglutaryl rather than 3',3'-dimethylsuccinyl C-3 ester side chain, had a higher antiviral EC₅₀ value (0.23 μ M), confirming the importance of the positioning of the dimethyl substitution as discussed in Chapter 3.

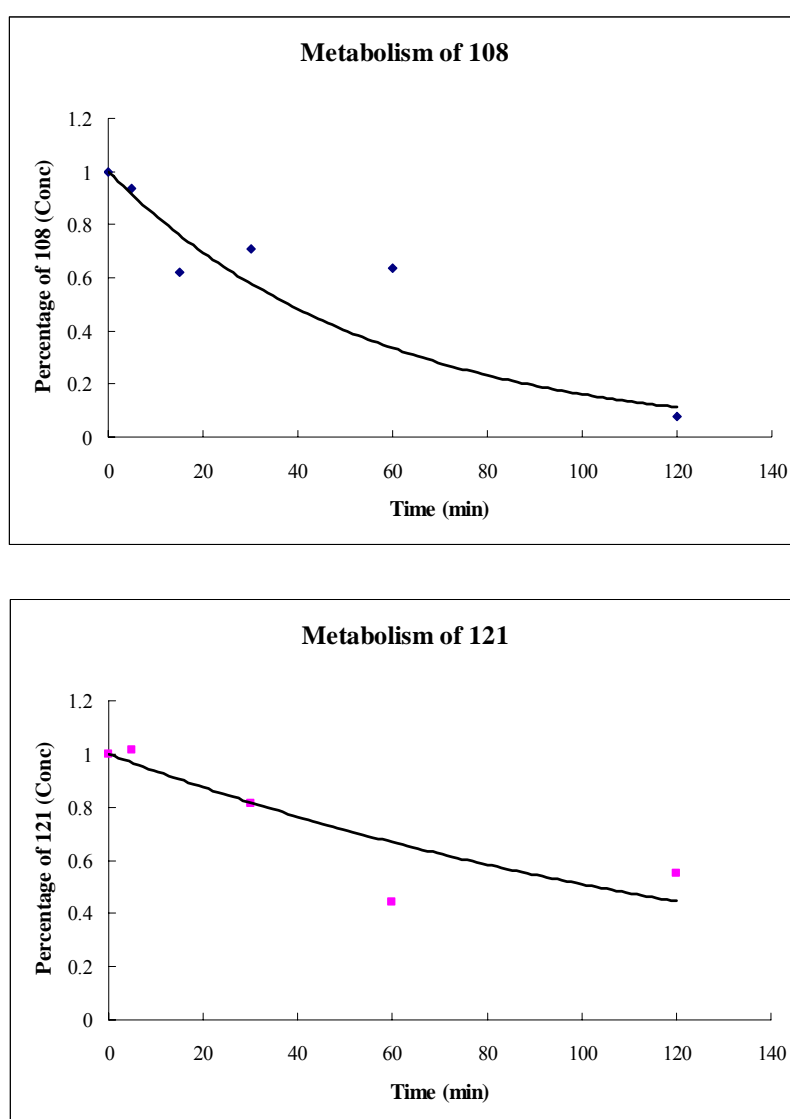


Figure 5-3. Metabolic stability of 108 and 121. Y scale: percentage of parent compound (concentration); X scale: time. Data presented are averaged from two separate experiments.

Because we previously found that introduction of a second amide bond is necessary for enhanced anti-HIV-1 entry activity of C-28 modified BA analogs, we also synthesized and evaluated **125-128**, which have different amide substituents linked to the terminal carboxylic acid of **121**. Moreover, the C-3 side chain of **58** was also incorporated into the C-3 position of the newly synthesized metabolically stable BA analogs **125-128**, to provide 3,28-disubstituted target compounds **129-132**. Their antiviral potency was then tested against both HIV-1_{IIIB} and HIV-1_{NL4-3} isolates.

From the results, we discovered that **125-128** only showed weak antiviral potency. This result is likely due to the slightly reduced length of the new C-28 side chain compared with previous 8-aminooctanoic chain (**108**). Indeed, the BA analog with 7-aminoheptanoic acid introduced to the C-28 position showed a 16-fold decreased anti-HIV activity compared with **108**, confirming the importance of the length of C-28 side chain.¹³¹

Compounds **131** and **132**, derived from **127** and **128**, which contain a morpholine ring at the end of C-28 side chain that is separated from the terminal amide bond by a short alkyl spacer (two or three methylenes), exhibited extremely potent anti-HIV-1 replication activity with EC₅₀ values of 0.007 μ M and 0.006 μ M, respectively, which are around 2-fold better than that of DSB (**58**). Their activities are also 2-3 fold more potent than the previous best entry inhibitors IC9564 (**48**) and A43D (**94**). Compound **130**, derived from **126**, with morpholine directly involved in the amide bond, had similar anti-HIV-1 potency (EC₅₀: 0.011 μ M) to that of **58**. Compound **129** with methylamine at the end of C-28 showed a slightly decreased

antiviral potency compared with **58**. From these results, we postulate that a longer C-28 chain is important for enhanced antiviral activity in 3, 28-disubstituted BA analogs. The better potency of **131** and **132** indicates that the high antiviral activity of **58** can be further increased with proper C-28 substitution. Moreover, because the C-28 side chains in all prior potent HIV inhibitors terminate in a free carboxylic acid or amide, the success of **131** and **132** also demonstrates that other polar groups at the end of this side chain can also increase antiviral potency.

To conclude, in this study, different modifications were performed at C-3 and C-28 positions of BA in order to improve the antiviral activity and physicochemical profiles of the compounds. Bioisosteric replacement of the C-3 ester bond in a 3,28-disubstituted analog with an amide bond (**124**) actually decreased antiviral potency, confirming again the importance of C-3 esterification to antiviral activity. Using a cyclic secondary amine moiety (piperidine) rather than a primary amine to form the C-28 amide bond significantly increased the metabolic stability of the derivatives in pooled human liver microsome assessment. Subsequent introduction of a second amide bond at the carboxylic terminus of this metabolically stable C-28 side chain and introduction of the 3',3'-dimethylsuccinyl side chain at the C-3 position resulted in the discovery of **131** and **132**, which showed extremely potent antiviral activity, slightly better than that of AZT and bevirimat (**58**). Both compounds have a morpholine moiety linked to the second amide bond through a short methylene chain and showed good solubility. **131** and **132** also showed good metabolic stability. Thus, they should serve as better leads for the development of a next generation of

BA-derived 3,28-disubstituted HIV-1 inhibitors.

Table 5-1. Anti-HIV-1 replication activities of 121-132

Compd	HIV-1 _{IIIB} ^a			HIV-1 _{NL4-3} ^b		
	EC ₅₀ (μM)	IC ₅₀ (μM)	TI	EC ₅₀ (μM)	IC ₅₀ (μM)	TI
AZT	0.056	1,870	33,115	- ^c	-	-
58	0.012	42.88	3,573	- ^c	-	-
48	- ^c	-	-	0.089	> 10	> 112.4
94	- ^c	-	-	0.085	> 10	> 117.6
121	21.72	41.05	1.15	- ^c	-	-
122	0.015	20.83	1,389	- ^c	-	-
123	0.23	33.24	144.5	- ^c	-	-
124	13.2	35.87	2.7	- ^c	-	-
125	NT ^d	NT ^d	-	- ^c	-	-
126	> 3.6 ^e	23.99	-	- ^c	-	-
127	> 0.35 ^e	14.50	-	- ^c	-	-
128	> 0.34 ^e	23.43	-	- ^c	-	-
129	0.067	33.31	497.2	0.24	> 10	> 41.7
130	0.011	19.23	1,748	0.07	8.8	121.4
131	0.007	17.31	2,473	0.035	8.5	283.9
132	0.006	18.52	3,087	0.031	8.6	245.7

^a All data presented are averages of at least two separate experiments performed by Panacos Pharmaceutical Inc., Gaithersburg, MD. ^b All data presented are averages of at least two separate experiments performed by Dr. Chin-Ho Chen, Duke University, NC. ^c not tested in the experiment. ^d not tested due to solubility issue. ^e endpoint not achieved. EC₅₀: concentration that inhibits HIV-1 replication by 50%. IC₅₀: concentration that inhibits mock-infected cell growth by 50%. TI = IC₅₀/EC₅₀.

5. Experimental Section

5-1. Chemistry

Melting points were measured with a Fisher Johns melting apparatus without correction. ^1H NMR spectra were measured on a 300MHz Varian Gemini 2000 spectrometer using Me_4Si (TMS) as internal standard. The solvent used was CDCl_3 unless otherwise indicated. Mass spectra were measured on Shimadzu LCMS-2010 (ESI-MS). Optical rotations were measured with a Jasco Dip-2000 digital polarimeter at 20 °C at the sodium D line. Thin-layer chromatography (TLC) and preparative thin-layer chromatography (PTLC) were performed on Merck precoated silica gel 60 F-254 plates. Flash+TM and CombiFlash systems were used as medium pressure column chromatography. Silica gel (200-400 mesh) from Aldrich, Inc., was used for column chromatography. All other chemicals were obtained from Sigma-Aldrich, Inc.

3-Deoxy-betulinic acid (133): To a solution of betulinic acid (2 g, 1eq) in DMF was added pyridium dichromate (PDC, 2 eq). The mixture was stirred at room temperature for 2 h. The reaction mixture was diluted with EtOAc (30 mL) and the precipitate was filtered through a short pack of Florisil. The solution was washed with 20% HCl and distilled water. The organic layer was dried over anhydrous Na_2SO_4 and concentrated to dryness under vacuum. The residue was chromatographed using a silica gel column to yield 1.68 g (87%) of pure **133**, white powder. Mp 246-248 °C. MS (ESI-) m/z : 453.3 ($\text{M}^- - \text{H}$) for $\text{C}_{30}\text{H}_{46}\text{O}_3$. ^1H NMR (300 MHz, CDCl_3): δ 4.72, 4.58 (1H each, s, H-29), 3.09 (1H, m, H-19), 2.41-2.26 (2H, m, H-2), 1.69 (3H, s, H-30), 0.98, 0.97, 0.96, 0.92, 0.89 (3H each, s, $5 \times \text{CH}_3$).

Methyl *N*-[3-Deoxy-lup-20(29)-en-28-oyl]-leucinate (134): A solution of **133** (500 mg, 1 eq), DMAP (0.6 eq) and EDCI (1.6 eq) in CH₂Cl₂ was stirred at 0 °C for 30 min. Leucine methyl ester (1.6 eq) and Et₃N (1 eq) was then added into the system and stirred at room temperature overnight. The reaction was diluted with CH₂Cl₂ (20 mL) and washed with brine. The organic layer was then dried over anhydrous Na₂SO₄ and concentrated to dryness under vacuum. The residue was chromatographed using a silica gel column to yield 372 mg (58%) of pure **134**, white amorphous powder. Mp 191-193 °C. MS (ESI+) *m/z*: 582.5 (M⁺ + H) for C₃₇H₅₉NO₄. ¹H NMR (300 MHz, CDCl₃): δ 5.87 (1H, d, *J* = 8.4 Hz, -CONH-), 4.70, 4.59 (1H each, s, H-29), 4.64 (1H, m, -NHCH-), 3.73 (3H, s, -COOCH₃), 3.05 (1H, m, H-19), 2.41-2.26 (2H, m, H-2), 1.68 (3H, s, H-30), 1.06, 1.02 (3H each, s, leucine moiety -(CH₃)₂), 0.98 (3H, s, CH₃), 0.96 (6H, s, 2 × CH₃), 0.92, 0.89 (3H each, s, 2 × CH₃).

Methyl *N*-[3-Oxime-lup-20(29)-en-28-oyl]-leucinate (135): A solution of **134** (230 mg, 1eq), and hydroxylamine hydrochloride (4 eq) in pyridine (10 mL) was heated at 50 °C for 2 h. After cooling to room temperature, the reaction mixture was diluted with CH₂Cl₂ and washed three times by 20% HCl and brine. The organic layer was then dried over anhydrous Na₂SO₄ and concentrated to dryness under vacuum. The residue was chromatographed using a silica gel column to yield 235 mg (90%) of pure **135**, white amorphous powder. Mp 213-215 °C. MS (ESI+) *m/z*: 582.5 (M⁺ + H) for C₃₇H₅₉NO₄. ¹H NMR (300 MHz, CDCl₃): δ 5.87 (1H, d, *J* = 8.4 Hz, -CONH-), 4.70, 4.59 (1H each, s, H-29), 4.64 (1H, m, -NHCH-), 3.73 (3H, s, -COOCH₃), 3.05 (1H, m, H-19), 2.20-2.15 (2H, m, H-2), 1.67 (3H, s, H-30), 1.05, 1.02 (3H each, s,

leucine moiety $-(\text{CH}_3)_2$, 0.98 (3H, s, CH_3), 0.96 (6H, s, $2 \times \text{CH}_3$), 0.94, 0.92 (3H each, s, $2 \times \text{CH}_3$).

Methyl *N*-[3 β -Amino-lup-20(29)-en-28-oyl]-leucinate (136): To a solution of **135** (100 mg, 1eq) and ammonium acetate (15 eq) in MeOH was added sodium cyanoborohydride (NaCNBH_3 , 20 eq) under nitrogen atmosphere. The reaction was cooled to 0 °C, and 15% aqueous titanium trichloride (TiCl_3 , 3 eq) was added dropwise over 45 min. The mixture was stirred at room temperature overnight, and then treated with 2N NaOH until pH = 10. The solution was dried under vacuum and the resided aqueous solution was extracted with CH_2Cl_2 and washed with distilled water until pH = 7. The organic layer was then dried over anhydrous Na_2SO_4 and concentrated to dryness under vacuum. The residue was chromatographed using a silica gel column to yield 80 mg (82%) of pure **136**, white amorphous powder. Mp 135-137 °C. MS (ESI+) m/z : 582.5 ($\text{M}^+ + \text{H}$) for $\text{C}_{37}\text{H}_{59}\text{NO}_4$. ^1H NMR (300 MHz, CDCl_3): δ 5.86 (1H, d, $J = 7$ Hz, $-\text{CONH}-$), 4.72, 4.58 (1H each, s, H-29), 4.64 (1H, m, $-\text{NHCH}-$), 3.73 (3H, s, $-\text{COOCH}_3$), 3.05 (1H, m, H-19), 2.44 (1H, m, H-3), 2.10-1.90 (1H, m, H-13), 1.68 (3H, s, H-30), 0.97 (9H, s, CH_3 -23, leucine moiety- $(\text{CH}_3)_2$), 0.96, 0.94, 0.93, 0.92 (3H each, s, $4 \times \text{CH}_3$).

Methyl *N*-[3 β -Acetoxy-lup-20(29)-en-28-oyl]-4-piperidine butanoate (138): Oxalyl chloride solution (2M in CH_2Cl_2 , 10mL) was added to **114** (800 mg, 1 eq) in CH_2Cl_2 (10 mL) and stirred for 2 h. After concentration under vacuum, the residual mixture was treated with 4-piperidine butyric acid methyl ester (1.6 eq) and triethylamine (Et_3N , 0.1 mL) in CH_2Cl_2 . The mixture was stirred at room temperature

overnight until no starting material was observed by TLC. Then, the solution was diluted with CH₂Cl₂ (20 mL) and washed three times with brine and distilled water. The organic layer was dried over anhydrous Na₂SO₄ and concentrated to dryness under reduced pressure. The residue was chromatographed using a silica gel column to yield 1.02 g (94%) of pure **138**, white amorphous powder. Mp 195–197 °C. MS (ESI+) *m/z*: 666.5 (M⁺ + H) for C₄₂H₆₇NO₅. ¹H NMR (300 MHz, CDCl₃): δ 4.72, 4.57 (1H each, s, H-29), 4.47 (1H, dd, *J* = 11.1, 5.7 Hz, H-3), 3.67 (3H, s, -COOCH₃), 3.67-3.47 (4H, m, 28-CON(CH₂CH₂)₂CH-), 2.99 (1H, m, H-19), 2.31 (2H, t, *J* = 7 Hz, -CH₂COOCH₃), 2.05 (3H, s, OCOCH₃), 1.68 (3H, s, H-30), 0.96 (6H, s, 2 × CH₃), 0.94, 0.82, 0.75 (3H each, s, 3 × CH₃).

Synthesis of BA derivatives 121 and 124. To a solution of the appropriate ester intermediates **138** or **137** (1 eq) in MeOH (8 mL) and THF (4 mL) was added 2N NaOH (4 mL). The mixture was stirred overnight, and then neutralized with 20% HCl. The solution was dried under vacuum and reconstituted with EtOAc. The organic layer was washed with brine and dried over anhydrous Na₂SO₄ and concentrated to dryness under reduced pressure. The residue was chromatographed using a silica gel column to yield the pure target compounds.

***N*-[3β-Hydroxy-lup-20(29)-en-28-oyl]-4-piperidine butyric acid (121):** 190 mg (100%) starting from 200 mg of **138**, white amorphous powder. Mp 145-146 °C. MS (ESI-) *m/z*: 608.4 (M⁻ - H) for C₃₉H₆₃NO₄. ¹H NMR (300 MHz, CDCl₃): δ 4.72, 4.57 (1H each, s, H-29), 3.67-3.47 (4H, m, 28-CON(CH₂CH₂)₂CH-), 3.19 (1H, m, H-3), 2.99 (1H, m, H-19), 2.31 (2H, t, *J* = 8.4 Hz, -CH₂COOH), 1.68 (3H, s, H-30),

0.96 (6H, s, 2 × CH₃), 0.94, 0.82, 0.81 (3H each, s, 3 × CH₃). [α]_D²⁵ -22.7 ° (c = 0.33, MeOH).

***N'*-[3 β -*N*-(3',3'-Dimethylsuccinyl)-lup-20(29)-en-28-oyl]-leucine (124):** 24 mg (98%) starting from 25 mg of **137**; white amorphous powder. Mp 248-250 °C. MS (ESI-) *m/z*: 695.5 (M⁻ - H) for C₄₂H₆₈N₂O₆. ¹H NMR (300 MHz, CDCl₃): δ 5.87 (1H, d, *J* = 7.6 Hz, -CONH-), 4.72, 4.58 (1H each, s, H-29), 4.64 (1H, m, -NHCH-), 3.59 (1H, m, H-3), 2.99 (1H, m, H-19), 2.64-2.42 (2H, m, H-2'), 1.68 (3H, s, H-30), 1.30, 1.26 (3H each, s, 2 × CH₃-3'), 1.00 (6H, s, leucine moiety -(CH₃)₂), 0.96 (6H, s, 2 × CH₃), 0.89, 0.86, 0.85 (3H each, s, 3 × CH₃). [α]_D²⁵ -16.1 ° (c = 0.28, MeOH).

Synthesis of BA derivatives 125-128. A solution of **121** (1 eq), EDCI (2 eq), HOBT (1 eq), Et₃N (0.05 mL) and appropriate amine (2 eq) in anhydrous CH₂Cl₂ (8 mL) was stirred at room temperature overnight until the starting material was not observed by TLC. The solution was diluted with CH₂Cl₂ (20 mL) and washed three times with brine and distilled water. The organic layer was dried over anhydrous Na₂SO₄ and concentrated to dryness under reduced pressure. The residue was chromatographed using a silica gel column to yield pure target compounds.

***N'*-[*N*-[3 β -Hydroxy-lup-20(29)-en-28-oyl]-4-piperidine-butanoyl]-aminomethane (125):** 46 mg (100%) starting from 50 mg of **121**, off-white amorphous powder. Mp 202-204 °C. MS (ESI+) *m/z*: 623.5 (M⁺ + H) for C₄₀H₆₆N₂O₃. ¹H NMR (300 MHz, CDCl₃): δ 5.44 (1H, *br s*, -CONHCH₃), 4.69, 4.54 (1H each, s, H-29), 3.58-3.54 (4H, m, 28-CON(CH₂CH₂)₂CH-), 3.16 (1H, m, H-3), 2.95 (1H, m, H-19), 2.78 (3H, d, *J* = 4.8 Hz, -CONHCH₃), 2.16 (2H, t, *J* = 7.5 Hz, -CH₂CONHCH₃), 1.66

(3H, s, H-30), 0.93 (6H, s, $2 \times \text{CH}_3$), 0.92, 0.90, 0.79 (3H each, s, $3 \times \text{CH}_3$). $[\alpha]_D^{25}$ -10.7 ° (c = 0.19, MeOH).

***N'*-[*N*-[3 β -Hydroxy-lup-20(29)-en-28-oyl]-4-piperidine-butanoyl]-morpholine (126):** 53 mg (87%) starting from 50 mg of **121**, white amorphous powder. Mp 132-133 °C. MS (ESI+) *m/z*: 679.5 ($\text{M}^+ + \text{H}$) for $\text{C}_{43}\text{H}_{70}\text{N}_2\text{O}_4$. ^1H NMR (300 MHz, CDCl_3): δ 4.69, 4.54 (1H each, s, H-29), 3.66-3.60 (8H, m, 28-CON(CH_2CH_2) $_2$ CH-, -CON(CH_2CH_2) $_2$ O), 3.42 (4H, m, -CON(CH_2CH_2) $_2$ O), 3.14 (1H, m, H-3), 2.95-2.60 (1H, m, H-19), 2.27 (2H, t, $J = 9.2$ Hz, - $\text{CH}_2\text{CON}(\text{CH}_2\text{CH}_2)_2\text{O}$), 1.65 (3H, s, H-30), 0.93 (3H each, s, $2 \times \text{CH}_3$), 0.91, 0.83, 0.79 (3H each, s, $3 \times \text{CH}_3$). $[\alpha]_D^{25}$ -20.0 ° (c = 0.31, MeOH).

***N'*-[*N*-[3 β -Hydroxy-lup-20(29)-en-28-oyl]-4-piperidine-butanoyl]-2-aminoethylmorpholine (127):** 54 mg (91%) starting from 55 mg of **121**, white amorphous powder. Mp 114-116 °C. MS (ESI+) *m/z*: 722.6 ($\text{M}^+ + \text{H}$), 744.5 ($\text{M}^+ + \text{Na}$) for $\text{C}_{45}\text{H}_{75}\text{N}_3\text{O}_4$. ^1H NMR (300 MHz, CDCl_3): δ 6.79 (1H, br, s, -CONHCH $_2$ -), 4.68, 4.53 (1H each, s, H-29), 3.69-3.67 (8H, m, 28-CON(CH_2CH_2) $_2$ CH-, -CH $_2$ N(CH_2CH_2) $_2$ O), 3.31 (2H, m, -CONHCH $_2$ -), 3.17 (1H, m, H-3), 2.95-2.60 (1H, m, H-19), 2.43 (6H, m, -CH $_2$ N(CH_2CH_2) $_2$ O), 2.17 (2H, t, $J = 7.5$ Hz, -CH $_2$ CONHCH $_2$ -), 1.63 (3H, s, H-30), 0.93 (3H each, s, $2 \times \text{CH}_3$), 0.90, 0.79, 0.72 (3H each, s, $3 \times \text{CH}_3$). $[\alpha]_D^{25}$ -10.6 ° (c = 0.15, MeOH).

***N'*-[*N*-[3 β -Hydroxy-lup-20(29)-en-28-oyl]-4-piperidine-butanoyl]-3-amino propylmorpholine (128):** 54 mg (90%) starting from 50 mg of **121**, white amorphous powder. Mp 122-124 °C. MS (ESI+) *m/z*: 736.6 ($\text{M}^+ + \text{H}$) for $\text{C}_{46}\text{H}_{77}\text{N}_3\text{O}_4$. ^1H NMR

(300 MHz, CDCl₃): δ 5.93 (1H, br, s, -CONHCH₂-), 4.69, 4.54 (1H each, s, H-29), 3.70-3.67 (8H, m, 28-CON(CH₂CH₂)₂CH-, -CH₂N(CH₂CH₂)₂O), 3.33 (2H, dd, J = 12, 6, -CONHCH₂-), 3.15 (1H, m, H-3), 2.95-2.60 (1H, m, H-19), 2.47-2.41 (6H, m, -CH₂N(CH₂CH₂)₂O), 2.16 (2H, t, J = 7.5 Hz, -CH₂CONHCH₂-), 1.65 (3H, s, H-30), 0.93 (3H each, s, 2 \times CH₃), 0.91, 0.79, 0.72 (3H each, s, 3 \times CH₃). $[\alpha]_D^{25}$ -7.5 ° (c = 0.18, MeOH).

Synthesis of 122-123, 137, 129-132. A solution of the appropriate BA analogs (1 eq), DMAP (1.5 eq) and the appropriate acid anhydride (5 eq) in anhydrous pyridine (1.5 mL) was stirred at 160 °C for 3 h using microwave. The reaction mixture was diluted with EtOAc (15 mL) and washed three times with 20% HCl solution and distilled water. The organic layer was dried over anhydrous Na₂SO₄ and concentrated to dryness under reduced pressure. The residue was chromatographed using a silica gel column to yield pure target compounds.

***N*-[3 β -*O*-(3',3'-Dimethylsuccinyl)-lup-20(29)-en-28-oyl]-4-piperidine**

butyric acid (122): 20 mg (41%) starting from 50 mg of **121**, white amorphous powder. Mp 116-118 °C. MS (ESI+) m/z : 738.6 (M⁺ + H), (ESI-) m/z : 736.5 (M⁻ - H) for C₄₅H₇₁NO₇. ¹H NMR (300 MHz, CDCl₃): δ 4.72, 4.57 (1H each, s, H-29), 4.47 (1H, t, J = 7.5, H-3), 3.65-3.50 (4H, m, 28-CON(CH₂CH₂)₂CH-), 2.98 (1H, m, H-19), 2.64-2.42 (2H, m, H-2'), 2.30 (2H, t, J = 7.2 Hz, -CH₂COOH), 1.68 (3H, s, H-30), 1.27, 1.25 (3H each, s, 2 \times CH₃-3'), 0.95, 0.93, 0.84, 0.83, 0.82 (3H each, s, 5 \times CH₃). $[\alpha]_D^{25}$ -27.7 ° (c = 0.30, MeOH).

***N*-[3 β -*O*-(4',4'-Dimethylglutaryl)-lup-20(29)-en-28-oyl]-4-piperidine**

butyric acid (123): 12 mg (38%) starting from 30 mg of **121**, white amorphous powder. Mp 143-145 °C. MS (ESI+) m/z : 752.4 ($M^+ + H$), (ESI-) m/z : 750.4 ($M^- - H$) for $C_{46}H_{73}NO_7$. 1H NMR (300 MHz, $CDCl_3$): δ 4.72, 4.57 (1H each, s, H-29), 4.47 (1H, t, $J = 7.5$, H-3), 3.65-3.50 (4H, m, 28-CON(CH_2CH_2) $_2$ CH-), 3.00 (1H, m, H-19), 2.35-2.30 (4H, m, H-2', - CH_2COOH), 1.68 (3H, s, H-30), 1.27, 1.25 (3H each, s, $2 \times CH_3-3'$), 0.96 (6H, s, $2 \times CH_3$), 0.89, 0.86, 0.82 (3H each, s, $3 \times CH_3$). $[\alpha]^{25}_D -23.1^\circ$ ($c = 0.20$, MeOH).

Methyl N' -[3 β - N -(3',3'-Dimethylsuccinyl)-lup-20(29)-en-28-oyl]-leucinate (137): 37 mg (38%) starting from 80 mg of **136**; white amorphous powder. Mp 187-189 °C. MS (ESI+) m/z : 711.5 ($M^+ + H$), 733.4 ($M^+ + Na$) for $C_{43}H_{70}N_2O_6$. 1H NMR (300 MHz, $CDCl_3$): δ 5.69 (1H, *br* s, -CONH-), 4.70, 4.58 (1H each, s, H-29), 4.62 (1H, m, -NHCH-), 3.73 (3H, s, -COOCH $_3$), 3.59 (1H, m, H-3), 2.99 (1H, m, H-19), 2.64-2.42 (2H, m, H-2'), 1.68 (3H, s, H-30), 1.30, 1.26 (3H each, s, $2 \times CH_3-3'$), 1.09 (6H, s, leucine moiety -(CH $_3$) $_2$), 0.97 (6H, s, $2 \times CH_3$), 0.92, 0.82, 0.80 (3H each, s, $3 \times CH_3$).

N' -[N -[3 β - O -(3',3'-Dimethylsuccinyl)-lup-20(29)-en-28-oyl]-4-piperidine-butanoyl]-aminomethane (129): 17 mg (48%) starting from 30 mg of **125**, white amorphous powder. Mp 166-169 °C. MS (ESI+) m/z : 751.6 ($M^+ + H$) for $C_{46}H_{74}N_2O_6$. 1H NMR (300 MHz, $CDCl_3$): δ 5.43 (1H, *br* s, -CONHCH $_3$), 4.69, 4.54 (1H each, s, H-29), 4.47 (1H, t, $J = 7.5$, H-3), 3.68-3.60 (4H, m, 28-CON(CH_2CH_2) $_2$ CH-), 2.98 (1H, m, H-19), 2.79 (3H, d, $J = 3.4$ Hz, -CONHCH $_3$), 2.67-2.62 (2H, m, H-2'), 2.14 (2H, t, $J = 6.8$ Hz, - $CH_2CONHCH_3$), 1.65 (3H, s, H-30), 1.30, 1.25 (3H each, s, $2 \times$

CH₃-3'), 0.93, 0.91 (3H each, s, 2 × CH₃), 0.90, 0.80, 0.79 (3H each, s, 3 × CH₃).

[α]²⁵_D -25.0 ° (c = 0.12, MeOH).

***N'*-[*N*-[3β-*O*-(3',3'-Dimethylsuccinyl)-lup-20(29)-en-28-oyl]-4-piperidine-butanoyl]-morpholine (130):** 23 mg (55%) starting from 35mg of **126**, off-white amorphous powder. Mp 122-124 °C. MS (ESI+) *m/z*: 807.6 (M⁺ + H) for C₄₉H₇₈N₂O₇. ¹H NMR (300 MHz, CDCl₃): δ 4.69, 4.54 (1H each, s, H-29), 4.45 (1H, t, *J* = 6.9, H-3), 3.66-3.61 (8H, m, 28-CON(CH₂CH₂)₂CH-, -CON(CH₂CH₂)₂O), 3.45-3.42 (4H, m, -CON(CH₂CH₂)₂O), 2.99-2.82 (1H, m, H-19), 2.67-2.52 (2H, m, H-2'), 2.28 (2H, t, *J* = 7.8 Hz, -CH₂CON(CH₂CH₂)₂O), 1.65 (3H, s, H-30), 1.26 (6H, s, 2 × CH₃-3'), 0.92, 0.90 (3H each, s, 2 × CH₃), 0.79 (6H, s, 2 × CH₃), 0.77 (3H, s, CH₃). [α]²⁵_D -19.1 ° (c = 0.41, MeOH).

***N'*-[*N*-[3β-*O*-(3',3'-Dimethylsuccinyl)-lup-20(29)-en-28-oyl]-4-piperidine-butanoyl]-2-aminoethylmorpholine (131):** 14 mg (41%) starting from 30 mg of **127**, white amorphous powder. Mp 121-123 °C. MS (ESI+) *m/z*: 850.4 (M⁺ + H) for C₅₁H₈₃N₃O₇. ¹H NMR (300 MHz, CDCl₃): δ 7.01 (1H, br, s, -CONHCH₂-), 4.70, 4.54 (1H each, s, H-29), 4.45 (1H, t, *J* = 10.2, H-3), 3.81-3.78 (8H, m, 28-CON(CH₂CH₂)₂CH-, -CH₂N(CH₂CH₂)₂O), 3.48 (2H, m, -CONHCH₂-), 2.85-2.70 (7H, m, -CH₂N(CH₂CH₂)₂O, H-19), 2.60-2.52 (2H, m, H-2'), 2.14 (2H, t, *J* = 7.5 Hz, -CH₂CONHCH₂-), 1.25 (6H, s, 2 × CH₃-3'), 1.63 (3H, s, H-30), 0.93 (3H each, s, 2 × CH₃), 0.90, 0.79, 0.72 (3H each, s, 3 × CH₃). [α]²⁵_D -18.0 ° (c = 0.16, MeOH).

***N'*-[*N*-[3β-*O*-(3',3'-Dimethylsuccinyl)-lup-20(29)-en-28-oyl]-4-piperidine-butanoyl]-3-aminopropylmorpholine (132):** 17 mg (47%) starting from 30 mg of

128, white amorphous powder. Mp 1125-127 °C. MS (ESI+) m/z : 864.6 ($M^+ + H$) for $C_{52}H_{85}N_3O_7$. 1H NMR (300 MHz, $CDCl_3$): δ 6.76 (1H, br, s, -CONHCH₂-), 4.69, 4.54 (1H each, s, H-29), 4.30 (1H, m, H-3), 3.81-3.67 (8H, m, 28-CON(CH₂CH₂)₂CH-, -CH₂N(CH₂CH₂)₂O), 3.28 (2H, m, -CONHCH₂-), 2.96 (1H, m, H-19), 2.80-2.73 (6H, m, -CH₂N(CH₂CH₂)₂O), 2.60-2.52 (2H, m, H-2'), 2.16 (2H, t, $J = 7.5$ Hz, -CH₂CONHCH₂-), 1.65 (3H, s, H-30), 1.25, 1.24 (6H, s, $2 \times CH_3$ -3'), 0.92, 0.90 (3H each, s, $2 \times CH_3$), 0.80, 0.79, 0.78 (3H each, s, $3 \times CH_3$). $[\alpha]_D^{25}$ -14.1 ° ($c = 0.24$, MeOH).

5-2. *In Vitro* Metabolic Stability Assessment in Human Liver Microsomes

5-2-1. *Materials*

BA derivatives **108**, **121** and **122** were synthesized and characterized in our study. NADPH, $MgCl_2$, KH_2PO_4 , formic acid and ammonium acetate were purchased from Sigma-Aldrich. HPLC-grade acetonitrile and water was purchased from VWR. Pooled human liver microsomes were purchased from BD biosciences (Woburn, MA).

5-2-2. *Sample Preparation*

Stock solutions of **108** and **121** (1 mg/ml) were prepared by dissolving the pure compound in methanol and stored at 4°C. For measurement of metabolic stability, **108** and **121** were brought to a final concentration of 3 μ M with 0.1 M potassium phosphate buffer at pH 7.4, which contained 0.2 mg/ml human liver microsome and 5 mM $MgCl_2$. The incubation volumes were 800 μ l. Reactions were started by adding 80 μ l of NADPH (final concentration of 1.0 mM) and stopped by taking the aliquots

over time, then adding to 1.5 volumes of ice-cold acetonitrile. Incubations of all samples were conducted in duplicate. For each sample, 100 µl aliquots were taken out at 0, 5, 15, 30, 60, 120 min time points. After addition of 150 µl ice-cold acetonitrile, the mixture was centrifuged at 12,000 rpm for 5 min at 0 °C. The Supernatant was collected and 20 µl of the supernatant was directly injected to LCMS. The following controls were also conducted: 1) positive control incubations that contain liver microsomes, NADPH and the substrate propranolol; 2) negative control incubations that omit NADPH and 3) baseline control that only contain liver microsomes and NADPH.

5-2-3. HPLC-MS Conditions

Analysis was carried out on Shimadzu LCMS-20 with an electrospray ionization source. An Alltima C18 5µm 150mm x 2.1mm column was used with a gradient elution at a flow rate of 1.5 ml/min. The initial elution condition was acetonitrile (B) in water (A, with 0.1% formic acid and 5mM ammonium acetate) at 55%. After staying at initial condition for 3 min, the concentration of B increased linearly to 90% at 15 min, and stayed at 90% for 2 min. The mobile phase was then returned to the initial condition and re-equilibrated for 3 min. The MS conditions were optimized to detector voltage: +1.35 kV, acquisition mode: SIM of the appropriate molecular weights of the testing compounds. The CDL temperature is 200 °C, heat block is 230 °C and neutralizing gas flow is 1.5 L/min. Samples were injected by auto-sampler. Electrospray ionization was operated in the positive ion mode. Full-scan spectra were also monitored over the range of 180 - 1000 m/z.

5-3. HIV-1_{III}B Replication Inhibition Assay in MT-2 Cell Lines^{145,152}

This screening was performed by Panacos Pharmaceutical Inc. The general procedure was described previously in Chapter 3, 5-2.

5-4. HIV-1_{NL4-3} Replication Inhibition Assay in MT-4 Cell Lines^{133,148}

This screening was performed by Dr. Chin-Ho Chen, Duke University. The general procedure was described previously in Chapter 4, 5-3.

Chapter 6. Concluding Remarks and Perspectives for Future Directions of Research on BA Derivatives

1. BA Derivatives as Potent HIV-1 Inhibitors

1-1. SAR Conclusions of BA Derivatives as Potent HIV-1 Inhibitors Targeting Maturation and Entry Processes

In this study, three series of compounds were designed, synthesized and bio-evaluated as a continuing study of BA derivatives as potent HIV-1 inhibitors. Based on the screening results assessed in HIV-1_{IIIB} infected MT-2 lymphocytes and HIV-1_{NL4-3} infected MT-4 lymphocytes, we determined the following SAR conclusions.

A C-3 dimethylsuccinyl side chain is a key pharmacophore for HIV-1 maturation inhibition activity of BA analogs. Dimethyl substitution at the C-3' position within the C-3 side chain, especially the 3'S-methyl group (as in **78**), is critical for the extremely high antiviral potency of DSB (**58**). Enlarging one of the C-3' methyls to an ethyl group further enhanced anti-HIV-1 activity, as was seen with **82**. In contrast, C-3 side chains containing pendant rings (conformationally restricted) dramatically decreased antiviral activity. C-28 and C-30 substitutions did not harm the high antiviral potency of C-3 modified BA analogs. Actually, the existence of appropriate C-28 side chains can further increase the derivatives' anti-HIV-1 potency.

At C-28, a long methylene side chain and a second amide bond near its end are critical for HIV-1 entry inhibition activity of BA analogs. The metabolic stability of the C-28 amide bond was increased significantly by replacing the primary amine moiety with a secondary cyclic amine (specifically piperidine). Introduction of a morpholine-containing moiety at the end of the C-28 side chain increased the antiviral activity of 3, 28-disubstituted BA analogs **131** and **132** by several-fold. The success of these two compounds suggests that larger substituents can be tolerated near the C-28 amide bond and that a third nitrogen at the end of the C-28 side chain can further increase activity. The high antiviral potency of 3, 28-disubstituted BA analogs may be due to synergistic effects. These findings give us a new direction for the development of BA-derived potent HIV-1 inhibitors.

Except for amine moieties and a hydroxyl group, the C-30 position can accommodate certain substitutions through an ether bond that do not significantly affect the antiviral potency of the BA derivatives. This result suggests that the C-30 position can serve as a good place to incorporate water-solubilizing moieties, which can improve the physicochemical properties of BA analogs. Indeed, compound **112**, which contains a morpholine moiety in its C-30 substituent, showed very potent antiviral activity and much increased solubility.

1-2. Future Research Directions

3,28,30-Trisubstituted BA derivatives can be synthesized starting from 28,30-disubstituted analogs. These tri-substituted BA analogs are very likely to show

significant antiviral maturation and entry activities as well as promising physicochemical properties suitable for clinical development, because the C-3 and C-28 modifications ensure high potency, while C-30 water-solubilizing substitutions can significantly improve hydrophilicity. For example, compound **139** (Figure 6-1) can be synthesized starting from **112**. Based on our prior SAR conclusions, **139** incorporates important pharmacophores and is very likely to exhibit potent antiviral potency and significantly increased solubility.

For BA-derived HIV-1 entry inhibitors, improving the pharmacodynamic and pharmacokinetic properties of the long lipophilic C-28 side chain should be the main focus of future design. Currently, this class of compounds shows high lipophilicity and relatively low metabolic stability. In the present study, we demonstrated that the C-28 position could tolerate cyclic secondary amine substitutions (piperidine) with similar antiviral activity and increased metabolic stability. Accordingly, we feel that incorporating heteroatoms in the middle of the C-28 side chain is a good approach to increase hydrophilicity of future compounds, while maintaining good antiviral potency. Therefore, compound **140** (Figure 6-1) was designed. Replacement of the piperidine moiety with a piperazine moiety increases the calculated Log P value of the derivative to around 7.6, which is much lower than that of the original piperidine analogs. Moreover, analogs with a piperazine moiety are likely to have better metabolic stability compared to ones with primary amines. Because **140** contains a longer C-28 side chain critical for anti-entry activity, it should exhibit potent antiviral activity similar to **108**. Thus, development of C-28 piperazine analogs (**140** and its

analogues) is a good direction for the next generation of BA-derived HIV-1 entry inhibitors. The best entry inhibitors can be further developed into 3,28-disubstituted bi-functional HIV inhibitors, such as **141** (Figure 6-1).

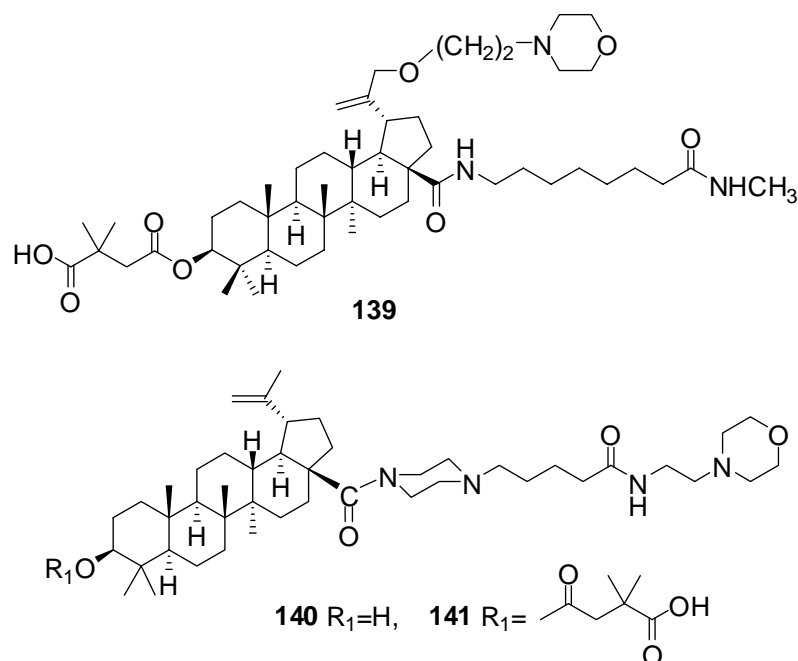


Figure 6-1. Design for future BA derived HIV-1 inhibitors.

2. Modeling of BA Analogs

2-1. PASS Prediction of BA and DSB Biological Activities

To date, there are more than 1,000 publications discussing BA (**44**). In addition, nearly 50 patents and patent applications relating to **44** were identified in a literature search. Many of these publications and patents pertain to the pharmaceutical application of **44** for the treatment of cancer, viral infections, hair loss, and other conditions.¹⁵⁸ Because **44** shows a good safety profile *in vivo*, it was further screened by using PASS Inet software (Prediction of Activity Spectra for Substances) (<http://195.178.207.233/PASS/>) in an attempt to identify new activities that may

provide new therapeutic indications.

The approach used in PASS is based on the suggestion that $Activity=f(Structure)$. Thus, by "comparing" the structure of a new compound with structures of well-known biologically active substances, it is possible to estimate if a new compound may have a particular effect. The PASS training set contains about 46,000 biologically active compounds. They include about 16,000 already launched drugs and 30,000 drug-candidates now under clinical or advanced preclinical testing. The similarity of compounds is characterized by the Euclidean distance (di) between compounds in multi-dimensional space of normalized descriptors. The mathematical approach is the leave-one-out cross-validated procedure.

Table 6-1. Some of the PASS-predicted biological activities of BA (44)

Pa^a	Pi^b	Predicted Biological Activity
0.912	0.007	Phosphatase inhibitor
0.857	0.004	DNA ligase (ATP) inhibitor
0.781	0.015	Membrane integrity antagonist
0.759	0.011	GABA A receptor antagonist
0.733	0.006	Hepatoprotectant
0.715	0.008	Antinephritic
0.707	0.007	Hepatic disorders treatment
0.701	0.005	Retinol dehydrogenase inhibitor
0.712	0.020	Oxidoreductase inhibitor
0.660	0.007	Phospholipase C inhibitor

^a: the estimates of probability for the compound to be active. ^b: the estimates of probability for the compound to be inactive. $Pa > 0.7$ the compound is very likely to reveal this activity in experiments; $0.5 < Pa < 0.7$ the compound is likely to reveal this activity in experiments.

Besides the known antineoplastic and apoptosis agonist activities of **44**, PASS also predicts that **44** can function as a phosphatase inhibitor, DNA ligase inhibitor, etc. These effects may be the mechanisms for its numerous activities. Some interesting predicted activities of **44** are listed in Table 6-1.

Potential biological activities of DSB (**58**) have also been predicted by PASS. One interesting result is that PASS estimates that **58** can also function as apoptosis agonist, suggesting that it may be developed as an anticancer agent. Some of the interesting predictions are summarized in Table 6-2.

Table 6-2. Some of the PASS-predicted biological activities of DSB (58)

Pa^a	Pi^b	Predicted Biological Activity
0.879	0.014	Phosphatase inhibitor
0.842	0.007	Apoptosis agonist
0.761	0.018	Membrane integrity antagonist
0.709	0.021	GABA A receptor antagonist
0.663	0.006	DNA ligase (ATP) inhibitor
0.597	0.008	Phospholipase C inhibitor

^a: the estimates of probability for the compound to be active. ^b: the estimates of probability for the compound to be inactive. $Pa > 0.7$ the compound is very likely to reveal this activity in experiments; $0.5 < Pa < 0.7$ the compound is likely to reveal this activity in experiments.

2-2. Pharmacophore Elucidation Using MOE 2007.09

Because the exact binding target of BA derivatives is still not clear and the X-ray structures of the possible binding targets are not available at this time, computational modeling approaches to guide rational drug design of novel

BA-derived HIV-1 inhibitors focus mainly on ligand-based drug design. Three-dimensional alignment of putative ligands can be used to deduce structural requirements for biological activity. For example, CoMFA¹⁵⁹ uses a 3D molecular alignment as input. Another strategy is pharmacophore elucidation in which several ligands are aligned, and a small collection of essential molecular features required for biological activity is derived from the alignment.¹⁶⁰ Methodologies based upon 3D alignment for finding biologically active ligands generally make use of the qualitative assumption that if two ligands have similar biological activity and bind in similar modes, then the bound conformations of the two ligands align well and inferences can be made about the nature of the receptor.

The purpose of the pharmacophore elucidator is to generate a collection of pharmacophore queries from a collection of compounds, some or all of which are active against a particular biological target, such that all or most of the active compounds satisfy the generated queries. In the absence of receptor information, it is hoped that geometric features common to many of the actives will contain information related to important interactions between the bound conformations of the actives and the receptor. The fundamental approach for pharmacophore elucidation is to exhaustively search for all pharmacophore queries that induce a good overlay of most of the active molecules and that separate actives from inactives (when inactives are present). Thus, the plausibility of the pharmacophore is measured by overlay of actives (common binding mode), and the relationship to activity is measured by classification accuracy.

Because pharmacophore elucidation is a much faster approach to obtain information on molecular features and visualized models, it was chosen to align the BA-derived HIV-1 inhibitors. MOE (Molecular Operating Environment, Version 2007.09, Chemical Computing Group, Montreal, Quebec, Canada) was used in this preliminary study, and the most active BA-derived HIV-1 inhibitors (**122**, **129-132**) (Figure 6-2) were selected to search for the best conformational space.

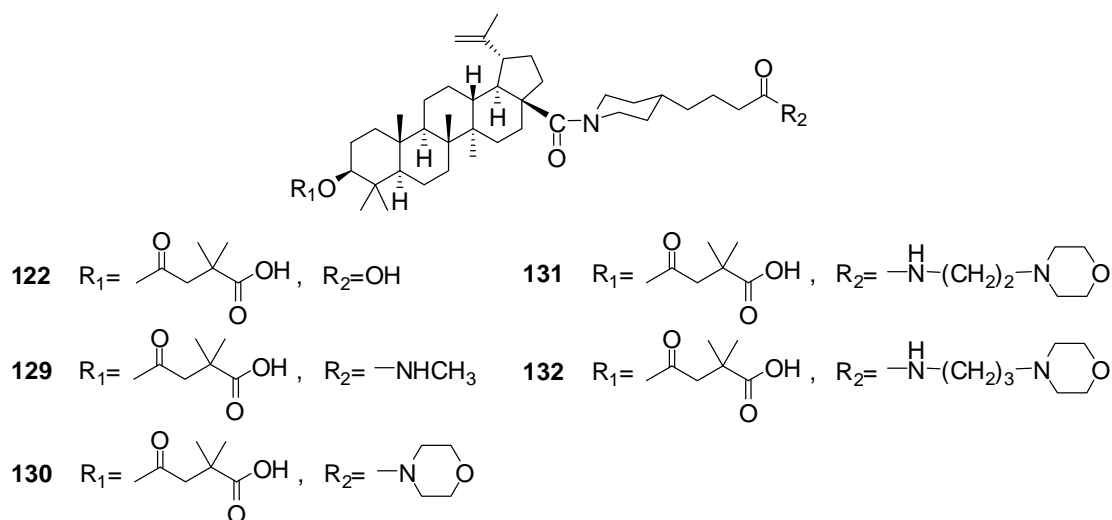


Figure 6-2. Structures of selected active compounds for pharmacophore model

To find common features, MOE can align ligands and maximize overlap over a set of pre-determined features. The features are derived from the following qualitative notions of a good alignment: 1) the strain energy of each molecule is small, 2) molecules have similar shapes, 3) molecules have similar LogP (octanol/water) values, 4) molecules have comparable molar refractivity,; 5) aromatic atoms overlap, 6) hydrogen bond donors and acceptors overlap, 7) acidic groups and basic groups overlap, 8) atoms of similar partial charge overlap, and 9) hydrophobic areas overlap.

The resulted pharmacophore model is shown in Figure 6-3. The model

indicates that all of the active compounds can attain similar conformations. The BA skeleton provides good hydrophobic interactions with the binding pocket, while the tails of the C-3 and C-28 side chains form necessary hydrogen bonds with the target. In addition, the model indicates that polar moieties could also be accommodated near the BA skeleton's C-28 area. This finding supports our intent to incorporate more polar moieties into this position to increase the derivatives' hydrophilicity. The synthesis and evaluation of **140** and **141** may validate this design.

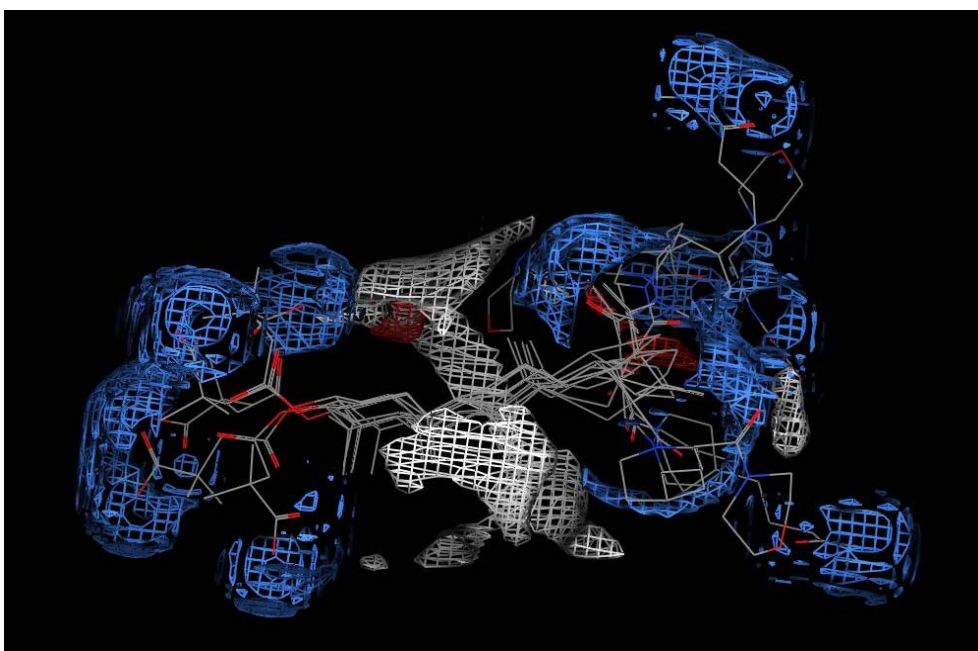


Figure 6-3. MOE predicted pharmacophore model for compound 122, 129-132.

White: hydrophobic interaction; Blue: donor-functionality; Red: acceptor-functionality.

To validate this pharmacophore model, it is necessary to screen a database including both active BA-derived HIV-1 entry inhibitors and inactive structures. If the pharmacophore search can successfully separate the active and inactive groups, this

model is considered predictable. Nevertheless, the initial result of this pharmacophore elucidation still provides us a straightforward visualized model of the predicted interaction between binding targets and active BA derivatives.

2-3. Future Studies on Modeling of BA Analogs Using Variable Selection kNN QSAR Method

Two-dimensional kNN (k-Nearest Neighbor) QSAR method is also a ligand-based method of analysis. It is very suitable for building QSAR models of a group of small molecules with related structures and varying bioactivities, and using these QSAR models to screen different databases to identify new leads. The 2D descriptors could accelerate processing time. By generating kNN QSAR models of BA-derived anti-HIV-1 agents and running database mining, we may be able to identify hits that can serve as good leads for future drug development as anti-HIV-1 maturation inhibitors and/or entry inhibitors.

2-3-1. Introduction

In general, the kNN QSAR method uses the kNN classification principle combined with the variable selection procedure. A subset of n_{var} (number of selected variables) descriptors between 1 and the total number of the original descriptors is selected randomly as a hypothetical descriptor pharmacophore (HDP). The HDP selection is optimized by leave-one out cross-validation method where the HDP biological activity is predicted by k most similar molecules in the training set ($k=1-5$)

with one compound eliminated from the training set. The similarity of compounds is characterized by the Euclidean distance (d_i) between compounds in multi-dimensional space of normalized descriptors (range-scaled). To enhance the kNN QSAR approach, distance weighted activity values of the closest neighbors were developed for the predictions of activity. The measure of the model performance is the value of the leave-one-out cross-validated $R^2(q^2)$. A flowchart of currently employed kNN methodology is displayed in Figure 6-4.

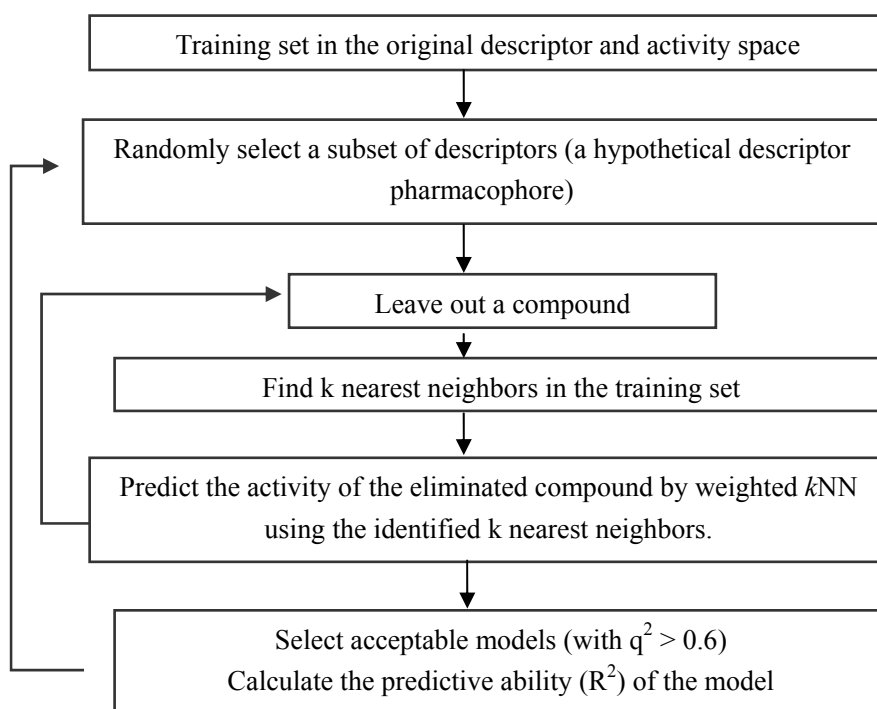


Figure 6-4. Flowchart of kNN Method

2-3-2. Model Validation: Training and Test Set Compound Selection

The overall modeling process of building the kNN QSAR model of BA-derived HIV-1 inhibitors is illustrated in Figure 6-5. The whole data set is divided into multiple training and test sets. Several criteria are used to build kNN QSAR models

for the training data set and select validated models. We will consider a model successful if the following values apply. (1) Both the q^2 values for the training data set and the R^2 for the corresponding test data set exceed 0.6. (2) The coefficient of determination of R_o (observed) is similar to R^2 (predicted), i.e., $|R^2 - R_o^2| / R^2 < 0.1$. (3) The slope of regression of predicted vs observed values is between 0.85 and 1.15.

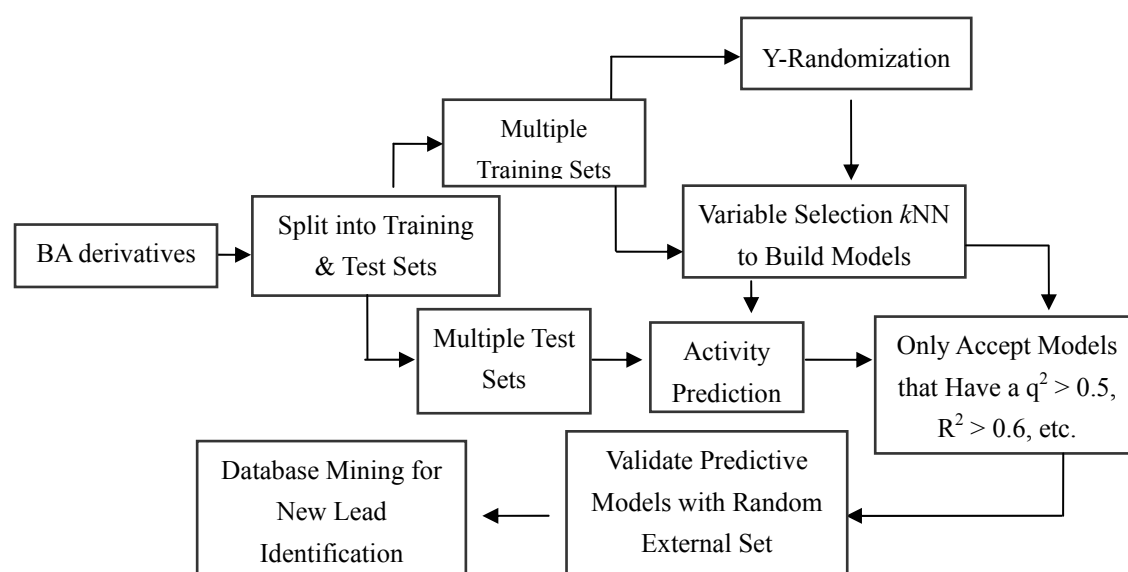


Figure 6-5. The workflow of k NN QSAR modeling

2-3-3. Robustness of QSAR Models

The statistical significance of QSAR models for training sets is tested by the standard hypothesis with one tail Z test at the significance level of $\alpha=0.05$ based on the following hypothesis. The null hypothesis states that the q^2 of the actual QSAR model is not significantly better than other random QSAR models, whereas the alternative hypothesis states that the q^2 of the actual QSAR model is significantly better than other QSAR random models. (i) H_0 , $h=\mu$; (ii) H_1 , $h>\mu$ (where μ is the

average value of q^2 for random QSAR models and h is the value of q^2 for the experimental QSAR model).

2-3-4. Database Mining

Validated QSAR models generated by a modified kNN approach will be used to mine novel lead anti-HIV-1 agents from different chemical databases, such as Chemdiv (over 750,000 compounds). The overall workflow of the data mining procedures is shown in Figure 6-6.

The Euclidean distance (di) in the descriptor pharmacophore space is used to evaluate the similarity of all chemical structures in the database and all active probes (corresponding descriptors for 10 best QSAR models). All structures are ranked in the database by their similarity to a probe, and M structures are selected within a certain similarity threshold. The biological activities of these M structures are predicted based on the previously generated best kNN QSAR models. Structures with higher biological activity predicted by all or a majority of generated QSAR models are selected as computational hits.

To summarize, a ligand-based 2D kNN QSAR method provides us an efficient approach to build QSAR models and mine different databases for novel hits. Its application into the study of BA-derived HIV-1 inhibitors may help us to expand this research into more diverse compound structures.

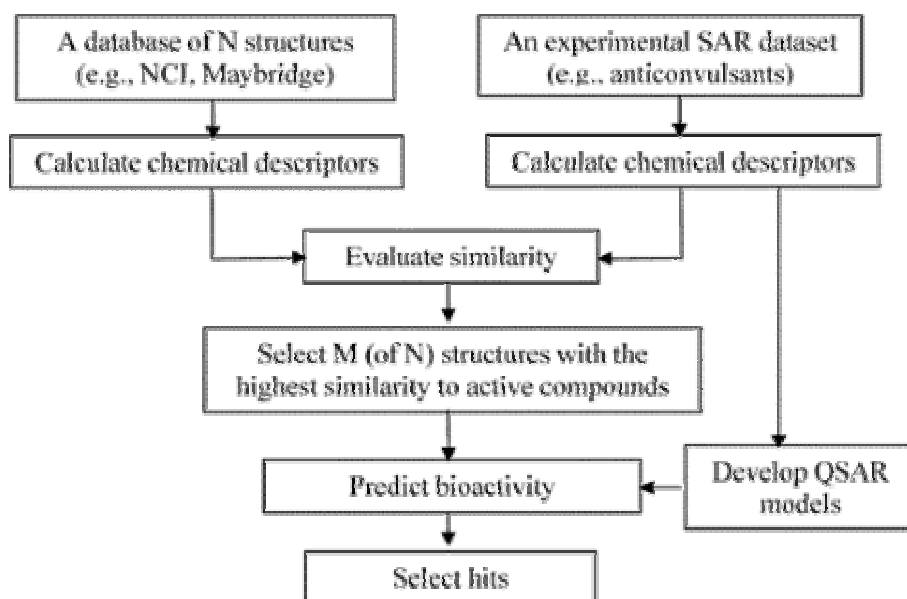


Figure 6-6. Workflow of the data mining procedures.

3. BA Derivatives as Potent Proteasome Inhibitors

3-1. Introduction

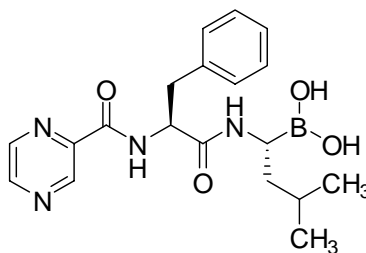
BA (**44**) is cytotoxic against several tumor varieties including melanoma, neuroectodermal tumor, and malignant brain tumor.^{161,162} It appears to function by inducing apoptosis in cells, irrespective of their p53 status.^{162,163} While **44** exhibited no toxic effects in mice even at a concentration of 500 mg/kg, doses of **44** as low as 5 mg/kg were determined to significantly impede tumor development.¹⁶¹ Together, these encouraging findings have made **44** a very attractive candidate for clinical treatment of various forms of cancers.

Proteasomes are responsible for more than 80% of intracellular protein degradation.¹⁶⁴ The β subunits of proteasomes have three major proteolytic activities: chymotrypsin-like ($\beta 5$), trypsin-like ($\beta 2$), and caspase-like ($\beta 1$). These proteolytic activities enable the proteasome to cleave proteins into small peptides. Proteasomes

are involved in many essential cellular functions, such as cell cycle regulation, cell differentiation, signal transduction pathways, antigen processing for appropriate immune responses, stress signaling, inflammatory responses, and apoptosis. Interestingly, despite the presence of proteasomes in all eukaryotic cells, malignant cells are more sensitive to the loss of proteasome function.¹⁶⁵ Possible reasons for this difference may be because 1) malignant cells often proliferate rapidly and have aberrant cell-cycle checkpoints, which leads to the accumulation of defective proteins and increases dependency on proteasomes as a disposal mechanism and 2) inhibition of proteasome activity causes a reversal or bypass of some mutational effects in cell-cycle and apoptotic checkpoints. In other words, inhibition of the 26S proteasome could result in selective inhibition of malignant cell growth. Thus, proteasome inhibition has become a strategy for anticancer chemotherapy, and numerous agents have been identified to inhibit proteasomes and kill tumor cells, overcome drug resistance, and enhance radiation sensitivity.

Bortezomib (PS341, Velcade, **142**) was the first proteasome inhibitor approved by the US FDA on May 2003 for treatment of multiple myeloma.¹⁶⁶ It shows high-affinity specificity and selectivity for the chymotryptic activity of the proteasome targeting the active site N-terminal threonine residue.^{167,168} As a result, **142** stabilizes I κ B and the CDK inhibitors p21 and p27, activates c-Jun-N-terminal kinase, and stabilizes the tumor suppressor p53 and pro-apoptotic proteins, which results in apoptosis or inhibits cancer cell proliferation.^{167,169} The successful development of **142** into a clinical drug provides us with a valid example of the

potential applicability of proteasome inhibitors as anticancer agents.



142 Bortezomib (PS341, Velcade)

3-2. Proteasome Inhibition Activities of DSB and C-30 Modified BA Analogs

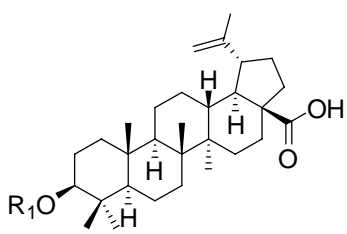
Our investigation indicated that HIV-1 virions produced in the presence of DSB (**58**) contained much higher amounts of the cellular protein APOBEC3G. Because APOBEC3G is subject to proteasome degradation in HIV-1 infected cells, we then postulated that the elevated APOBEC3G level in the treated viral particles may due to inhibition of proteasomes by **58**.

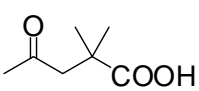
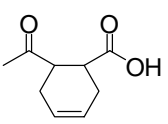
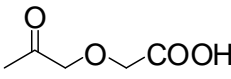
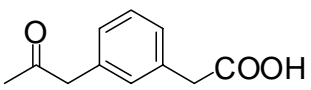
Further screening of **58** on 20S proteasome activity demonstrated that it inhibited chymotrypsin-like activity with an IC_{50} value of 7.2 μ M, did not inhibit caspase-like activity, and was a very weak inhibitor (IC_{50} : 20.5 μ M) of trypsin-like activity. These results are favorable because normal cells may suffer fewer consequences from treatment with **58**, because two of the main proteolytic activities are retained. In our screening, **58** did not inhibit the cellular proteases cathepsin B (cysteine protease) and DPPIV (DPP4, CD26, serine protease). Thus, **58** may have reduced side effects compared with other proteasome inhibitors such as peptide aldehydes and peptide boronates, which also inhibit these cellular proteases.

Because **58** is a C-3 modified BA derivative, we then synthesized two

additional compounds (**143** and **144**) to investigate the impact of the modification on proteasome inhibition. These two compounds plus BA (**44**) and **74** were tested against chymotrypsin-like activity of human 20S proteasomes. The results are summarized in Table 6-3. From the limited data, we concluded that addition of a C-3 ester group to **44** can confer activity, and the identity of the ester group can influence potency. Within the C-3 side chain, a polar oxygen atom (**143**) was not tolerated and larger lipophilic moieties (**58**, **74**, **144**) were favored.

Table 6-3. Proteasome inhibition activity of 3-substituted BA analogs ^a



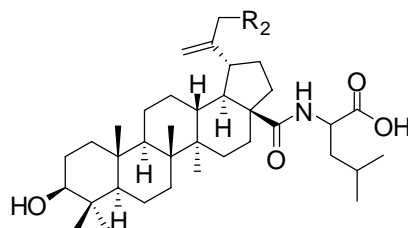
Compound	R ₁	IC ₅₀ (μM)
44	H	NS
58		7.2
74		< 3
143		NS
144		1.6


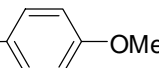
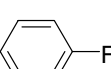
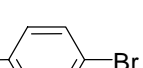
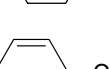
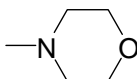
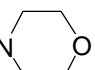
^a All data presented are averages of at least two separate experiments performed by Dr. Chin-Ho Chen, Duke University, NC. IC₅₀: concentration that inhibits the chymotrypsin-like activity of human 20S proteasomes by 50%. NS: no inhibition.

In our prior results, modification of the C-19 isopropenyl moiety of **44** did not affect antiviral potency, but did slightly increase cytotoxicity. Thus, we hypothesized that the C-19 position is also related to proteasome inhibition activity. Therefore, eleven 28,30-disubstituted compounds (**96-98**, **100-107**) with varying functionalities appended to the C-19 isopropenyl group were screened for inhibition of proteasome activity. Their structures and anti-proteasome activities are summarized in Table 6-4. The preliminary screening data confirmed our hypothesis that substitution at the C-30 position could increase anti-proteasome activity of **44** analogs. The most active derivative **102** had an IC₅₀ value of 1.7 μ M, making it five-fold more active than **58**. From the bioassay data, we concluded that aromatic ring systems at C-30 can significantly increase the anti-proteasome chymotrypsin-like activity of 28,30-disubstituted BA derivatives. Comparatively, polar moieties only slightly enhanced anti-proteasome activity.

Two C-28 monosubstituted BA derivatives were also screened against chymotrypsin-like activity of human 20S proteasomes in order to investigate the effect of C-28 modification on proteasome inhibition activity. These compounds included IC9564 (**48**) with a long C-28 side chain and 15bh (**95**) with a short C-28 side chain (Table 6-4). However, neither of the compounds exhibited anti-proteasome activity. Whether introduction of other functional groups at C-28, rather than aminoalkanoic acid groups, will increase proteasome inhibition activity needs to be further evaluated.

Table 6-4. Proteasome inhibition activities of 28,30-disubstituted BA analogs ^a



Compound	R ₂	IC ₅₀ (μM)
96	—Br	5.9
97	—OCH ₂ CH ₃	13.2
98	—O(CH ₂) ₂ CH ₃	3.7
100	—O(CH ₂) ₂ — 	1.8
101	—O(CH ₂) ₂ — 	2.3
102	—O(CH ₂) ₂ — 	1.7
103	—O(CH ₂) ₂ — 	++ (> 90%)
104	—O(CH ₂) ₂ — 	++ (> 90%)
105	— 	+ (40-60%)
106	—O(CH ₂) ₂ — 	+ (40-60%)
107	—OH	+ (40-60%)

^a All data presented are averages of at least two separate experiments performed by Dr. Chin-Ho Chen, Duke University, NC. IC₅₀: concentration that inhibits the chymotrypsin-like activity of human 20S proteasomes by 50%. ++: strongly inhibits (> 90%) the chymotrypsin-like activity of human 20S proteasomes at test concentration (10 μg/ml). +: moderately inhibits (40-60%) the chymotrypsin-like activity of human 20S proteasomes at test concentration (10 μg/ml).

In conclusion, we discovered that C-3 and C-30 modification with lipophilic moieties and aromatic rings can significantly increase the anti-proteasome activity of BA derivatives. Comparatively, analogs with C-28 amidoalkanoic acids rather than leucine side chains had no proteasome inhibition activity. These results suggest that 3,30-disubstituted BA analogs may possess enhanced anti-proteasome activity and have a better potential to be developed into potent proteasome inhibitors and potential anticancer drugs.

3-3. Future Planned Studies on Novel BA Analogs as Potent Anti-proteasome Agents

3,30-Disubstituted BA analogs with different functionalities as shown in Figure 6-7 can be synthesized and evaluated against human 20S proteasome. This design incorporates the favored substitutions in monosubstituted BA analogs into one BA molecule. The C-28 carboxylic acid will be kept free in order to increase the compound's solubility. The synthetic methods for these novel compounds are summarized in Scheme 6-1.

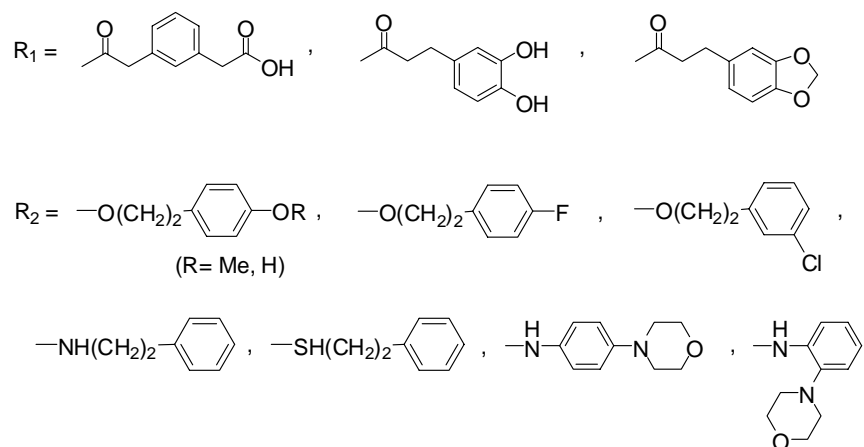
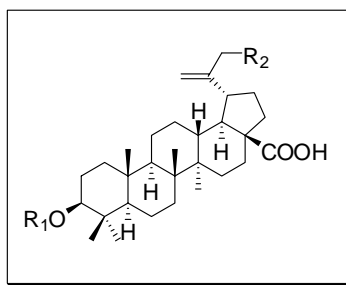
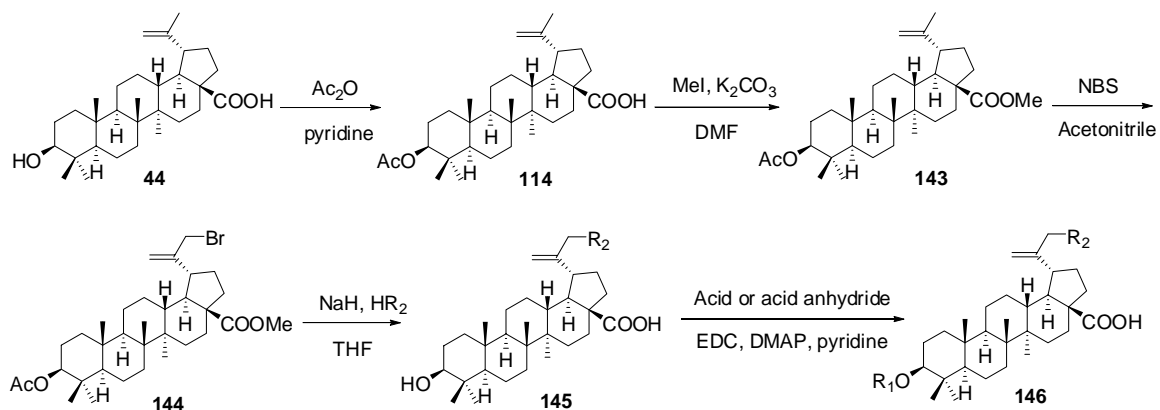


Figure 6-7. 3,30-disubstituted BA analogs to increase anti-proteasome activity



Scheme 6-1. General synthetic route for 3,30-disubstituted BA analogs

REFERENCES

- (1) UNAIDS. AIDS epidemic update, December 2007.
- (2) Varghese, B.; Maher, J. E.; Peterman, T. A.; Branson, B. M.; Steketee, R. W. Reducing the risk of sexual HIV transmission: quantifying the per-act risk for HIV on the basis of choice of partner, sex act, and condom use. *Sex Transm Dis* **2002**, *29*, 38-43.
- (3) Kaplan, E. H.; Heimer, R. HIV incidence among New Haven needle exchange participants: updated estimates from syringe tracking and testing data. *J Acquir Immune Defic Syndr Hum Retrovirol* **1995**, *10*, 175-176.
- (4) Coovadia, H. Antiretroviral agents--how best to protect infants from HIV and save their mothers from AIDS. *N Engl J Med* **2004**, *351*, 289-292.
- (5) Buchbinder, S. P.; Katz, M. H.; Hessel, N. A.; O'Malley, P. M.; Holmberg, S. D. Long-term HIV-1 infection without immunologic progression. *Aids* **1994**, *8*, 1123-1128.
- (6) Levy, J. A. HIV pathogenesis and long-term survival. *Aids* **1993**, *7*, 1401-1410.
- (7) Gao, F.; Yue, L.; Robertson, D. L.; Hill, S. C.; Hui, H. et al. Genetic diversity of human immunodeficiency virus type 2: evidence for distinct sequence subtypes with differences in virus biology. *J Virol* **1994**, *68*, 7433-7447.
- (8) Arien, K. K.; Vanham, G.; Arts, E. J. Is HIV-1 evolving to a less virulent form in humans? *Nat Rev Microbiol* **2007**, *5*, 141-151.
- (9) Reeves, J. D.; Doms, R. W. Human immunodeficiency virus type 2. *J Gen Virol* **2002**, *83*, 1253-1265.
- (10) Russo-Marie, F. [HIV and macrophage]. *Pathol Biol (Paris)* **1997**, *45*, 137-145.
- (11) Lu, M.; Blacklow, S. C.; Kim, P. S. A trimeric structural domain of the HIV-1 transmembrane glycoprotein. *Nat Struct Biol* **1995**, *2*, 1075-1082.
- (12) Kwong, P. D.; Wyatt, R.; Robinson, J.; Sweet, R. W.; Sodroski, J. et al. Structure of an HIV gp120 envelope glycoprotein in complex with the CD4 receptor and a neutralizing human antibody. *Nature* **1998**, *393*, 648-659.
- (13) Morrow, C. D.; Park, J.; Wakefield, J. K. Viral gene products and replication of the human immunodeficiency type 1 virus. *Am J Physiol* **1994**, *266*, C1135-1156.
- (14) Gallo, R. C. The AIDS virus. *Sci Am* **1987**, *256*, 46-56.

- (15) Caputo, A.; Grossi, M. P.; Rossi, C.; Campioni, D.; Balboni, P. G. et al. The tat gene and protein of the human immunodeficiency virus type 1. *New Microbiol* **1995**, *18*, 87-110.
- (16) Symensma, T. L.; Giver, L.; Zapp, M.; Takle, G. B.; Ellington, A. D. RNA aptamers selected to bind human immunodeficiency virus type 1 Rev in vitro are Rev responsive in vivo. *J Virol* **1996**, *70*, 179-187.
- (17) Park, I. W.; Sodroski, J. Functional analysis of the vpx, vpr, and nef genes of simian immunodeficiency virus. *J Acquir Immune Defic Syndr Hum Retrovirol* **1995**, *8*, 335-344.
- (18) Strebel, K.; Klimkait, T.; Martin, M. A. A novel gene of HIV-1, vpu, and its 16-kilodalton product. *Science* **1988**, *241*, 1221-1223.
- (19) McGovern, S. L.; Caselli, E.; Grigorieff, N.; Shoichet, B. K. A common mechanism underlying promiscuous inhibitors from virtual and high-throughput screening. *J Med Chem* **2002**, *45*, 1712-1722.
- (20) Tomaras, G. D.; Greenberg, M. L. Mechanisms for HIV-1 Entry: Current Strategies to Interfere with This Step. *Curr Infect Dis Rep* **2001**, *3*, 93-99.
- (21) Reeves, J. D.; Hibbitts, S.; Simmons, G.; McKnight, A.; Azevedo-Pereira, J. M. et al. Primary human immunodeficiency virus type 2 (HIV-2) isolates infect CD4-negative cells via CCR5 and CXCR4: comparison with HIV-1 and simian immunodeficiency virus and relevance to cell tropism in vivo. *J Virol* **1999**, *73*, 7795-7804.
- (22) Edwards, T. G.; Hoffman, T. L.; Baribaud, F.; Wyss, S.; LaBranche, C. C. et al. Relationships between CD4 independence, neutralization sensitivity, and exposure of a CD4-induced epitope in a human immunodeficiency virus type 1 envelope protein. *J Virol* **2001**, *75*, 5230-5239.
- (23) Reeves, J. D.; Piefer, A. J. Emerging drug targets for antiretroviral therapy. *Drugs* **2005**, *65*, 1747-1766.
- (24) Hoffman, T. L.; LaBranche, C. C.; Zhang, W.; Canziani, G.; Robinson, J. et al. Stable exposure of the coreceptor-binding site in a CD4-independent HIV-1 envelope protein. *Proc Natl Acad Sci U S A* **1999**, *96*, 6359-6364.
- (25) Pani, A.; Loi, A. G.; Mura, M.; Marceddu, T.; La Colla, P. et al. Targeting HIV: old and new players. *Curr Drug Targets Infect Disord* **2002**, *2*, 17-32.
- (26) Pommier, Y.; Johnson, A. A.; Marchand, C. Integrase inhibitors to treat HIV/AIDS. *Nat Rev Drug Discov* **2005**, *4*, 236-248.
- (27) Freed, E. O. HIV-1 gag proteins: diverse functions in the virus life cycle. *Virology* **1998**, *251*, 1-15.

- (28) Girard, M. P.; Osmanov, S. K.; Kieny, M. P. A review of vaccine research and development: the human immunodeficiency virus (HIV). *Vaccine* **2006**, *24*, 4062-4081.
- (29) Cervia, J. S.; Smith, M. A. Enfuvirtide (T-20): a novel human immunodeficiency virus type 1 fusion inhibitor. *Clin Infect Dis* **2003**, *37*, 1102-1106.
- (30) Carter, N. J.; Keating, G. M. Maraviroc. *Drugs* **2007**, *67*, 2277-2288; discussion 2289-2290.
- (31) Croxtall, J. D.; Lyseng-Williamson, K. A.; Perry, C. M. Raltegravir. *Drugs* **2008**, *68*, 131-138.
- (32) Huang, P.; Farquhar, D.; Plunkett, W. Selective action of 3'-azido-3'-deoxythymidine 5'-triphosphate on viral reverse transcriptases and human DNA polymerases. *J Biol Chem* **1990**, *265*, 11914-11918.
- (33) Chapman, T.; McGavin, J.; Noble, S. Tenofovir disoproxil fumarate. *Drugs* **2003**, *63*, 1597-1608.
- (34) Spence, R. A.; Kati, W. M.; Anderson, K. S.; Johnson, K. A. Mechanism of inhibition of HIV-1 reverse transcriptase by nonnucleoside inhibitors. *Science* **1995**, *267*, 988-993.
- (35) Esnouf, R. M.; Ren, J.; Hopkins, A. L.; Ross, C. K.; Jones, E. Y. et al. Unique features in the structure of the complex between HIV-1 reverse transcriptase and the bis(heteroaryl)piperazine (BHAP) U-90152 explain resistance mutations for this nonnucleoside inhibitor. *Proc Natl Acad Sci U S A* **1997**, *94*, 3984-3989.
- (36) Debouck, C. The HIV-1 protease as a therapeutic target for AIDS. *AIDS Res Hum Retroviruses* **1992**, *8*, 153-164.
- (37) Ho, D. D.; Neumann, A. U.; Perelson, A. S.; Chen, W.; Leonard, J. M. et al. Rapid turnover of plasma virions and CD4 lymphocytes in HIV-1 infection. *Nature* **1995**, *373*, 123-126.
- (38) Hammer, S. M.; Katzenstein, D. A.; Hughes, M. D.; Gundacker, H.; Schooley, R. T. et al. A trial comparing nucleoside monotherapy with combination therapy in HIV-infected adults with CD4 cell counts from 200 to 500 per cubic millimeter. AIDS Clinical Trials Group Study 175 Study Team. *N Engl J Med* **1996**, *335*, 1081-1090.
- (39) Gulick, R. M.; Meibohm, A.; Havlir, D.; Eron, J. J.; Mosley, A. et al. Six-year follow-up of HIV-1-infected adults in a clinical trial of antiretroviral therapy with indinavir, zidovudine, and lamivudine. *Aids* **2003**, *17*, 2345-2349.
- (40) Chun, T. W.; Carruth, L.; Finzi, D.; Shen, X.; DiGiuseppe, J. A. et al. Quantification of latent tissue reservoirs and total body viral load in HIV-1 infection. *Nature* **1997**, *387*, 183-188.
- (41) Finzi, D.; Hermankova, M.; Pierson, T.; Carruth, L. M.; Buck, C. et al. Identification of a

- reservoir for HIV-1 in patients on highly active antiretroviral therapy. *Science* **1997**, 278, 1295-1300.
- (42) Wong, J. K.; Hezareh, M.; Gunthard, H. F.; Havlir, D. V.; Ignacio, C. C. et al. Recovery of replication-competent HIV despite prolonged suppression of plasma viremia. *Science* **1997**, 278, 1291-1295.
 - (43) Piscitelli, S. C.; Flexner, C.; Minor, J. R.; Polis, M. A.; Masur, H. Drug interactions in patients infected with human immunodeficiency virus. *Clin Infect Dis* **1996**, 23, 685-693.
 - (44) Louie, M.; Markowitz, M. Goals and milestones during treatment of HIV-1 infection with antiretroviral therapy: a pathogenesis-based perspective. *Antiviral Res* **2002**, 55, 15-25.
 - (45) Boden, D.; Hurley, A.; Zhang, L.; Cao, Y.; Guo, Y. et al. HIV-1 drug resistance in newly infected individuals. *Jama* **1999**, 282, 1135-1141.
 - (46) Wegner, S. A.; Brodine, S. K.; Mascola, J. R.; Tasker, S. A.; Shaffer, R. A. et al. Prevalence of genotypic and phenotypic resistance to anti-retroviral drugs in a cohort of therapy-naïve HIV-1 infected US military personnel. *Aids* **2000**, 14, 1009-1015.
 - (47) Hammer, S. M.; Pedneault, L. Antiretroviral resistance testing comes of age. *Antivir Ther* **2000**, 5, 23-26.
 - (48) Speck, R. F.; Wehrly, K.; Platt, E. J.; Atchison, R. E.; Charo, I. F. et al. Selective employment of chemokine receptors as human immunodeficiency virus type 1 coreceptors determined by individual amino acids within the envelope V3 loop. *J Virol* **1997**, 71, 7136-7139.
 - (49) Chan, D. C.; Fass, D.; Berger, J. M.; Kim, P. S. Core structure of gp41 from the HIV envelope glycoprotein. *Cell* **1997**, 89, 263-273.
 - (50) Weissenhorn, W.; Dessen, A.; Harrison, S. C.; Skehel, J. J.; Wiley, D. C. Atomic structure of the ectodomain from HIV-1 gp41. *Nature* **1997**, 387, 426-430.
 - (51) Melikyan, G. B.; Markosyan, R. M.; Hemmati, H.; Delmedico, M. K.; Lambert, D. M. et al. Evidence that the transition of HIV-1 gp41 into a six-helix bundle, not the bundle configuration, induces membrane fusion. *J Cell Biol* **2000**, 151, 413-423.
 - (52) Mondor, I.; Ugolini, S.; Sattentau, Q. J. Human immunodeficiency virus type 1 attachment to HeLa CD4 cells is CD4 independent and gp120 dependent and requires cell surface heparans. *J Virol* **1998**, 72, 3623-3634.
 - (53) Moulard, M.; Lortat-Jacob, H.; Mondor, I.; Roca, G.; Wyatt, R. et al. Selective interactions of polyanions with basic surfaces on human immunodeficiency virus type 1 gp120. *J Virol* **2000**, 74, 1948-1960.

- (54) Callahan, L. N.; Phelan, M.; Mallinson, M.; Norcross, M. A. Dextran sulfate blocks antibody binding to the principal neutralizing domain of human immunodeficiency virus type 1 without interfering with gp120-CD4 interactions. *J Virol* **1991**, *65*, 1543-1550.
- (55) Boyd, M. R.; Gustafson, K. R.; McMahon, J. B.; Shoemaker, R. H.; O'Keefe, B. R. et al. Discovery of cyanovirin-N, a novel human immunodeficiency virus-inactivating protein that binds viral surface envelope glycoprotein gp120: potential applications to microbicide development. *Antimicrob Agents Chemother* **1997**, *41*, 1521-1530.
- (56) Dey, B.; Lerner, D. L.; Lusso, P.; Boyd, M. R.; Elder, J. H. et al. Multiple antiviral activities of cyanovirin-N: blocking of human immunodeficiency virus type 1 gp120 interaction with CD4 and coreceptor and inhibition of diverse enveloped viruses. *J Virol* **2000**, *74*, 4562-4569.
- (57) Botos, I.; O'Keefe, B. R.; Shenoy, S. R.; Cartner, L. K.; Ratner, D. M. et al. Structures of the complexes of a potent anti-HIV protein cyanovirin-N and high mannose oligosaccharides. *J Biol Chem* **2002**, *277*, 34336-34342.
- (58) Van Damme, L.; Wright, A.; Depraetere, K.; Rosenstein, I.; Vandersmissen, V. et al. A phase I study of a novel potential intravaginal microbicide, PRO 2000, in healthy sexually inactive women. *Sex Transm Infect* **2000**, *76*, 126-130.
- (59) Smita, J.; Soma, D.; Beverly, B.; Albert, P.; JoAnn, K. et al. Phase I safety study of 0.5% PRO 2000 vaginal Gel among HIV un-infected women in Pune, India. *AIDS Res Ther* **2006**, *3*, 4.
- (60) Huang, L.; Chen, C. H. Molecular targets of anti-HIV-1 triterpenes. *Curr Drug Targets Infect Disord* **2002**, *2*, 33-36.
- (61) Jacobson, J. M.; Israel, R. J.; Lowy, I.; Ostrow, N. A.; Vassilatos, L. S. et al. Treatment of advanced human immunodeficiency virus type 1 disease with the viral entry inhibitor PRO 542. *Antimicrob Agents Chemother* **2004**, *48*, 423-429.
- (62) Jacobson, J. M.; Lowy, I.; Fletcher, C. V.; O'Neill, T. J.; Tran, D. N. et al. Single-dose safety, pharmacology, and antiviral activity of the human immunodeficiency virus (HIV) type 1 entry inhibitor PRO 542 in HIV-infected adults. *J Infect Dis* **2000**, *182*, 326-329.
- (63) Moore, J. P.; Sattentau, Q. J.; Klasse, P. J.; Burkly, L. C. A monoclonal antibody to CD4 domain 2 blocks soluble CD4-induced conformational changes in the envelope glycoproteins of human immunodeficiency virus type 1 (HIV-1) and HIV-1 infection of CD4⁺ cells. *J Virol* **1992**, *66*, 4784-4793.
- (64) Kuritzkes, D. R.; Jacobson, J.; Powderly, W. G.; Godofsky, E.; DeJesus, E. et al. Antiretroviral activity of the anti-CD4 monoclonal antibody TNX-355 in patients infected with HIV type 1. *J Infect Dis* **2004**, *189*, 286-291.

- (65) Lin, P. F.; Blair, W.; Wang, T.; Spicer, T.; Guo, Q. et al. A small molecule HIV-1 inhibitor that targets the HIV-1 envelope and inhibits CD4 receptor binding. *Proc Natl Acad Sci U S A* **2003**, *100*, 11013-11018.
- (66) Guo, Q.; Ho, H. T.; Dicker, I.; Fan, L.; Zhou, N. et al. Biochemical and genetic characterizations of a novel human immunodeficiency virus type 1 inhibitor that blocks gp120-CD4 interactions. *J Virol* **2003**, *77*, 10528-10536.
- (67) Ho, H. T.; Fan, L.; Nowicka-Sans, B.; McAuliffe, B.; Li, C. B. et al. Envelope conformational changes induced by human immunodeficiency virus type 1 attachment inhibitors prevent CD4 binding and downstream entry events. *J Virol* **2006**, *80*, 4017-4025.
- (68) Si, Z.; Madani, N.; Cox, J. M.; Chruma, J. J.; Klein, J. C. et al. Small-molecule inhibitors of HIV-1 entry block receptor-induced conformational changes in the viral envelope glycoproteins. *Proc Natl Acad Sci U S A* **2004**, *101*, 5036-5041.
- (69) Kadow, J.; Wang, H. G.; Lin, P. F. Small-molecule HIV-1 gp120 inhibitors to prevent HIV-1 entry: an emerging opportunity for drug development. *Curr Opin Investig Drugs* **2006**, *7*, 721-726.
- (70) Zhao, Q.; Ma, L.; Jiang, S.; Lu, H.; Liu, S. et al. Identification of N-phenyl-N'-(2,2,6,6-tetramethyl-piperidin-4-yl)-oxalamides as a new class of HIV-1 entry inhibitors that prevent gp120 binding to CD4. *Virology* **2005**, *339*, 213-225.
- (71) Vermeire, K.; Zhang, Y.; Princen, K.; Hatse, S.; Samala, M. F. et al. CADA inhibits human immunodeficiency virus and human herpesvirus 7 replication by down-modulation of the cellular CD4 receptor. *Virology* **2002**, *302*, 342-353.
- (72) Vermeire, K.; Bell, T. W.; Choi, H. J.; Jin, Q.; Samala, M. F. et al. The Anti-HIV potency of cyclotriazadisulfonamide analogs is directly correlated with their ability to down-modulate the CD4 receptor. *Mol Pharmacol* **2003**, *63*, 203-210.
- (73) Bell, T. W.; Anugu, S.; Bailey, P.; Catalano, V. J.; Dey, K. et al. Synthesis and structure-activity relationship studies of CD4 down-modulating cyclotriazadisulfonamide (CADA) analogues. *J Med Chem* **2006**, *49*, 1291-1312.
- (74) Vermeire, K.; Schols, D.; Bell, T. W. CD4 down-modulating compounds with potent anti-HIV activity. *Curr Pharm Des* **2004**, *10*, 1795-1803.
- (75) Berger, E. A.; Murphy, P. M.; Farber, J. M. Chemokine receptors as HIV-1 coreceptors: roles in viral entry, tropism, and disease. *Annu Rev Immunol* **1999**, *17*, 657-700.
- (76) Berger, E. A.; Doms, R. W.; Fenyo, E. M.; Korber, B. T.; Littman, D. R. et al. A new classification for HIV-1. *Nature* **1998**, *391*, 240.

- (77) Zhu, T.; Mo, H.; Wang, N.; Nam, D. S.; Cao, Y. et al. Genotypic and phenotypic characterization of HIV-1 patients with primary infection. *Science* **1993**, *261*, 1179-1181.
- (78) Moyle, G. J.; Wildfire, A.; Mandalia, S.; Mayer, H.; Goodrich, J. et al. Epidemiology and predictive factors for chemokine receptor use in HIV-1 infection. *J Infect Dis* **2005**, *191*, 866-872.
- (79) Cormier, E. G.; Dragic, T. The crown and stem of the V3 loop play distinct roles in human immunodeficiency virus type 1 envelope glycoprotein interactions with the CCR5 coreceptor. *J Virol* **2002**, *76*, 8953-8957.
- (80) Briz, V.; Poveda, E.; Soriano, V. HIV entry inhibitors: mechanisms of action and resistance pathways. *J Antimicrob Chemother* **2006**, *57*, 619-627.
- (81) Liu, R.; Paxton, W. A.; Choe, S.; Ceradini, D.; Martin, S. R. et al. Homozygous defect in HIV-1 coreceptor accounts for resistance of some multiply-exposed individuals to HIV-1 infection. *Cell* **1996**, *86*, 367-377.
- (82) Samson, M.; Libert, F.; Doranz, B. J.; Rucker, J.; Liesnard, C. et al. Resistance to HIV-1 infection in caucasian individuals bearing mutant alleles of the CCR-5 chemokine receptor gene. *Nature* **1996**, *382*, 722-725.
- (83) Cocchi, F.; DeVico, A. L.; Garzino-Demo, A.; Arya, S. K.; Gallo, R. C. et al. Identification of RANTES, MIP-1 alpha, and MIP-1 beta as the major HIV-suppressive factors produced by CD8+ T cells. *Science* **1995**, *270*, 1811-1815.
- (84) Lederman, M. M.; Veazey, R. S.; Offord, R.; Mosier, D. E.; Dufour, J. et al. Prevention of vaginal SHIV transmission in rhesus macaques through inhibition of CCR5. *Science* **2004**, *306*, 485-487.
- (85) Trkola, A.; Ketas, T. J.; Nagashima, K. A.; Zhao, L.; Cilliers, T. et al. Potent, broad-spectrum inhibition of human immunodeficiency virus type 1 by the CCR5 monoclonal antibody PRO 140. *J Virol* **2001**, *75*, 579-588.
- (86) Baba, M.; Nishimura, O.; Kanzaki, N.; Okamoto, M.; Sawada, H. et al. A small-molecule, nonpeptide CCR5 antagonist with highly potent and selective anti-HIV-1 activity. *Proc Natl Acad Sci U S A* **1999**, *96*, 5698-5703.
- (87) Dragic, T.; Trkola, A.; Thompson, D. A.; Cormier, E. G.; Kajumo, F. A. et al. A binding pocket for a small molecule inhibitor of HIV-1 entry within the transmembrane helices of CCR5. *Proc Natl Acad Sci U S A* **2000**, *97*, 5639-5644.
- (88) Seto, M.; Aikawa, K.; Miyamoto, N.; Aramaki, Y.; Kanzaki, N. et al. Highly potent and orally active CCR5 antagonists as anti-HIV-1 agents: synthesis and biological activities of

- 1-benzazocine derivatives containing a sulfoxide moiety. *J Med Chem* **2006**, *49*, 2037-2048.
- (89) Imamura, S.; Ichikawa, T.; Nishikawa, Y.; Kanzaki, N.; Takashima, K. et al. Discovery of a piperidine-4-carboxamide CCR5 antagonist (TAK-220) with highly potent Anti-HIV-1 activity. *J Med Chem* **2006**, *49*, 2784-2793.
- (90) Dorr, P.; Westby, M.; Dobbs, S.; Griffin, P.; Irvine, B. et al. Maraviroc (UK-427,857), a potent, orally bioavailable, and selective small-molecule inhibitor of chemokine receptor CCR5 with broad-spectrum anti-human immunodeficiency virus type 1 activity. *Antimicrob Agents Chemother* **2005**, *49*, 4721-4732.
- (91) Wood, A.; Armour, D. The discovery of the CCR5 receptor antagonist, UK-427,857, a new agent for the treatment of HIV infection and AIDS. *Prog Med Chem* **2005**, *43*, 239-271.
- (92) Armour, D.; de Groot, M. J.; Edwards, M.; Perros, M.; Price, D. A. et al. The discovery of CCR5 receptor antagonists for the treatment of HIV infection: hit-to-lead studies. *ChemMedChem* **2006**, *1*, 706-709.
- (93) Price, D. A.; Armour, D.; de Groot, M.; Leishman, D.; Napier, C. et al. Overcoming HERG affinity in the discovery of the CCR5 antagonist maraviroc. *Bioorg Med Chem Lett* **2006**, *16*, 4633-4637.
- (94) Castonguay, L. A.; Weng, Y.; Adolfsen, W.; Di Salvo, J.; Kilburn, R. et al. Binding of 2-aryl-4-(piperidin-1-yl)butanamines and 1,3,4-trisubstituted pyrrolidines to human CCR5: a molecular modeling-guided mutagenesis study of the binding pocket. *Biochemistry* **2003**, *42*, 1544-1550.
- (95) Tagat, J. R.; McCombie, S. W.; Nazareno, D.; Labroli, M. A.; Xiao, Y. et al. Piperazine-based CCR5 antagonists as HIV-1 inhibitors. IV. Discovery of 1-[(4,6-dimethyl-5-pyrimidinyl)carbonyl]-4-[4-[2-methoxy-1(R)-4-(trifluoromethyl)phenyl]ethyl-3(S)-methyl-1-piperazinyl]-4-methylpiperidine (Sch-417690/Sch-D), a potent, highly selective, and orally bioavailable CCR5 antagonist. *J Med Chem* **2004**, *47*, 2405-2408.
- (96) Strizki, J. M.; Tremblay, C.; Xu, S.; Wojcik, L.; Wagner, N. et al. Discovery and characterization of vicriviroc (SCH 417690), a CCR5 antagonist with potent activity against human immunodeficiency virus type 1. *Antimicrob Agents Chemother* **2005**, *49*, 4911-4919.
- (97) Tsamis, F.; Gavrilov, S.; Kajumo, F.; Seibert, C.; Kuhmann, S. et al. Analysis of the mechanism by which the small-molecule CCR5 antagonists SCH-351125 and SCH-350581 inhibit human immunodeficiency virus type 1 entry. *J Virol* **2003**, *77*, 5201-5208.
- (98) Seibert, C.; Ying, W.; Gavrilov, S.; Tsamis, F.; Kuhmann, S. E. et al. Interaction of small molecule inhibitors of HIV-1 entry with CCR5. *Virology* **2006**, *349*, 41-54.

- (99) Cohenl, C., Dejesus, E., Mills, A., Pierone, G., Kumar, Jr. P., Ruane, P., Elion, R., Fusco, G., Levy, R., Solomon, K., Erickson-Viitanen, S., Potent Antiretroviral Activity of the Once-daily CCR5 Antagonist INCB009471 over 14 Days of Monotherapy. *4th IAS Conference on HIV Pathogenesis, Treatment and Prevention* **2007**, July, Sydney, Australia.
- (100) Maeda, K.; Nakata, H.; Koh, Y.; Miyakawa, T.; Ogata, H. et al. Spirodiketopiperazine-based CCR5 inhibitor which preserves CC-chemokine/CCR5 interactions and exerts potent activity against R5 human immunodeficiency virus type 1 in vitro. *J Virol* **2004**, 78, 8654-8662.
- (101) Watson, C.; Jenkinson, S.; Kazmierski, W.; Kenakin, T. The CCR5 receptor-based mechanism of action of 873140, a potent allosteric noncompetitive HIV entry inhibitor. *Mol Pharmacol* **2005**, 67, 1268-1282.
- (102) Kazmierski WM, A. C., Bifulco N, Boros EE, Chauder BA, Chong PY, Duan M, Deanda F, Koble CS, McLean EW, Peckham JP, Perkins AC, Thompson JB, Vanderwall D *WO* 2004054974.
- (103) Howard, O. M.; Korte, T.; Tarasova, N. I.; Grimm, M.; Turpin, J. A. et al. Small molecule inhibitor of HIV-1 cell fusion blocks chemokine receptor-mediated function. *J Leukoc Biol* **1998**, 64, 6-13.
- (104) Chen, X.; Yang, L.; Zhang, N.; Turpin, J. A.; Buckheit, R. W. et al. Shikonin, a component of chinese herbal medicine, inhibits chemokine receptor function and suppresses human immunodeficiency virus type 1. *Antimicrob Agents Chemother* **2003**, 47, 2810-2816.
- (105) Dorn, C. P.; Finke, P. E.; Oates, B.; Budhu, R. J.; Mills, S. G. et al. Antagonists of the human CCR5 receptor as anti-HIV-1 agents. part 1: discovery and initial structure-activity relationships for 1 -amino-2-phenyl-4-(piperidin-1-yl)butanes. *Bioorg Med Chem Lett* **2001**, 11, 259-264.
- (106) Finke, P. E.; Meurer, L. C.; Oates, B.; Shah, S. K.; Loebach, J. L. et al. Antagonists of the human CCR5 receptor as anti-HIV-1 agents. Part 3: a proposed pharmacophore model for 1-[N-(methyl)-N-(phenylsulfonyl)amino]-2-(phenyl)-4-[4-(substituted)piperidin-1-yl]butanes. *Bioorg Med Chem Lett* **2001**, 11, 2469-2473.
- (107) Hale, J. J.; Budhu, R. J.; Holson, E. B.; Finke, P. E.; Oates, B. et al. 1,3,4-Trisubstituted pyrrolidine CCR5 receptor antagonists. Part 2: lead optimization affording selective, orally bioavailable compounds with potent anti-HIV activity. *Bioorg Med Chem Lett* **2001**, 11, 2741-2745.
- (108) Kim, D.; Wang, L.; Caldwell, C. G.; Chen, P.; Finke, P. E. et al. Discovery of human CCR5 antagonists containing hydantoins for the treatment of HIV-1 infection. *Bioorg Med Chem Lett* **2001**, 11, 3099-3102.

- (109) Tachibana, K.; Hirota, S.; Iizasa, H.; Yoshida, H.; Kawabata, K. et al. The chemokine receptor CXCR4 is essential for vascularization of the gastrointestinal tract. *Nature* **1998**, *393*, 591-594.
- (110) Zou, Y. R.; Kottmann, A. H.; Kuroda, M.; Taniuchi, I.; Littman, D. R. Function of the chemokine receptor CXCR4 in haematopoiesis and in cerebellar development. *Nature* **1998**, *393*, 595-599.
- (111) Ma, Q.; Jones, D.; Borghesani, P. R.; Segal, R. A.; Nagasawa, T. et al. Impaired B-lymphopoiesis, myelopoiesis, and derailed cerebellar neuron migration in CXCR4- and SDF-1-deficient mice. *Proc Natl Acad Sci U S A* **1998**, *95*, 9448-9453.
- (112) Blanco, J.; Barretina, J.; Henson, G.; Bridger, G.; De Clercq, E. et al. The CXCR4 antagonist AMD3100 efficiently inhibits cell-surface-expressed human immunodeficiency virus type 1 envelope-induced apoptosis. *Antimicrob Agents Chemother* **2000**, *44*, 51-56.
- (113) Hatse, S.; Princen, K.; De Clercq, E.; Rosenkilde, M. M.; Schwartz, T. W. et al. AMD3465, a monomacrocyclic CXCR4 antagonist and potent HIV entry inhibitor. *Biochem Pharmacol* **2005**, *70*, 752-761.
- (114) Seibert, C.; Sakmar, T. P. Small-molecule antagonists of CCR5 and CXCR4: a promising new class of anti-HIV-1 drugs. *Curr Pharm Des* **2004**, *10*, 2041-2062.
- (115) Stone, N. D.; Dunaway, S. B.; Flexner, C.; Tierney, C.; Calandra, G. B. et al. Multiple-dose escalation study of the safety, pharmacokinetics, and biologic activity of oral AMD070, a selective CXCR4 receptor inhibitor, in human subjects. *Antimicrob Agents Chemother* **2007**, *51*, 2351-2358.
- (116) Ichiyama, K.; Yokoyama-Kumakura, S.; Tanaka, Y.; Tanaka, R.; Hirose, K. et al. A duodenally absorbable CXC chemokine receptor 4 antagonist, KRH-1636, exhibits a potent and selective anti-HIV-1 activity. *Proc Natl Acad Sci U S A* **2003**, *100*, 4185-4190.
- (117) Murakami, T.; Yoshida, A.; Tanaka, R.; Mitsuhashi, S.; Hirose, K.; Yanaka, M.; Yamamoto, N. and Tanaka, Y. KRH-2731: An Orally Bioavailable CXCR4 Antagonist Is a Potent Inhibitor of HIV-1 Infection. *11th Conference on Retroviruses and Opportunistic Infections* **2004**, *San Francisco, CA*, abstract #541.
- (118) Wild, C.; Oas, T.; McDanal, C.; Bolognesi, D.; Matthews, T. A synthetic peptide inhibitor of human immunodeficiency virus replication: correlation between solution structure and viral inhibition. *Proc Natl Acad Sci U S A* **1992**, *89*, 10537-10541.
- (119) Jiang, S.; Lin, K.; Strick, N.; Neurath, A. R. HIV-1 inhibition by a peptide. *Nature* **1993**, *365*, 113.

- (120) Poveda, E.; Briz, V.; Soriano, V. Enfuvirtide, the first fusion inhibitor to treat HIV infection. *AIDS Rev* **2005**, *7*, 139-147.
- (121) Robertson, D. US FDA approves new class of HIV therapeutics. *Nat Biotechnol* **2003**, *21*, 470-471.
- (122) Wild, C.; Greenwell, T.; Matthews, T. A synthetic peptide from HIV-1 gp41 is a potent inhibitor of virus-mediated cell-cell fusion. *AIDS Res Hum Retroviruses* **1993**, *9*, 1051-1053.
- (123) Weiss, C. D. HIV-1 gp41: mediator of fusion and target for inhibition. *AIDS Rev* **2003**, *5*, 214-221.
- (124) Poveda, E.; Rodes, B.; Lebel-Binay, S.; Faudon, J. L.; Jimenez, V. et al. Dynamics of enfuvirtide resistance in HIV-infected patients during and after long-term enfuvirtide salvage therapy. *J Clin Virol* **2005**, *34*, 295-301.
- (125) Lalezari, J. P.; Bellos, N. C.; Sathasivam, K.; Richmond, G. J.; Cohen, C. J. et al. T-1249 retains potent antiretroviral activity in patients who had experienced virological failure while on an enfuvirtide-containing treatment regimen. *J Infect Dis* **2005**, *191*, 1155-1163.
- (126) Markovic, I.; Clouse, K. A. Recent advances in understanding the molecular mechanisms of HIV-1 entry and fusion: revisiting current targets and considering new options for therapeutic intervention. *Curr HIV Res* **2004**, *2*, 223-234.
- (127) Martin-Carbonero, L. Discontinuation of the clinical development of fusion inhibitor T-1249. *AIDS Rev* **2004**, *6*, 61.
- (128) Debnath, A. K.; Radigan, L.; Jiang, S. Structure-based identification of small molecule antiviral compounds targeted to the gp41 core structure of the human immunodeficiency virus type 1. *J Med Chem* **1999**, *42*, 3203-3209.
- (129) Armand-Ugon, M.; Clotet-Codina, I.; Tintori, C.; Manetti, F.; Clotet, B. et al. The anti-HIV activity of ADS-J1 targets the HIV-1 gp120. *Virology* **2005**, *343*, 141-149.
- (130) Fujioka, T.; Kashiwada, Y.; Kilkuskie, R. E.; Cosentino, L. M.; Ballas, L. M. et al. Anti-AIDS agents, 11. Betulinic acid and platanic acid as anti-HIV principles from *Syzigium claviflorum*, and the anti-HIV activity of structurally related triterpenoids. *J Nat Prod* **1994**, *57*, 243-247.
- (131) Soler, F.; Poujade, C.; Evers, M.; Carry, J. C.; Henin, Y. et al. Betulinic acid derivatives: a new class of specific inhibitors of human immunodeficiency virus type 1 entry. *J Med Chem* **1996**, *39*, 1069-1083.
- (132) Mayaux, J. F.; Bousseau, A.; Pauwels, R.; Huet, T.; Henin, Y. et al. Triterpene derivatives that block entry of human immunodeficiency virus type 1 into cells. *Proc Natl Acad Sci U S A*

1994, *91*, 3564-3568.

- (133) Sun, I. C.; Chen, C. H.; Kashiwada, Y.; Wu, J. H.; Wang, H. K. et al. Anti-AIDS agents 49. Synthesis, anti-HIV, and anti-fusion activities of IC9564 analogues based on betulinic acid. *J Med Chem* **2002**, *45*, 4271-4275.
- (134) Yu, D.; Sakurai, Y.; Chen, C. H.; Chang, F. R.; Huang, L. et al. Anti-AIDS agents 69. Moronic acid and other triterpene derivatives as novel potent anti-HIV agents. *J Med Chem* **2006**, *49*, 5462-5469.
- (135) Labrosse, B.; Pleskoff, O.; Sol, N.; Jones, C.; Henin, Y. et al. Resistance to a drug blocking human immunodeficiency virus type 1 entry (RPR103611) is conferred by mutations in gp41. *J Virol* **1997**, *71*, 8230-8236.
- (136) Labrosse, B.; Treboute, C.; Alizon, M. Sensitivity to a nonpeptidic compound (RPR103611) blocking human immunodeficiency virus type 1 Env-mediated fusion depends on sequence and accessibility of the gp41 loop region. *J Virol* **2000**, *74*, 2142-2150.
- (137) Holz-Smith, S. L.; Sun, I. C.; Jin, L.; Matthews, T. J.; Lee, K. H. et al. Role of human immunodeficiency virus (HIV) type 1 envelope in the anti-HIV activity of the betulinic acid derivative IC9564. *Antimicrob Agents Chemother* **2001**, *45*, 60-66.
- (138) Yuan, X.; Huang, L.; Ho, P.; Labranche, C.; Chen, C. H. Conformation of gp120 determines the sensitivity of HIV-1 DH012 to the entry inhibitor IC9564. *Virology* **2004**, *324*, 525-530.
- (139) Huang, L.; Lai, W.; Ho, P.; Chen, C. H. Induction of a nonproductive conformational change in gp120 by a small molecule HIV type 1 entry inhibitor. *AIDS Res Hum Retroviruses* **2007**, *23*, 28-32.
- (140) Lai, W.; Huang, L.; Ho, P.; Li, Z.; Montefiori, D. et al. Betulinic Acid Derivatives That Target gp120 and Inhibit Multiple Genetic Subtypes of Human Immunodeficiency Virus Type 1. *Antimicrob Agents Chemother* **2008**, *52*, 128-136.
- (141) Huang, L.; Zhang, L.; Chen, C. H. Potential drug targets on the HIV-1 envelope glycoproteins, gp120 and gp41. *Curr Pharm Des* **2003**, *9*, 1453-1462.
- (142) Yu, D.; Wild, C. T.; Martin, D. E.; Morris-Natschke, S. L.; Chen, C. H. et al. The discovery of a class of novel HIV-1 maturation inhibitors and their potential in the therapy of HIV. *Expert Opin Investig Drugs* **2005**, *14*, 681-693.
- (143) Kashiwada, Y.; Hashimoto, F.; Cosentino, L. M.; Chen, C. H.; Garrett, P. E. et al. Betulinic acid and dihydrobetulinic acid derivatives as potent anti-HIV agents. *J Med Chem* **1996**, *39*, 1016-1017.

- (144) Kanamoto, T.; Kashiwada, Y.; Kanbara, K.; Gotoh, K.; Yoshimori, M. et al. Anti-human immunodeficiency virus activity of YK-FH312 (a betulinic acid derivative), a novel compound blocking viral maturation. *Antimicrob Agents Chemother* **2001**, *45*, 1225-1230.
- (145) Li, F.; Goila-Gaur, R.; Salzwedel, K.; Kilgore, N. R.; Reddick, M. et al. PA-457: a potent HIV inhibitor that disrupts core condensation by targeting a late step in Gag processing. *Proc Natl Acad Sci U S A* **2003**, *100*, 13555-13560.
- (146) Martin, D. E.; Blum, R.; Wilton, J.; Doto, J.; Galbraith, H. et al. Safety and pharmacokinetics of Bevirimat (PA-457), a novel inhibitor of human immunodeficiency virus maturation, in healthy volunteers. *Antimicrob Agents Chemother* **2007**, *51*, 3063-3066.
- (147) Smith, P. F.; Ogundele, A.; Forrest, A.; Wilton, J.; Salzwedel, K. et al. Phase I and II study of the safety, virologic effect, and pharmacokinetics/pharmacodynamics of single-dose 3-o-(3',3'-dimethylsuccinyl)betulinic acid (bevirimat) against human immunodeficiency virus infection. *Antimicrob Agents Chemother* **2007**, *51*, 3574-3581.
- (148) Huang, L.; Ho, P.; Lee, K. H.; Chen, C. H. Synthesis and anti-HIV activity of bi-functional betulinic acid derivatives. *Bioorg Med Chem* **2006**, *14*, 2279-2289.
- (149) Martin, D. E.; Blum, R.; Doto, J.; Galbraith, H.; Ballow, C. Multiple-dose pharmacokinetics and safety of bevirimat, a novel inhibitor of HIV maturation, in healthy volunteers. *Clin Pharmacokinet* **2007**, *46*, 589-598.
- (150) Keyling-Bilger, F.; Schmitt, G.; Beck, A.; Luu, B. Synthesis of optically active diastereomers of a nonproteic neurotrophic mimetic. *Tetrahedron* **1996**, *52*, 14891-14904.
- (151) Kawasaki, M.; Shinada, T.; Hamada, M.; Ohfune, Y. Total synthesis of (-)-kaitocephalin. *Org Lett FIELD Full Journal Title:Organic letters* **2005**, *7*, 4165-4167.
- (152) Qian, K.; Nakagawa-Goto, K.; Yu, D.; Morris-Natschke, S. L.; Nitz, T. J. et al. Anti-AIDS agents 73: structure-activity relationship study and asymmetric synthesis of 3-O-monomethylsuccinyl-betulinic acid derivatives. *Bioorg Med Chem Lett* **2007**, *17*, 6553-6557.
- (153) Roehm, N. W.; Rodgers, G. H.; Hatfield, S. M.; Glasebrook, A. L. An improved colorimetric assay for cell proliferation and viability utilizing the tetrazolium salt XTT. *J Immunol Methods* **1991**, *142*, 257-265.
- (154) Demirov, D. G.; Ono, A.; Orenstein, J. M.; Freed, E. O. Overexpression of the N-terminal domain of TSG101 inhibits HIV-1 budding by blocking late domain function. *Proc Natl Acad Sci U S A* **2002**, *99*, 955-960.
- (155) Kiernan, R. E.; Ono, A.; Englund, G.; Freed, E. O. Role of matrix in an early postentry step in

the human immunodeficiency virus type 1 life cycle. *J Virol* **1998**, *72*, 4116-4126.

- (156) Evers, M.; Poujade, C.; Soler, F.; Ribeill, Y.; James, C. et al. Betulinic acid derivatives: a new class of human immunodeficiency virus type 1 specific inhibitors with a new mode of action. *J Med Chem* **1996**, *39*, 1056-1068.
- (157) Sun, I. C.; Wang, H. K.; Kashiwada, Y.; Shen, J. K.; Cosentino, L. M. et al. Anti-AIDS agents. 34. Synthesis and structure-activity relationships of betulin derivatives as anti-HIV agents. *J Med Chem* **1998**, *41*, 4648-4657.
- (158) Cichewicz, R. H.; Kouzi, S. A. Chemistry, biological activity, and chemotherapeutic potential of betulinic acid for the prevention and treatment of cancer and HIV infection. *Med Res Rev* **2004**, *24*, 90-114.
- (159) Cramer, R. D., 3rd; Patterson, D. E.; Bunce, J. D. Recent advances in comparative molecular field analysis (CoMFA). *Prog Clin Biol Res* **1989**, *291*, 161-165.
- (160) Martin, Y. C.; Bures, M. G.; Danaher, E. A.; DeLazzer, J.; Lico, I. et al. A fast new approach to pharmacophore mapping and its application to dopaminergic and benzodiazepine agonists. *J Comput Aided Mol Des* **1993**, *7*, 83-102.
- (161) Pisha, E.; Chai, H.; Lee, I. S.; Chagwedera, T. E.; Farnsworth, N. R. et al. Discovery of betulinic acid as a selective inhibitor of human melanoma that functions by induction of apoptosis. *Nat Med* **1995**, *1*, 1046-1051.
- (162) Schmidt, M. L.; Kuzmanoff, K. L.; Ling-Indeck, L.; Pezzuto, J. M. Betulinic acid induces apoptosis in human neuroblastoma cell lines. *Eur J Cancer* **1997**, *33*, 2007-2010.
- (163) Fulda, S.; Friesen, C.; Los, M.; Scaffidi, C.; Mier, W. et al. Betulinic acid triggers CD95 (APO-1/Fas)- and p53-independent apoptosis via activation of caspases in neuroectodermal tumors. *Cancer Res* **1997**, *57*, 4956-4964.
- (164) Nencioni, A.; Grunebach, F.; Patrone, F.; Ballestrero, A.; Brossart, P. Proteasome inhibitors: antitumor effects and beyond. *Leukemia* **2007**, *21*, 30-36.
- (165) Kanagasabay, P.; Morgan, G. J.; Davies, F. E. Proteasome inhibition and multiple myeloma. *Curr Opin Investig Drugs* **2007**, *8*, 447-451.
- (166) Cheriya, V.; Jacobs, B. S.; Hussein, M. A. Proteasome inhibitors in the clinical setting: benefits and strategies to overcome multiple myeloma resistance to proteasome inhibitors. *Drugs R D* **2007**, *8*, 1-12.
- (167) Hideshima, T.; Richardson, P.; Chauhan, D.; Palombella, V. J.; Elliott, P. J. et al. The proteasome inhibitor PS-341 inhibits growth, induces apoptosis, and overcomes drug

- resistance in human multiple myeloma cells. *Cancer Res* **2001**, *61*, 3071-3076.
- (168) Adams, J. The proteasome: a suitable antineoplastic target. *Nat Rev Cancer* **2004**, *4*, 349-360.
- (169) Lee, A. H.; Iwakoshi, N. N.; Anderson, K. C.; Glimcher, L. H. Proteasome inhibitors disrupt the unfolded protein response in myeloma cells. *Proc Natl Acad Sci U S A* **2003**, *100*, 9946-9951.